

Electronic Thesis and Dissertation Repository

7-21-2020 2:00 PM

Development of an Active Infection Monitoring Knee Spacer for Two-Stage Revision

Michael K. Lavdas, *The University of Western Ontario*

Supervisor: Teeter, Matthew G., *Robarts Research Institute*

Co-Supervisor: Holdsworth, David W., *Robarts Research Institute*

A thesis submitted in partial fulfillment of the requirements for the Master of Engineering Science degree in Biomedical Engineering

© Michael K. Lavdas 2020

Follow this and additional works at: <https://ir.lib.uwo.ca/etd>



Part of the [Biomedical Devices and Instrumentation Commons](#)

Recommended Citation

Lavdas, Michael K., "Development of an Active Infection Monitoring Knee Spacer for Two-Stage Revision" (2020). *Electronic Thesis and Dissertation Repository*. 7285.

<https://ir.lib.uwo.ca/etd/7285>

This Dissertation/Thesis is brought to you for free and open access by Scholarship@Western. It has been accepted for inclusion in Electronic Thesis and Dissertation Repository by an authorized administrator of Scholarship@Western. For more information, please contact wlsadmin@uwo.ca.

Abstract

Infections requiring surgical revision occur in ~3% of total knee arthroplasty (TKA) procedures. The standard treatment for TKA infection in North America is referred to as the two-stage revision process. Unfortunately, the success rate of the two-stage revision is low, at roughly 85%. There are indications that the two-stage revision may fail to clear the infection due to unsatisfactory diagnostic tools. This thesis depicts the development and evaluation of a novel telemetric sensing package designed for integration into the two-stage revision process. Studies within evaluate its performance through sensor validation, thermal insulation testing, radio frequency penetration evaluation, a cadaveric loading study to confirm durability, a micro CT evaluation of the sensor's impact on implant integrity and a comparison of internal vs external joint temperature during joint movement.

The results of this work describe a largely effective implantable tool for measuring, logging and transmitting diagnostic information about orthopaedic infection. Accuracy and precision of the sensing package were found to be $\pm 0.24^{\circ}\text{C}$ and 0.09°C respectively with negligible hysteresis. Thermal insulation caused by the implant itself was found to produce a thermal time constant of 262.67 ± 4.56 seconds, which results in a very manageable ~17 minute rise time. Bluetooth stability was suitable for data and instruction transmission to both iOS and Android devices while the implant was *in situ*. Following cyclic loading of the cadaveric specimen with the instrumented implants installed, imaging and debridement revealed no obvious issues related to mechanical integrity of the bone cement spacer. However, some bone cement integration issues were observed. Although some engineering iteration and further testing is required, this research contributes a feasible proof-of-concept platform technology for ongoing investigation in orthopaedic infection and implantable telemetrics.

Keywords

wireless telemetry; orthopaedic infection; sensors; embedded systems; smart implant; total knee arthroplasty; two-stage revision; 3D printing; cadaver; temperature sensing

Summary for Lay Audience

Knee replacement surgeries are among the most commonly performed operation in North America. Generally, these procedures are quite successful but occasionally complications arise. Serious complications may require further surgery to rectify. Currently, the most common cause for additional “revision” surgeries is infection. Unfortunately, current solutions are unable to eliminate the infection in an alarming ~15% of cases, which may result in serious long-term mobility challenges, amputation or even death. The hypothesis suggests that the diagnostic tools being used are insufficient for determining infection status during treatment. This project outlines the development of a novel sensing package intended for seamless integration with the current North American standard treatment protocol, the “two-stage revision”. This implantable device will collect biometric (temperature) readings and store them for bulk wireless offloading to a physician’s mobile device for analysis. Future human trials will be used to hopefully find a correlation between infection and mean knee temperature during treatment.

This thesis outlines the entire design process including an evaluation of current tools, problem definition, concept generation/selection, implementation and design validation. During testing of this device, temperature sensing performance was evaluated using a custom-built, programmable temperature chamber in addition to a water bath. The device was then surgically installed in a cadaver knee to demonstrate appropriate sensing, telemetric and mechanical capabilities while in a simulated working environment.

The exciting test performance results of this device imply great optimism, not only for the success of the proposed project, but for sensing applications throughout the healthcare industry.

Acknowledgments

This research would not have been possible without a great deal of support. My primary supervisor, Dr. Matthew Teeter, has been nothing short of outstanding throughout my graduate studies. Matt was incredible in connecting me with any resource required and guiding my development in grasping the biological side of this project. Further, Matt recognized my desire to excel in the medical devices industry and afforded me every opportunity to develop an entrepreneurial skillset in tandem with my research, which has been a huge bonus to my graduate studies and has shaped my next steps in life.

I would also like to thank Dr. David Holdsworth, my co-supervisor, who has been challenging me to improve my methods of problem solving and presenting evidence-based opinion for many years. On many occasions I left David's office with a fundamentally reformed understanding of a topic I thought I already grasped. David's generosity with his wealth of knowledge and experience on a staggering array of topics is something I admire greatly and aspire to achieve within my career.

Dr. Brent Lanting has been an excellent advisor to my research. Despite working long days in the operating room, Brent always found time to offer an opinion on the practicality of my designs for clinical use. Brent also performed the mock surgery on the cadaveric specimen for my study and went out of his way to involve me in the procedure to teach me more about knee replacement than I could have ever learned in the classroom.

I would also like to acknowledge Dr. Ryan Willing for his assistance and patience in the kinematic loading portion of the cadaveric study. Without his guidance, and access to his resources, this study would have never come together in the way that it did.

My fellow graduate student, Sydney Wilson, also played a substantial role in the success of this research. Her intuitive knowledge of circuitry and assistance with circuit layout tools was invaluable. Similarly, on the software side, Riley Bloomfield was always there to bounce ideas off of and help with code debugging. Chaithanya Nair, a summer student, surpassed all expectations and was instrumental in the search for an appropriate device battery manufacturer.

Doctors Ali Tavallaei and Daniel Gelman were my original two lab mates when I began at Robarts Research as a summer student nearly a decade ago. Both have offered nothing but respect, friendship and seemingly bottomless knowledge over the years.

Dr. Maria Drangova will always be the person who believed in my technical and scientific potential enough to give me a chance. Our coincidental meeting began my pursuit for scientific knowledge and her guidance over the years has been perhaps the most valuable I have ever received.

Shannon Woodhouse and the entire Bone & Joint Institute have been relentlessly supportive of my ongoing development through mentorship, education and support. They have been a truly outstanding organization with incredible people behind it. I also thank them for including me in the Collaborative Training Program in Musculoskeletal Health Research and offering me both the Undergraduate Trainee Bursary and the Graduate Transdisciplinary Training Award.

Western Engineering and the School of Biomedical Engineering, namely Whitney Barrett and Dr. Abbas Samani have afforded me every opportunity over the last two years and have always been incredible to work with on a personal and professional level. I very much appreciated their assistance while I applied for and secured both the Ontario Graduate Scholarship and Natural Sciences and Engineering Research Council of Canada's Master's Scholarship. Beyond this, Abbas was an outstanding course instructor to TA with throughout my entire time in the program. Also, Eugen Porter and Chris Vandelaar are some of the finest educators one could ever hope for. I attribute so much of my technical development to their perpetual willingness to share knowledge.

I would like to thank my family for offering me every opportunity to succeed, sharing their love of all things technical, and encouraging me to always strive for excellence.

Finally, I would like to thank Page for her many years of true partnership and more kinds support than I could ever put down on paper.

Table of Contents

Abstract	ii
Keywords	ii
Summary for Lay Audience	iii
Acknowledgments	iv
Table of Contents	vi
List of Tables	ix
List of Figures	x
List of Acronyms	xiii
1 Chapter 1—Project Overview	1
1.1 Introduction	1
1.2 Motivation	2
1.2.1 Knee Anatomy	2
1.2.2 Osteoarthritis	4
1.2.3 Total Knee Arthroplasty	6
1.2.4 Infections of Total Knee Arthroplasty	7
1.3 Diagnostics & Treatment of Total Knee Arthroplasty Infection	8
1.4 Problem Definition, Thesis Scope & Hypotheses	13
2.1 Thesis Outline	17
2.2 2 Chapter 2—System Design	18
2.2.1 Data Collection & Logging in Medical Applications	18
2.3 Embedded Systems & Wireless Telemetry	20
Concept Generation, Selection & Implementation	22
Temperature Sensing	26
Concept Generation, Selection & Implementation	29

	Power Management, Source, and Safety	31
	Concept Generation, Selection & Implementation	33
	Encapsulation Strategy.....	37
2.4	Hermetic, Near-Hermetic & Non-Hermetic Implant Packaging	37
2.4.1	Additive & Subtractive Manufacturing of Case Materials	39
2.5	Conformal Encapsulant.....	40
2.5.1	Bone Cement & Potting Considerations.....	41
2.5.2	Thermal Insulation of the Sensor	42
2.5.3	Kinematic Loading Expectations	42
2.5.4	Concept Selection & Implementation.....	44
2.5.5	Concept Selection & Implementation.....	44
2.5.6	Concept Selection & Implementation.....	44
2.5.7	Concept Selection & Implementation.....	44
3	Chapter 3—Experimental Evaluation of Prototype	54
3.1	Introduction.....	54
3.2	Methods.....	56
3.2.1	Study Design.....	56
3.2.2	Specimen Design, Manufacture, and Inspection.....	57
3.2.3	Specimen Design, Manufacture, and Inspection.....	57
3.2.4	CAD Workflow, Manufacture, and Programming	59
3.2.5	Testing.....	59
3.3	Statistical Analysis.....	66
3.3.1	Statistical Analysis.....	66
3.3.2	Results.....	67
3.3.3	Specimen Manufacturing	67
3.3.4	Sensing Precision	68
3.3.5	Sensing Precision	68
3.3.6	Sensor Characterization, Sensing Accuracy & Hysteresis	68
3.3.7	Sensor Characterization, Sensing Accuracy & Hysteresis	68
3.3.7	Thermal Equilibrium & Insulation.....	71
	Radio Frequency Penetration.....	72
	Data Collection During Anatomic Loading.....	72
	Mechanical Integrity	73

	Discussion	78
4	Chapter 4—Summary, Discussion, and Conclusion	82
	Summary of Device Performance	82
3.4	Ramifications of Performance on Utility	83
	Limitations, Recommendations & Future Work.....	87
4.1	Conclusion	88
4.2	Conclusion	88
4.3	References.....	90
4.4	Curriculum Vitae	111

List of Tables

Table 2.1—Go/No-Go screening of embedded system solutions. This is an engineering selection tool for filtering considered devices.	25
Table 2.2—Go/No-Go screening of encapsulation strategies. This is an engineering selection tool used to filter potential solutions.....	47
Table 2.3—Engineering decision matrix for optimal encapsulation strategy. This is a secondary design tool to select the optimal solution from a list of feasible ones.	48
Table 3.1—Bluetooth Signal Strength Before & After Implantation	72

List of Figures

Figure 1.1—Diagram of the right tibial tray displaying relevant internal structures. Accessed through a Creative Commons 4.0 License at [7]. 2

Figure 1.2—Depiction of the right knee from the anterior direction identifying internal structures. Accessed through a Creative Commons 4.0 License at [7]...... 3

Figure 2.1—Mbientlabs MMC microcontroller as depicted with ruler for scale. It is a 25mm ARM based MCU with extensive peripheral support..... 22

Figure 2.2—TI CC2650MODA microcontroller as depicted with a ruler for scale. It is a thumbnail sized device with a rich featureset. 23

Figure 2.3—ELSRA BT03 microcontroller as depicted with a ruler for scale. It is seen here soldered down to a supplied breakout board..... 24

Figure 2.4—Schematic of the custom printed circuit board layout which depicts the battery, short circuit/undervoltage protection, sensor and microcontroller with integrated antenna... 36

Figure 2.5—Two titanium superstructures, pictured with the intentionally textured pattern (left) and the smooth alternative (right). 49

Figure 2.6—Completed instrumentation package including MCU, sensor and battery. 51

Figure 2.7—Custom fixture is installed, suspending instrumentation package for the first silicone stage..... 51

Figure 2.8—The fixture is removed following Step 5 with the package suspended by cured first stage..... 51

Figure 2.9—Sensing packages in Step 8 of assembly depicting the second silicone stage curing in vacuum chamber..... 52

Figure 2.10— Depiction of the prototype encapsulated system. The protruding wires are only for prototype purposes and clipped before use. 52

Figure 3.1—Specimen B, an encapsulated sensing package, which has been potted in bone cement to demonstrate similar thermal insulation characteristics to the implanted embodiment..... 58

Figure 3.2—Approximate location of the Specimens C1 & C2 within the cadaveric specimen prior to bone cement application. The femur is above, while the tibia is below. 62

Figure 3.3—Cadaveric knee featuring InterSpace articulating components and novel instrumentation as seen in flexion..... 63

Figure 3.4—Cadaveric knee featuring InterSpace articulating components and novel instrumentation as seen in extension..... 63

Figure 3.5—Depiction of the cadaveric knee with the installed articulating spacer and sensors mounted to the VIVO apparatus for the purposes of anatomic loading. 64

Figure 3.6—Retroactively identified oxidation on decoupling capacitor as a result of fluidic condensation during testing and delay before debridement..... 67

Figure 3.7—Graph depicting the comparison of the reference sensor readings vs. the experimental sensor readings and visualization of the characteristic equation of the calibration dataset. 68

Figure 3.8—A visual representation of the validation dataset. This depicts the relationship between the experimentally captured values regressed to degrees Celsius and their paired samples from the reference sensor..... 69

Figure 3.9—Graphical depiction of the hysteresis observed at each temperature step. The mean value (-0.001°C) is displayed in blue..... 70

Figure 3.10—Graph of "Thermal Step Response" with 15 repeated trials of package temperature rise superimposed. Dotted lines highlight the average amount of time required for 63.2% of rise, also known as the thermal time constant. 71

Figure 3.11— Graph of "Temperature Readings vs. Loading Cycles" depicting the temperature captured by the instrumented implant throughout cyclic loading..... 72

Figure 3.12—An axial view of the articulating surfaces following the loading cycle and debridement. Note excess bone cement on the tibial tray has been worn smooth..... 73

Figure 3.13—An auxiliary view of the tibia and femur following the loading cycles and debridement. No spacer separation or major fracturing was observed. 73

Figure 3.14—Micro CT image depicting a region on the posterior face of the potted sensing package in the tibia where poor bone cement coverage is observed. 74

Figure 3.15—Micro CT image depicting a sagittal view of the tibial implant where three regions of poor bone cement integration with the implanted instrumentation can be observed. 75

Figure 3.16—Two areas with insufficient bone cement can be observed on the tibial keel. . 76

Figure 3.17—A third area with a void of bone cement coverage on the tibial keel. 76

Figure 3.18—Explanted femoral spacer component clamped in a bench vice displaying superior bone cement coverage of the sensing package. 77

List of Acronyms

ACL – Anterior Cruciate Ligament

BLE – Bluetooth Low Energy

CRP – C-Reactive Protein

CT – Computed Tomography

DoF – Degree(s) of Freedom

ECM – Extracellular Matrix

ESR – Erythrocyte Sedimentation Rate

I²C – Inter-Integrated Circuit

IDE – Integrated Development Environment

IO – Input/Output

LCL – Lateral Collateral Ligament

LTC – Lithium Thionyl Chloride

MCL – Medial Collateral Ligament

MCU – Microcontroller Unit

OA – Osteoarthritis

PCB – Printed Circuit Board

PCL – Posterior Cruciate Ligament

PET – Positron Emission Tomography

PJI – Periprosthetic Joint Infection

RF – Radio Frequency

SPI – Serial Protocol Interface

SSR – Single Stage Revision

TI – Texas Instruments

TKA – Total Knee Arthroplasty

TPBS – Triple Phase Technetium-99 Bone Scan

TSR – Two Stage Revision

WBC – White Blood Cell Count

1 Chapter 1—Project Overview

Introduction

1.1 Total Knee Arthroplasty (TKA), colloquially known as “knee replacement” is one of the most prolific surgical procedures in North America. An aging population suggests that the popularity of this procedure is likely to continue growing.

There are several scenarios that call for a total knee arthroplasty including end-stage rheumatoid arthritis, osteoarthritis, hemophilia, gout, disorders resulting in unusual bony ingrowth or osteonecrosis. There also exists a plurality of other less common issues that ultimately result sub-optimal operation of the load bearing tissues and necessitate a replacement [1]. However, osteoarthritis (OA) is responsible for over 90% of knee replacements so this will be a focal point of discussion [2].

Although there are various types and approaches to knee replacement, ultimately the goal of any procedural style is to replace the bearing surface(s) and/or supporting tissue of the knee joint with a synthetic substitute after the natural mechanisms have failed.

TKA is a generally successful surgery with low revision rates. However, the single most common situation requiring further intervention is infection (up to 3% of cases) [3] [4] [5].

The sheer volume of patients means that even a small percentage represents a substantial affected population Sections 1.2.4 and 1.2.5 offer a comprehensive discussion of the statistics, infection, diagnostics, and the gold standard treatments for TKA infection.

Unfortunately, knees requiring revision processes for infection become reinfected at a rate of roughly 15% with devastating ramifications [6]. Although there may be several explanations for this, Section 1.2.5 discusses high likelihood that improved diagnostic measures for these TKA infections, specifically *during* the treatment protocol, would be extremely valuable in reducing reinfection.

Ultimately, the focus of this thesis is the engineering of a novel instrumentation and telemetric package with the intent to log and transmit diagnostic information regarding infection status to a physician during the treatment process. Design validation is also presented though a combination of benchtop analyses and a cadaveric study. The performance observed suggests promising utility not only in its current form, but the possibility of this platform technology receiving slight modifications for more diverse biometric applications. The majority of Chapter 1 explains the biological background and reasoning for the pursuit of this diagnostic tool.

Motivation

1.2 Knee Anatomy

1.2.1 Before describing the pathway a patient takes to a total knee replacement an understanding of the structures and mechanisms within the knee joint alongside the ramifications of any component failing was essential. The knee is a synovial hinge joint that translates primarily on the sagittal plane but to a lesser extent also has degrees of freedom in the coronal and transverse planes as well.

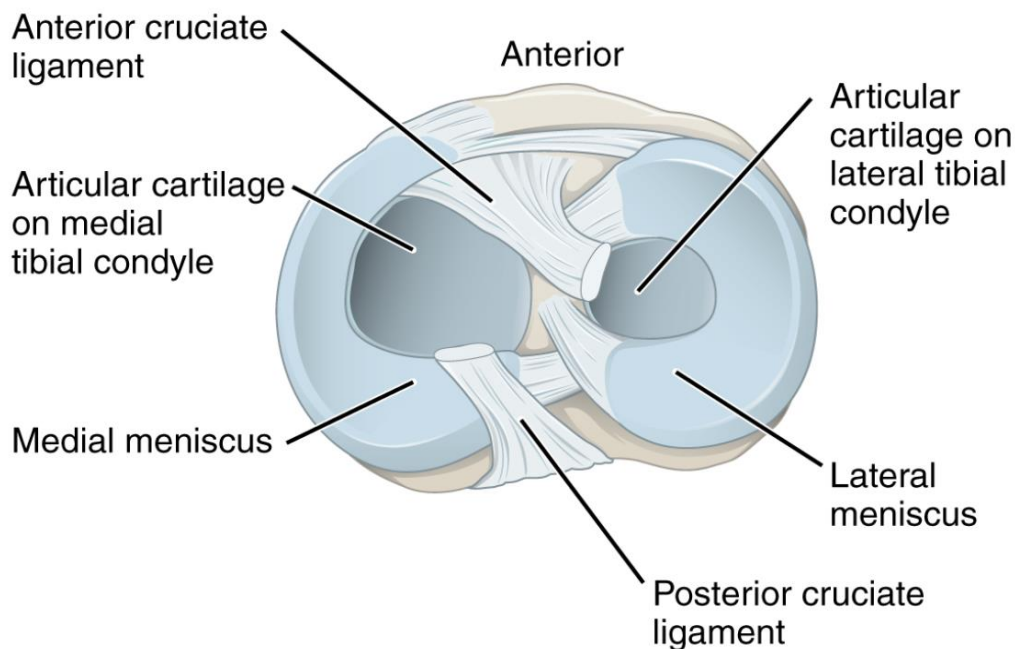


Figure 1.1—Diagram of the right tibial tray displaying relevant internal structures. Accessed through a Creative Commons 4.0 License at [7].

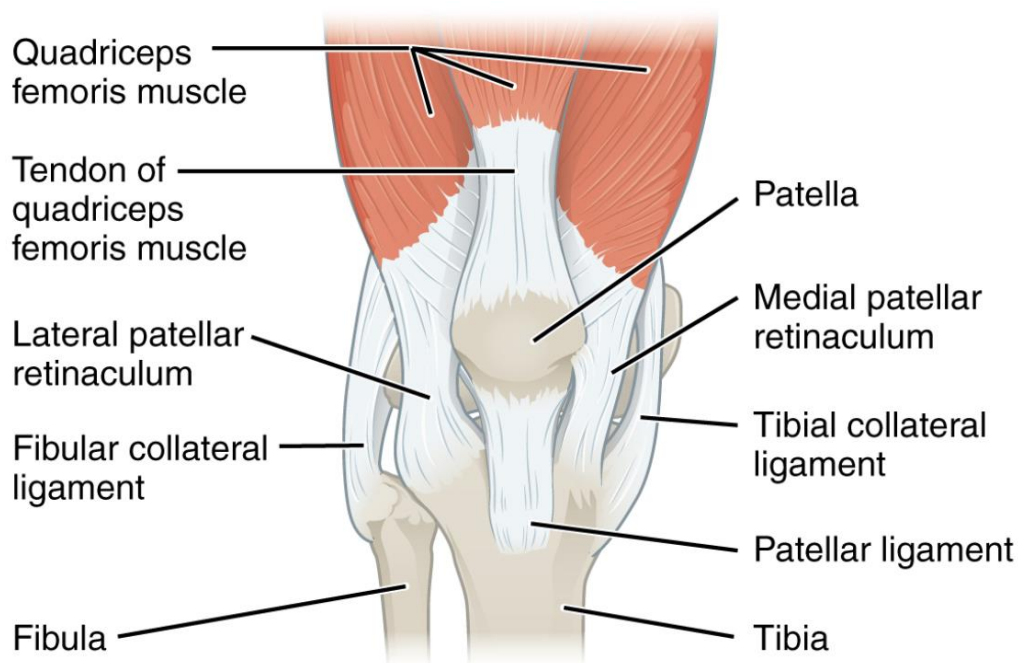


Figure 1.2—Depiction of the right knee from the anterior direction identifying internal structures. Accessed through a Creative Commons 4.0 License at [7].

A recent paper in the *Journal of Functional Morphology and Physiology* offers the basis for the following summary of knee anatomy [8]. There are four basic elements to knee composition: bony structures, cartilage, connective tissues, and muscles. Figures 1.2 and 1.2 (above) have been included as a precursor to the following content to orient the reader to the relative locations of each structure.

While the knee is fundamentally a junction of the femur and tibia, the patella is an additional, smaller bone that protects the anterior articular surfaces of the joint. It is attached to the joint by the quadriceps tendon and patellar ligament in the superior and inferior aspect respectively [9].

Two prominent cartilaginous structures in the knee are the lateral and medial meniscus. They contribute to force damping and lubrication of the joint actuation. Another function they serve is to distribute the loading evenly from one bone surface to the next despite any geometrical inconsistencies. More load is generally applied to the medial side of the

meniscus and as a result the cartilage of the medial meniscus tends to be stiffer than the lateral to maintain healthy joint alignment during ordinary dynamic loading. Articular cartilage, the primary site of osteoarthritic development envelops the load bearing surfaces of the tibia and femur. As patients advance in age, the entire meniscus tends to become stiffer/more fibrous and articular cartilage shows similar degenerative qualities, especially in obese patients [10] [11].

Bone and cartilage structures of the knee are enveloped in a two layer capsule. On the interior of this capsule, the synovium membrane secretes a lubricating fluid to assist and nourish the meniscus. The exterior layer of this capsule is comprised of five connective tissues. The quadriceps tendon joins the quadriceps to the patella. The medial and lateral collateral ligaments (MCL/LCL) stabilize the inner and outer portions of the knee respectively while the anterior and posterior cruciate ligaments (ACL/PCL) reduce forward and backward translation of the femur relative to the tibia.

Finally, there are two major muscle groups that cause the primary knee translation. Hamstrings run along the posterior of the femur and attaches just below the knee on the tibia. Quadriceps are four muscles that run along the anterior side of the femur to oppose the forces imparted by the hamstrings.

1.2.2

Osteoarthritis

The previous section outlined the overall knee anatomy and should orient the reader to how some of the concepts covered in this section might result in insufficient function.

Osteoarthritis is a disease resulting in the deterioration of articular cartilage, reducing the performance of load bearing joints and causing pain. One key characteristic of this disease for the time being is that physicians can often treat symptoms and slow disease progression, but there is no outright cure [12].

The pathology of OA is well characterized and generally known to progress in a few steps. It begins with the chondrocytes becoming unable to support loading applied in some regions of the cartilage. This is generally because of non-uniform loading, chronic or acute overloading. Their natural reaction is to cluster and excrete more growth factors

into the extracellular matrix (ECM), effectively an inflammation response. This is normal cartilage behavior. For much of the joint lifespan the articular cartilage can heal from this response by stimulating the regeneration of chondrocytes. However, when this fails to result in the desired healing, the chondrocytes undergo apoptosis at a higher rate than new ones are created and the ECM breaks down, leaving unsupported collagen fibers. At this stage the articular cartilage has somewhat “deflated”, and it becomes tough/fibrous. The end stage of OA involves bony ingrowth into the already toughened cartilage. This stage generally escalates to a bone-on-bone grinding effect.

Generally, treatment strategies taken are targeted around the early-stage inflammatory response. If the severity and length of that phase can be reduced, there is a higher likelihood that the cartilage will be able to replenish chondrocytes naturally [13]. Especially when it is caused by an acute injury. At this stage, the goal is to make chondrocyte production happen more quickly than apoptosis in order to prevent the ECM from becoming depleted.

Once the cartilage deteriorates beyond this point, the unsupported collagen becomes damaged from loading and there are few treatment options so knee replacement is considered [14]. The function of a knee replacement in this context is to completely remove the problematic cartilage and bone surfaces, leaving behind a low friction polyethylene on polished metal bearing surface in its place.

More recent research indicates that beyond the classical understanding of OA, there may be additional factors involved, specifically a discussion of bony ingrowth beginning in some regions of the cartilage *prior* to ECM collapse, thus creating the non-uniformly distributed loading/stress raisers commonly accepted to initiate OA [15].

This section previously alluded to total knee arthroplasty as the ultimate termination of treatment for osteoarthritis. For clarity, the Section 1.2.3 is a dedicated explanation of that process and depicts how TKA simply replaces the components failing to perform properly as OA progresses.

Total Knee Arthroplasty

1.2.3 Total knee arthroplasty is one of the most prolific surgeries in North America with ~700,000 performed annually [16]. TKA surgeries have become a fairly streamlined process with ever decreasing average length of stay in hospital and longer implant lifetime attributed to innovative design and improvements to healthcare [17]. Revision TKA surgeries in Canada for 2016–2017 were just 7.6% of total TKA surgeries, noting some of them would have been patients having components of their knee revised following a decade or more of good function [18].

Although strategies differ somewhat, specifically in the preservation of various supporting tendons and ligaments, this is a summarized procedure for TKA adapted from Varacello *et al.* [19]:

- 1) An incision is made across the anterior knee running in a proximal to distal direction. Note that minimally invasive approaches are now gaining popularity with shorter incisions.
- 2) The patella is moved to the side, permitting access to the articulating surfaces of the knee.
- 3) An intermedullary drilling operation is performed to permit access to the femoral canal.
- 4) Fixturing, guides, or other alignment equipment is affixed in preparation of an involved resection process on the femoral condyles. This fixturing is often located about the femoral canal geometry and pre-operative alignment analysis.
- 5) Surgical guides or fixtures are frequently used in resecting the tibial articulating surface to produce a flat surface on a plane that best supports proper knee alignment. Often a plane normal to the tibial axis is chosen, but other times a slight (2–3°) varus bias is applied.

- 6) The knee extension gap magnitude and geometry is assessed. This is often done by utilizing a spacing block in extension and an anteroposterior sizing guide in flexion. Adjustments to cutting guides affixed to the femur are applied as necessary.
- 7) The femur is resected with an anterior, posterior, anterior chamfer and posterior chamfer with assistance from installed surgical guides.
- 8) An intercondylar notch is cut from the femur, perpendicular to the native transepicondylar axis.
- 9) The femoral and tibial implants are either impacted or cemented in place. Care is taken to avoid internal rotation or component overhang. A polyethylene bearing is mated to the tibial component, sized to produce the desired joint geometry. Alignment is confirmed and the bearing may be switched if needed.
- 10) In some cases, the patella will also receive a bearing on the posterior surface.
- 11) The patella is repositioned, and the wound is closed.

While this description should clarify the process, the takeaway message is obvious: as OA progresses it causes the articulating cartilage and supporting bony structures to fail, this procedure simply replaces the regions that OA affects. It does however come with some risk, the most common of which is covered in Section 1.2.4.

Infections of Total Knee Arthroplasty

A drawback of any surgical procedure is risk of infection. It has been suggested that up to 5% of patients receiving any kind of surgery will develop a “surgical site infection” [20].

Revision rates in total knee arthroplasty attributed to infection are considerably lower than this at 1–3% of patients depending on the source [3] [4] [5] [21] [22] [23]. When considering the quantity of TKAs being performed annually in Canada (70,000) and the United States (>600,000) as many as 20,000 North American people require infection related revisions annually [18] [24].

Upon investigation of the types of infection, there are reports that 52.9% of infection can be attributed to staphylococcus, 5.9% to Escherichia coli, and 2.8% anaerobes. Other sources report that staphylococcus is the sole pathogen in 67.7% of cases while streptococci (another member of the Gram-positive bacterial group) was implicated in 19.2% of cases. Song *et al.* published results highlighting candida albicans in TKA infection, which implies fungus is another causative microorganism [25].

An infection, especially untreated, can be devastating. There are some intuitive symptoms including local heating, swelling, and pain. These localized symptoms can quickly progress to systemic infection, resulting in high fever, sepsis or even death [21] [26] [27] [28] [29]. This is coupled with up to 24× cost increase in overall treatment pathway for a patient who develops a periprosthetic joint infection (PJI) [30]. An additional challenge is that sometimes the symptom severity is low for a substantial period of time, meaning the patient is less likely to seek medical attention while in the meantime, an infectious biofilm is being formed on the implant components causing extreme infection resiliency [27].

1.2.5 **Diagnostics & Treatment of Total Knee Arthroplasty Infection**

Having understood the manifestation of infection in TKAs as discussed in Section 1.2.4, it became important to consider the methods currently being used to diagnose a primary TKA infection.

There are common clinical indicators of high interest as usually they are the easiest to observe by patients and primary caregivers at a glance. These indicators include persistent pain, swelling, erythema, localized warmth or wound drainage. Note that there are also examination findings that surround general tenderness and range of motion disproportionate to healing timeline, but if the infection is an “Acute PJI” (occurring in the first 4 weeks following surgery), it is difficult to discern ordinary localized pain or limited range of motion from an indication of infection so these two indicators are more valuable when evaluating a “Chronic PJI” (≥ 4 weeks post-surgery). Sensitivity of these evaluations are not as high as some other measurements, largely because meaningful

quantification of these symptoms is challenging. Also, they can be caused by other reasons (related or unrelated to the surgery) [30].

Serological tests are also popular tools, the two mainstays are erythrocyte sedimentation rate (ESR) evaluation and C-reactive protein (CRP) tests, although new markers such as IL-6 are being investigated [3].

ESR is a nonspecific indicator of inflammation that generally peaks 5–7 days following surgery and then decreases to a baseline over 3 months to a year. Ongoing ESR elevation is indicative of infection. It involves agitation of blood or serum and then measuring how long it takes for the red blood cells to separate/settle. ESR is imperfect however, featuring just 82% sensitivity and 87% specificity [31].

CRP is another inflammation correlated indicator, but it works differently than ESR. While ESR is not concerned with relative concentration, more so mechanical behavior, CRP testing is specifically checking the serum for concentration of these proteins. If CRP stays above a threshold of 10 pg/mL 14–21 days after TKA, the patient is still considered “infected”. Performed together, these tests have a sensitivity of 91% and specificity of 86% [31].

In some cases, the use of imaging tools to evaluate infection of TKA are used. Conventional radiography may be applied following the clinical observations above to seek any kinematic reasoning (such as fracture, loosening, or positional change) for the observed inflammatory symptoms instead of infection. This modality cannot specifically indicate that a patient is or is not infected, it can only positively identify kinematic abnormalities, which might be an alternative cause of symptoms [3].

There are various nuclear medicine approaches to imaging TKA infection, specifically, triple phase technetium-99 bone scan (TPBS), white blood cell (WBC) imaging using indium-111 as the emission source, or fluorodeoxyglucose positron emission tomography (PET). These modalities are applied to evaluate the bone remodelling behaviors or inflammatory responses and the correlation to infection. One source reported the overall

accuracy of these modalities as 81%, 84%, and 83% respectively in detecting TKA infection although no precision figure was offered [32].

Joint fluid/tissue analysis is another subcategory of PJI analysis. Knee aspiration involves using a syringe or vacuum device to extract fluid from the joint space. This can be performed simply to reduce pressure, but the synovial fluid collected can also inform physicians about the infection conditions after subsequent analysis [33].

The extracted aspirate can be sent for several different lab evaluations, which when combined, are one of the most effective ways to identify a primary infection. If there are >1100 leukocytes/ml of synovial fluid, *and* the amount of neutrophil (a type of leukocyte) as a percentage of the overall quantity of leukocytes is in excess of 64%, one can be 98.2% certain of infection. This confidence decreases when either one of these counts is below their respective thresholds [34]. Although very useful, there is one major drawback: if the patient has taken any antibiotics in the previous 4 weeks, these measurements plunge in reliability such that they are more suitable for an initial diagnosis than monitoring recovery as most patients will be put on antibiotics once the infection has been discovered [35] [36].

Although fungal infections are rare by comparison to bacterial, they do require their own evaluation strategies. While the clinical indicators of infection do still apply, usual joint aspiration protocols will not detect fungal infection. As a result, some hospitals choose to conduct a “potassium hydroxide mount” (a histological analysis) to rule out this possibility [37].

Once a patient has been diagnosed with an infection, there are some common options for their treatment. The preferred option is the cheapest and least invasive. It involves antibiotic suppression of the infection and is often coupled with irrigation and wound debridement but ultimately aims for implant retention. This is an easier solution for all involved, but there are two caveats:

- 1) These are only options for an acute infection diagnosis. Any infections older than 4 weeks are assumed to have developed into a deep infection or biofilm and are notoriously resilient [27].
- 2) Recall, once antibiotics are administered, the utility of the conventional aspiratory testing is severely compromised, so measuring treatment progress is difficult [34].

If the above fails to clear the infection, or the infection has been otherwise classified as “chronic” then it becomes likely that the region of the world the patient is in will dictate their treatment pathway.

In Europe, most patients should expect to undergo a single-stage revision (SSR) process. SSR involves one surgical procedure during which the infected implant is removed, any infected or necrotic tissue is resected, intermedullary canal is reamed, and insertion of a new “revision” implant meant to be a permanent replacement is cemented in place using a bone cement laced with antibiotic [38].

In North America, an alternative strategy, the two-stage revision (TSR) is preferred. As one might infer, a TSR involves two separate surgeries. The first does a lot of the same that the SSR does, but instead of aggressively reaming the canal to fit the revision knee at this stage, a smaller diameter cut is taken and an antibiotic loaded bone cement “spacer” is installed instead. This spacer passively elutes antibiotics and offers some surface antibiotic properties, which works to discourage the reformation of a bacterial biofilm on the implant surfaces. During this phase the patient is often dosed with a battery of oral and/or intravenous antibiotics. The spacer is recommended to remain in the patient for a period of approximately 6–10 weeks as the infection is cleared before another surgery is conducted to debride the spacer, ream the mating surfaces, and install the permanent revision total knee implant [38] [39].

Both solutions can be effective in their own way, but they certainly also have drawbacks. There are some suggested advantages of SSR over TSR. For example, if the revision is successful an entire surgical procedure is avoided. This is advantageous from a cost perspective but also means that the patient has one fewer operation to develop a

complication during and the patient recovery timeline can be expedited [25]. Although a concrete figure in knees has proven difficult to find, the same debate applied to hip arthroplasty in Australia suggests the cost difference between SSR and TSR is slightly more than 50% in an ideal SSR [40].

There is suggestion of some infection eradication advantage to two stage revision over SSR for several reasons. First, in TSR procedures the physician has the opportunity to revise to another spacer if they are unconvinced that the infection has been cleared in the treatment period of the first one. Furthermore, patients are more likely to have the bone volume remaining to permit these revisions because the tissues have not already been reamed out to fit the (wide bore) permanent knee as they would have with SSR [41]. Turning a two stage into a three stage revision has drawbacks but it is still preferable to reinfection of the permanent revision implant. Second, the volume of local antibiotics is increased over SSR with much more bone cement being used and therefore the useful elution period is also increased. Third, an antibiotic bone cement spacer leaves only antibiotic laden, non-metallic surfaces in the joint space. Assuming the right antibiotics are used, this creates a poor environment for biofilm formation and greatly reduced infection resiliency [42]. TSR strategy allows physicians to choose whether they are going to use a cemented or cement-less total knee revision implant on a case-by-case basis where SSR demands a cemented installation as the antibiotic cement is considered critical to the process [6].

When examining literature to compare the effectiveness of each style, it becomes clear that several factors negatively impact the chances of a fair comparison. It is easy to innocently introduce sampling bias into a comparative study in favour of SSR. This is because poor bone quality is often contraindicated for SSR so patients less healthy at pre-operation are more likely to receive TSR by default. Also, there may be some pressure to produce results in favour of SSR, especially in places where the healthcare payor is the same entity producing research funding. A well randomized, unbiased clinical trial is really needed to know with certainty which strategy is superior [38].

Regardless, the entire field can agree upon two things:

- 1) Both methods produce unacceptably high re-infection rates. A comprehensive 2019 review paper suggested ~15% reinfection for both strategies [6].
- 2) The ramifications of a “permanent” joint revision implant becoming reinfected are absolutely devastating, generally ending in lifelong mobility issues, amputation or mortality. Not to mention huge healthcare cost associated with reinfection, one study suggests a hip a reinfection costs roughly 5 times the price of a standard SSR [40].

One might find the high reinfection rate following either procedure unsurprising. Recalling discussion on diagnostic tools, the most common ones, leukocyte quantity and relative neutrophil content analyses following joint aspiration are negatively affected by antibiotic use. C-reactive protein tests are challenged as well, considering CRP levels change rapidly with variable inflammation levels [43]. It is reasonable that the same strategies used to diagnose a primary infection are not particularly suitable once the patient has begun their antibiotic therapy and enters the dynamic process of potential surgery and healing. There is the need for a better type of diagnostic tool for use once treatment has begun.

1.3

Problem Definition, Thesis Scope & Hypotheses

To review, this Chapter has offered discussion of the knee joint, the primary causes for replacement, the fundamental mechanism with which this is done, and some known issues with the process.

Section 1.2.5 offered detailed account of the infection related statistics, protocols and problems. This ultimately resulted in the argument that the current methods of monitoring infection status, specifically during treatment, are insufficient and improved diagnostic tools for this phase of recovery are required.

This suggests a problem definition. *“Develop a diagnostic solution specifically suitable for use during treatment for total knee arthroplasty infection.”*

The scope of this task was limited to address patients undergoing two stage revision considering a North American patient's most likely treatment pathway and the treatment protocol Canadian physicians are most comfortable with.

Tests observed working well at steady state (infected, or not infected) become less effective during recovery, either due to dynamic conditions or due to antibiotic interference [34].

Even the most rudimentary systems can only be accurately characterized and usefully leveraged with suitable data. To capture data needed in mapping a dynamic system, the key is almost always measurement *over time* [44]. When viewed from this perspective, reports of poor testing reliability during recovery seem reasonable if not probable. Every test for infection conducted on these patients comes down to a measurement every few weeks when the patient comes into clinic. How could any physician be expected to extrapolate on a continuously changing system with a sample rate of 1–2 times per month at an accuracy any higher than the current 85% when it is known some tracked metrics fluctuate by the hour [45] [46] [47]?

Recent advancement in embedded systems, wireless communications, sensors, and implant-safe batteries mean that innovators have the tools to offer physicians higher frequency information to aid in their treatment strategies. A patient may be sent home with an implantable or wearable sensing package that can collect and log biometric measurements every few minutes for later presentation of this telemetry (trended over time) to the physician. Medtronic has pursued this strategy for several years in the field of cardiac arrhythmia monitoring with FDA approval of their temporary LINQ™ implant and shown improved clinical outcomes by monitoring “at risk” patients remotely [48]. At this time, the researchers are unaware of any orthopaedic infection sensing equivalents.

By eliminating metrics inherently affected by antibiotic use and imaging modalities (infeasible to send home), this left a few choices for measurable indicators that may be a) correlated to infection status and b) converted into valid indicators by higher sample rates: functional pain, swelling, temperatures, ESR, and CRP measurement.

An evaluation of functional pain was discounted, the quantification of pain is an ongoing question so a sensing modality capable of measuring it in this context and timeline was unrealistic.

Erythrocyte sedimentation rate involves extraction of blood, timing of settling, and observation. Although very recent advancements in micro electromechanical systems are producing some incredibly interesting work on the topic of miniaturizing this test, a commercial embodiment of this technology, especially one feasible for implantation is years from reality [49].

C-reactive protein secretion is directly linked to inflammation, so “swelling” is also grouped into this category. This test has some real feasibility in implantable evaluation. A 2009 paper by Hsiao Chen *et al.* showcased an intriguing design for a MEMS chip capable of fitting a small lab-on-chip setup for this measurement in a 7×7 mm package. Unfortunately, this technology never made it to retail, likely because of the inherent sensitivity to micromanufacturing tolerances and complicated tuning processes making this a difficult sell [50]. If this technology were to appear commercially, it would be a great addition to this project.

The field of thermal measurement, both the sensors and system modelling, is well researched with dozens of high-quality sensors are available off-the-shelf. Another large advantage relative to other alternatives is that temperature can easily be measured through conduction if needed, which is advantageous from a biocompatibility/isolation perspective. Temperature sensing for infection monitoring does have challenges involving passive wound heating due to healing, and diurnal rhythm may have an impact as well, but these will later be discussed in detail.

At this stage, a decision had to be made: implantable or wearable? On one hand, implantable technologies come with many technical challenges like regulatory approvals, power supply, communication, and biocompatibility. On the other, wearables are likely to be less sensitive to joint space infection than an internal temperature measurement [51]. Most critically, a patient can remove it which brings up the dreaded topic of optional adherence. Under different circumstances the decision might have been more difficult,

but in this specific context, casting the sensing package directly into the antibiotic bone cement spacer simplified the technical challenges associated with implantation greatly, while removing adherence from the equation making implantation very attractive.

After careful consideration, and a deep-dive into existing technology developed for similar sensing applications (Section 2.1), it was decided to produce an orthopaedic implant integral to the bone cement spacer. This device is meant to capture and store periodic measurements of implant temperature, several times an hour, for weeks at a time between clinical visits. When the patient visits the clinic, the data will be wirelessly transmitted to the healthcare provider(s) to be evaluated for indications of infection subsidence or worsening.

The following pages depict development, fabrication, characterisation, and validation strategies of a device that may lay the groundwork for a fundamental change in orthopaedic infection management.

While this thesis is certainly design-heavy, it is not proposed in the absence of research questions. The researchers suggest two hypotheses:

- 1) The sensing package developed will offer sufficient sensing, power management, and communication performance to be feasibly used for the application of infection diagnostics in a knee spacer.
- 2) The integration of the overall instrumented package within a bone cement spacer is unlikely to cause mechanical or logistical issues during installation or use.

Section 1.4 clearly lays out the contents of each Chapter.

Thesis Outline

- 1.4 **CHAPTER 1** *Project Overview* – Introduces the knee anatomy, total knee arthroplasty, infection related conditions/diagnostics/treatments, the problem definition and a high level design approach.
- CHAPTER 2** *System Design* – Summarizes the sensing history of implantable devices. Project then broken into sub tasks. Engineering design thinking applied to each individual issue involved in the design of the instrumented implant. Manufacturing of sensing package discussed.
- CHAPTER 3** *Experimental Evaluation of Prototype* – Testing of the prototype including an evaluation of sensor precision, hysteresis, sensor accuracy, thermal time constant of cemented package, wireless communication from within a knee, data collection during anatomic loading, and instrumented spacer survivability.
- CHAPTER 4** *Summary, Discussion & Conclusion* – A final discussion of device performance, observations, future work is included and commentary regarding the high level ramifications of this project.

The objectives of this study were as follows:

- 1) Characterize the sensing device to identify a characteristic equation, sensing precision, sensing accuracy, and the thermal time constant of the cemented implant.
- 2) Assess wireless transmission of the device's temperature readings while in situ, and during exposure to anatomically relevant cyclic loading.
- 3) Investigate the integration of the sensing package within the bone cement spacer using imaging and destructive analysis.

2 Chapter 2—System Design

Having understood the need and problem definition, this chapter examined the history of sensing in orthopaedics and cover the design process this team underwent in the creation of a potential solution to infection diagnostics during two stage revision.

Data Collection & Logging in Medical Applications

In highly academic fields, data driven decision making is essential “due diligence” and is

- 2.1 what differentiates medicine from homeopathy. Quantitative measurement using implantable devices has been a research focus for decades, below is a brief summary.

Force sensing has historically been the primary driving factor for orthopaedic instrumentation as engineering decisions in implant design required quantitative information to form constraints. Implant instrumentation solutions originated in 1979. T. English and K. Kilvington published a paper depicting *in vivo* sensing of hip loads using an instrumented femoral implant [52]. The implant was primitive in design, utilising strain gauges positioned to measure axial loads with a battery powered transmitter. The battery and transmitter were encapsulated externally to the main body of the implant, but still inside the patient’s leg. Although the battery chemistry and transmission method were not discussed, it can be assumed that this system was non-rechargeable and communicated via low frequency radio waves to a dedicated receiver. As this implant was intended to be a permanent device, it is unclear if the battery and transmitter were intended to remain inside the body or be surgically detached from the rest of the implant and removed when depleted.

Shortly afterwards, in 1982, R. Brown *et al.* published a study depicting a more sophisticated device [53]. Their invention was a hip nail offering strain measurement about two separate degrees of freedom. It applied conventional FM radio technology to transmit readings, requiring impressive ingenuity as they transmitted two separate readings on a single frequency using no digital components. They effectively multiplexed the signal output using oscillators of asynchronous frequency (5 kHz and 4 kHz). Each oscillator fed a signal through one of the strain gauge (modified Wein) bridges, which

determined the amplitude and then both signals were superimposed for transmission. Signal deconstruction could then be performed by filtering out the 5 kHz and 4 kHz components using external computation hardware. Unfortunately, the oscillatory nature of this measurement strategy resulted in poor strain gauge performance. This was the most complex telemetric orthopaedic implant found prior to the use of onboard computational hardware separating the measurement circuit from transmission.

The industry was relatively quiet for several years until the early 2000s as researchers waited for more compact and power efficient mobile computing chips, better implantable battery technology, wireless charging options, and improved wireless communications. At that point, two groups took control of the orthopaedic sensing space.

Dr. D'Lima published a paper depicting a paradigm shift forward in this type of technology [54]. His team developed a knee implant that had computation available onboard utilizing an advanced (for the time) PIC16C microcontroller unit (MCU). This change permitted a separation of the power management, sensing, and transmission circuits. This device did not have an onboard power supply, rather relied on wireless excitation through an inductive coupling and rectification circuit. The microcontroller permitted several force sensors to be sampled sequentially and an integrated analog to digital converter (ADC) allowed digitization and therefore short-term storage of readings. The PIC16C also permitted integration of a radio frequency element allowing D'Lima's team to stream digitized readings to a proprietary receiving unit while the study subjects performed movements in his laboratory. Because this implant did not have a power supply, it relied on the patient being in the lab and hooked up through an inductively coupled knee brace to a power supply for excitation and reading capture. The upside to this mechanism was that there is nothing dangerous about leaving the instrumented implant in the body for an indefinite period as there were no batteries to leak.

Shortly thereafter, a German company called Orthoload collaborated with the Julius Wolff Institute to construct a device in this space considered the closest to "commercial" in instrumented orthopaedics. They have designed several orthopaedic implants for different joints that can collect kinematic information for 6 axis acceleration, loading, and

coarse resolution ($\sim 1^\circ\text{C}$) temperature [55]. Functionally it operates very similar to Dr. D’Lima’s solution, but they can include more sensing options due to a proprietary integrated circuit design. Orthoload does not sell these devices as commercial joint replacements for hospital purchase, instead they run clinical trials and sell the databases of collected kinematic information to research centers interested in developing their own (passive) implants, external prosthesis or other orthopaedic aids.

One final technology to discuss is not orthopaedic, but cardiac. Between 2014 and the present, St. Jude/Abbott Medical and Medtronic have produced at least four different implantable cardiac monitoring devices available for commercial use in the US. They allow remote monitoring with the ability to observe events between clinical visits and have been shown to capture 7.8 times more atrial fibrillation events in cryptogenic stroke patients (who are already closely monitored) over the course of one year [56].

The Medtronic LINQ (and competitive devices) set an approvals precedent for a clinically viable, battery powered implantable devices with the sole function of measuring a biological stimulus, logging that information over time, and wirelessly transmitting it to a physician for improved diagnostic capability over standard care. The adoption of this device bodes well for the approval of a similar device in orthopaedic infection sensing, which is the gap in technology that will be addressed in this thesis.

2.2

Embedded Systems & Wireless Telemetry

The rise of mobile computing is perhaps the most defining technological shift of the 2000s. It is difficult to pinpoint when the mainstream uptake began, some might argue the earliest pocket calculators, perhaps the earliest cell phones, but the 1996 PalmPilot1000 seems most representative of the beginning of modern mobile computing. Widely accepted customer requirements for mobile computing have remained largely unchanged since this first touchscreen handheld was designed: compact, lightweight, long battery life, quick performance, more storage, more connectivity, more multitasking capability, and low cost [57]. Microprocessors and their peripherals are a major design consideration for development of any mobile device as they influence all these priorities. For decades,

major manufacturers have consistently one-upped each other resulting in rapidly evolving mobile computing possibilities and the “smart” ecosystems.

When selecting the computational platform for this device, a degree of versatility was required as the MCU was one of the first components selected. At this stage, it was unclear what other components might be selected, so flexibility to integrate several different types of sensors, power supplies, and wireless communication strategies was advantageous.

To permit an 18-month design, fabrication and validation cycle, one constraint was a platform supported by a well-equipped development environment. An associated objective to find a pre-built package that would not require a custom printed circuit board (PCB) layout. The obvious caveat being an overall package size suitably small for an implantable application and availability of suitable hardware.

There was a necessity for a solution offering low sustained power consumption to afford the most flexibility in power supply. A target value was not chosen, but provided the selected platform was constrained to have some form of software-interruptible sleep/standby state, the net current draw for the MCU would be dwarfed by the power consumed for wireless transmission anyways.

To ensure compatibility with any potential sensor, it was preferable to have a microcontroller that contained an 11 + bit ADC, plus offered both Serial Peripheral Interface (SPI) and Inter-Integrated Circuit (I²C) communication options. Between these three options the selected microcontroller would be suitable to interface with nearly any commercially available sensor.

There was substantial motivation to select Bluetooth as the wireless modality. Most modern smartphones, laptops, and tablets offer Bluetooth as a native transmission feature. This sensing package was designed not only as a research tool, but also to be commercially viable. The cost reduction and ease of implementation if physicians could connect using their own devices so no dedicated transponder was required was extremely attractive. Suitable data security strategies for Bluetooth are also easy to implement

relative to some less popular technologies. However, it has been shown that 2.4 GHz signals do struggle to penetrate water. Literature suggested that Bluetooth *should* be capable of transmitting over the relatively short tissue depths required but there was certainly the objective to select a system that would permit an easy pivot to lower frequency communication should Bluetooth fail to penetrate the leg [58].

Concept Generation, Selection & Implementation

With these considerations in mind, the following four concept solutions were examined:

2.2.1

1) MbientLabs MetaMotion C

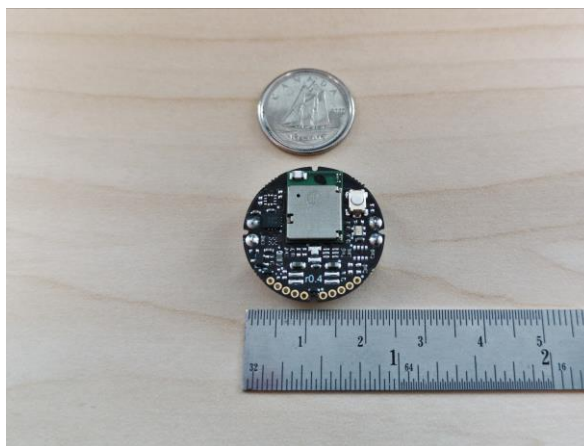


Figure 2.1—Mbientlabs MMC microcontroller as depicted with ruler for scale. It is a 25mm ARM based MCU with extensive peripheral support.

The Mbientlabs device shown in Figure 2.1 is a complete system, with integral microprocessor, Bluetooth antenna, several sensors, and plenty of sensor communication options. It is available with an integrated development environment (IDE) permitting C level language coding and wireless firmware updates. It was on the larger end of considered systems, a circular package of 25 mm diameter and is manufactured by a growing Chinese start up manufacturer [59].

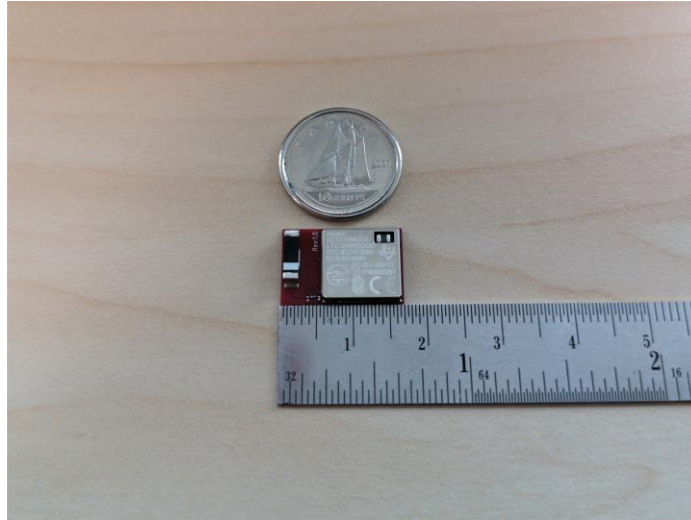


Figure 2.2—TI CC2650MODA microcontroller as depicted with a ruler for scale. It is a thumbnail sized device with a rich featureset.

2) Texas Instruments CC2650MODA

Texas Instruments (TI) has a rich heritage of mobile computational platforms and has recently produced a series of “SimpleLink” processors designed to make connected systems and “Internet of Things” a straightforward process. They make a range of chips that share similar architectures and identical pinout, but each integrates a different flavour of wireless capability. The suggested offering pictured in Figure 2.2 offers Bluetooth Low Energy (BLE) connectivity and an antenna integrated together on one small 10×12 mm PCB. This is designed to be soldered down to a custom breakout board containing sensors and a power supply of the engineer’s choosing with a full host of analog/digital input/output (IO), I²C, and SPI ports. For an additional fee, TI offers a prototyping kit and an IDE accepting a modified version of C programming [60].

3) ELSRA BT03

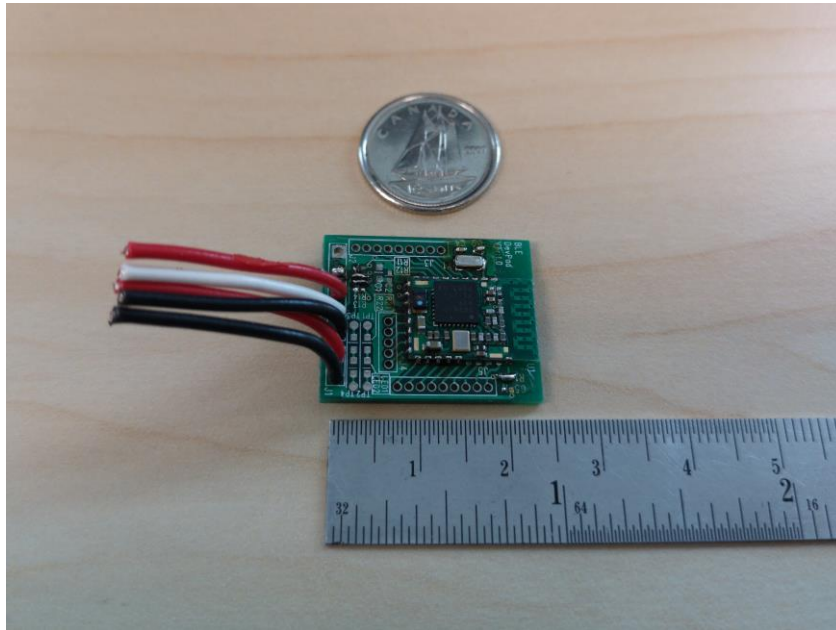


Figure 2.3—ELSRA BT03 microcontroller as depicted with a ruler for scale. It is seen here soldered down to a supplied breakout board.

ELSRA Electronics is a company based in Shenzhen, China. The BT03, seen in Figure 2.3, is a clone module of the CC2650MODA above but applies a newer, superior, TI processor (CC2640R2F). This module offers increased storage space and the ability to connect via BLE or Bluetooth 5.0, but at slightly higher cost. In theory, the same Texas Instruments prototyping kit and IDE are compatible [61].

4) Arduino / Arduino Compatible Systems

Systems like DFRobot’s BLE Beetle and competitors are capable, yet ultimately impractical modules. Arduino is extremely intuitive with excellent community support designed specifically to permit quick “minimum viable product” creation. Although it seemed like an obvious choice, there appears to be a surprising gap in technology. Even the smallest Bluetooth capable Arduino compatible devices are 25×33 mm and are not designed to be soldered down to a breakout PCB. Another challenge is that most of these

compact Arduino compatibles are sold by small third parties. This invited the opportunity for supply chain issues [62].

In the concept selection phase, reduction was conducted using a Go/No-Go Screening, which can be seen below in Table 2.1. This screening strategy eliminates potential solutions that “fail” any of the design constraints.

Table 2.1—Go/No-Go screening of embedded system solutions. This is an engineering selection tool for filtering considered devices.

	MbientLabs MMC	TI CC2650MODA	ELSRA BT03	Arduino Compatible
Sleep/Standby	Go	Go	Go	Go
Good IDE	No Go	Go	Go	Go
Compact	No Go	Go	Go	No Go
ADC, SPI & I2C	Go	Go	Go	Go
Bluetooth	Go	Go	Go	Go
Result:	Fail	Pass	Pass	Fail

The Texas Instruments and ELSRA platforms emerged from preliminary screening as the only solutions satisfying all constraints. Due to their similarities and low cost, they both would score competitively in an Engineering Decision Matrix so both solutions were purchased and tested.

Although powered by a superior processor, the ELSRA BT03 arrived with poor documentation and upon further inquiry, the customer support team was unable to implement their own hardware as advertised.

The TI branded CC2650MODA module also was not provided with thorough documentation for this application. It was originally designed to be applied as a Bluetooth transceiver module acting peripherally to a master microcontroller in a larger implementation. Nonetheless, the hardware capability *did* exist for it to be used in a standalone configuration and the Texas Instruments engineering staff were extremely

willing to provide additional resources. Using the TI Code Composer Studio IDE, software for this implant was developed in house. A custom PCB breakout to attach the sensor, a power supply, and breakaway programming interface was created.

The ultimate package size is just $12 \times 17 \times 3$ mm, about half the size of the smallest available Arduino platform. This platform also leverages three separate controllers on a single integrated circuit and managed by a real time operating system. The CC2650 includes a primary Cortex M3 processor in addition to a dedicated “sensor controller” and an “RF core” all on one 5×5 mm chip [60]. The peripheral processors can sleep/wake asynchronously from the main processor. This permits the power hungry M3 to idle or perform other tasks as the sensor controller independently samples the environment, stores the readings temporarily, and offloads them as appropriate to the Cortex M3. Similarly, the RF core has its own buffer to store and transmit information it has received wirelessly. As a result of this technology, the CC2650MODA can operate for months or years on a standard CR2032 coin cell depending on the application. It also has enough storage space after this device’s programming to hold 5500 readings before requiring a wireless information transfer to the physician’s phone. At such a time, the storage is wirelessly cleared, and further samples can be collected over several more weeks.

With the MCU selected, the next decision in the process was to determine which sensor would be selected for use. This is discussed in Section 2.3.

Temperature Sensing

It was decided early in the problem definition phase of this project that temperature sensing would be the operative biometric marker for this implant. Elevated temperature is a known indication of infection as the body’s immune system aims to weaken an infection with a localized or systemic feverish response [63]. Temperature sensing is likely to show some challenges in separating an infection “signal” from thermal “noise” resulting from factors discussed below but recalling Section 1.2.5, all metrics have individual hurdles. Temperature sensors are at least a mature technology, with alternate stimuli like ESR there would be concerns about performance of a novel sensor type in

addition to the questions about overall infection correlation. Note that the controller chosen in Section 2.2 was selected with the possibility of a future pivot to an alternate sensing modality as an alternate sensor would be almost “plug and play”, but prior to clinical testing, temperature sensing was the most logical starting point.

The first challenge was to determine a sensing resolution, precision, and accuracy that would be appropriate for this application. To be clear, resolution refers to the minimum detectable change, precision is synonymous with the standard deviation of a sensor reading at any given steady state condition and the accuracy refers to a range surrounding the “true” value of temperature reported by the sensor.

The decisions for appropriate constraints were challenging as is the first implantable sensor for this purpose. No dataset exists to say “if the patient is below X temperature for Y amount of time, the patient’s infection is cleared”. This will have to be discovered experimentally and is unlikely to be a single threshold value for all patients.

An investigation of expected temperature ranges began with an evaluation of previous literature. Research of “diurnal rhythm” – the body’s natural temperature fluctuation over time, was an initial consideration. Healthy human males have an average range of 0.9°C core temperature fluctuation throughout a 24 hour period, where females may show additional daily increase of up to 0.4°C depending on their menstrual cycle and other hormonal factors [64].

Other considerations included the observed increase in postoperative knee temperatures as recorded in healthy patients. A 2016 study published by Yirong Zeng *et al.* suggests that 5 days post-op, TKA patients experience an average increased knee skin temperature of 2.3°C relative to the contralateral knee, which stays fairly steady until the 30 day measurement. By 90 days, this temperature has begun to subside to 1.8°C. Their measurements were taken with a medical IR thermometer (Optris GmbH) offering a precision of 0.2°C and accuracy of $\pm 0.4^\circ\text{C}$ [65]. Notably, this study did not include any patients identified to have contracted a TKA infection.

Further investigation added another element to the story: internal wound temperature relative to surface skin temperature. Information on this subject is understandably limited considering a relative lack of measurement tools for this application. One relevant study was published in 2016 by Arjun Chanmugam *et al.* investigating deep wound temperature relative to skin surface temperature. Although based on a small sample size (just 6 patients), their metrics were very relevant to the proposed project. They used their proprietary implementation of Long Wave Infrared Thermography to image temperatures both at skin surface and at the wound bed depth. In their control patients without infection, they observed a gradient of 1.1–1.2°C from wound bed to surface while infected patients showed a much larger 4–5°C gradient. Another important finding in this study observed wound temperature changes in correlation with different stages of infection treatment [66]. Although it is difficult to draw firm conclusions from a small cohort study, it shows optimism that the stimulus at wound bed might be far more dramatic than at the skin surface and that with measuring at the infection site, infection correlation over time is feasible with implantable device.

Ultimately, the existing literature reveals that there are many reasons a patient's mean temperature may have a different baseline from another's. Fortunately, the strength of a logging platform is to characterize trended changes over time. Therefore, although accuracy is still a valuable metric, the top priority was a high *precision* sensor to track changes with reliability. After an evaluation of the related hardware and this rough idea of the ranges to expect, the following design constraints were selected based on the above literature: an accuracy of $\leq \pm 0.5^\circ\text{C}$, a precision of $\leq 0.2^\circ\text{C}$, and a resolution of $< 0.1^\circ\text{C}$ over a 35–40°C expected dynamic range. These constraints should well equip the implant to measure the patterns of temperature fluctuation with ample performance to capture the behaviour these studies suggest. While there is a challenge to decipher which biological phenomenon is causing an observed change, data collection with this level of detail will certainly offer a useable, first of its kind dataset to identify trends at the infection site and hopefully isolate an infection correlation during patient trials. Simply, if there is a statistical relationship to be found between temperature over time and infection status, a device meeting these constraints should be suitable to capture the required data.

The design decision was further limited by a need for small overall footprint. Ideally, an implementation involving no more than the sensor itself and perhaps a 0402 size decoupling capacitor as PCB real estate was at a premium.

Finally, power consumption was a consideration. Although the ability to “switch off” the sensor when not in use alleviated most energy consumption concerns, there was still an objective to reduce the amount of draw in use and while dormant.

Concept Generation, Selection & Implementation

2.3.1 Although many sensors were considered for this application, the following three were identified as plausible candidates:

1) Microchip Technologies MCP9808

This I²C temperature sensor is a staple enthusiast and commercial choice for many applications. Over the 35–40°C sensing range it reports a typical accuracy of just $\pm 0.25^\circ\text{C}$ ranging to a maximum of $\pm 0.5^\circ\text{C}$. The MCP9808 is precise to 0.0625°C . It consumes 200 μA in use and 0.1 μA in shutdown state [67].

2) Texas Instruments TMP235A2DCKR

The TMP235 series chip leverages current flow changes in thermal diodes to output an analog signal, this can be correlated to temperature. Although at first glance, it reports an unsuitable maximum accuracy of $\pm 2.5^\circ\text{C}$ (typically $\pm 0.5^\circ\text{C}$), this is over its very large (-40–150°C) dynamic range. A graph in Section 6.6 of the data sheet shows that accuracy within the 35–40°C range is $< \pm 0.5^\circ\text{C}$ with $> 99\%$ confidence. This device outputs an analog signal, meaning a resolution only limited by the selected MCU’s ample 12-bit ADC. Precision was not reported, but empirically found to be $< 0.1^\circ\text{C}$ with a five sample windowed average. It draws just 9 μA in operation and a does not require power while dormant. The optimal layout was determined to require just 1 decoupling capacitor for problem free operation [68]

3) Texas Instruments TMP117MAIDRV

This TI module is impressive in several ways. It is similar in operation to the MCP9808 above with the I²C interface but advertises superior performance. The data sheet suggests an impressive $\pm 0.1^{\circ}\text{C}$ accuracy in the operative range. The reported precision is tighter at $< 0.01^{\circ}\text{C}$. Active power consumption is also very low at $3.5\ \mu\text{A}$ with the caveat of a slow conversion cycle of 1 second per reading. Unfortunately, several peripheral components are required (pullup resistors and decoupling capacitors) to implement this device properly [69].

As these devices were all $< \$3$ USD, several samples of each were purchased for a benchtop evaluation selection strategy.

It was clear that although the MCP9808 and TMP117MAIDRV chips offered impressive performance, there were challenges to their implementation. First, they both relied on a “thermal pad” being soldered to the PCB rather than heating through the die jacket. Therefore, if the engineer desires environmental temperature sensing, these are best laid out on a PCB away from other components that generate heat. Unfortunately, in this case the system’s processor is located on the opposite side of the PCB and their footprints are superimposed. This raised concerns of the package reading the MCU heat rather than sensing environmental stimulus.

Another concern was the number of peripheral components required for their operation. The MCP9808 for example required 4–6 peripheral pullup resistors and decoupling capacitors for full functionality with acceptable noise levels. With circuit board real estate at a premium this was disadvantageous.

The TI TMP117MAIDRV platform came with the additional challenge of “blind” pins. When soldering the chip down, the pads were not accessible to a soldering iron and a heat soaking (hot air or hot plate) approach was required. While manageable in a single layer configuration, this was difficult to manufacture in-house as the MCU was already a blind soldering operation on the opposite side so uniform hot plate soldering was not feasible.

In an application where space was not at such a premium and the sensors could be located on the same side of the PCB as the microcontroller, the design decision may have been different.

The TMP235DCKR option was ultimately selected. While the theoretical performance was inferior to the other two options, following a rigorous evaluation (detailed in Section 3.2.4.1) it still satisfied all design constraints. Additionally, it was highly power efficient, was implementable with just one peripheral capacitor, and paired well with the rest of the embedded system layout.

Once the components to be used were selected, the team was able to calculate the power requirements for sustained operation of the sensor. The design process for this step, in addition to the safety considerations are discussed in Section 2.4.

Power Management, Source, and Safety

2.4

Supplying power to an implantable device in a way that is likely to be approved for use in humans is challenging. To accomplish this task, four basic mechanisms were considered.

Energy harvesting is a newer concept to consider in the context of compact devices. Essentially, this involves a compact generator that operates on energy already being wasted in the environment of the device [70]. A common example would be an automatic wristwatch that uses a rotor actuated by gravity and the kinetic force from the wearer's everyday movements to wind a mainspring. It is somewhat less popular in compact electronic devices as the rate of power generation is low and the engineer still usually requires a component to store the electricity once generated (a capacitor or battery). There are some innovators launching a wearable device that utilizes energy harvesting in a smartwatch application, this example runs on thermoelectric power. Unfortunately, it is not currently feasible to simply buy a suitable energy harvesting mechanism off the shelf [71].

Wireless charging has become a commercially available choice for developers of compact electronics. While still relatively new in mainstream consumer electronics, it has been applied in niche or research applications since the late 1800s where it was first

patented as a mechanism of powering electric rail cars [72]. It operates via an inductive coupling. At a fundamental level, alternating current is applied to a master coil by an external power supply, by Oersted's Law this generates an oscillating electromagnetic field [73]. This electromagnetic field interferes with a slave coil and by Faraday's Law the electromotive force drives electron flow on the device end [74]. This must then be rectified into a direct current and regulated to the appropriate voltage. When tuned appropriately, there is no longer a need for a large power reservoir on the receiving end of the inductive coupling, generally a capacitive storage solution is suitable provided the inductive coupling is always present during operation. Recalling Section 2.1, this is the option leveraged by both D'Lima and Orthoload in their instrumented implants. However, there are challenges. An internal rectifier/regulator circuit and coil take up a substantial amount of room and the transmission can be easily impeded by metallic objects. When applying an inductive system, the developer risks heating up his or her device if it is electrically conductive [75]. In the context of this temperature sensitive device this poses a great challenge.

The third option is to implant a battery. While by far away the simplest to implement, this has drawbacks as well. Batteries considered suitable for implantation have changed over time. The earliest battery powered implants were pacemakers, health regulators accepted more risk as they were a completely necessary device [76]. The chance of mercury-zinc batteries leaking or shorting over an extended period was preferable to an imminent heart failure. Now, medical battery safety is regulated in part by manufacturing guidelines in ISO 13485 and is required to demonstrate hermeticity. From an electrical/chemical safety standpoint ANSI/AAMEI ED 60601-1 depicts risk management strategies needed for medical power supplies and IEC 60086-4 / IEC 62133 cover battery safety/implementation for various chemistries [77]. Essentially there are four components to a successful implanted battery: manufacturing, chemistry, quality assurance, and implementation. These topics will be revisited in the following section.

In direct relation to the previous technology, the final concept involves coupling a wireless charging device with a rechargeable implantable battery. Recharging of batteries does add some (manageable) implementation challenges as accidental overcharging can

cause a casing rupture in addition to the usual short circuit risks [78]. It would also add substantial complexity and cost to the overall device. Truthfully, the biggest deterrent is the dependence on patient adherence to recharge the implant regularly.

In this design context, it became clear that a primary (non-rechargeable) battery was the optimal solution. It has strength in simplicity, and this project intrinsically has elements making a primary battery an easy choice. First, the implant is inherently temporary. As the sensing package is embedded in a knee spacer, it will not be left in the patient for more than 6–10 weeks before revision to the permanent knee. The power consumption of the electrical components selected are well known and straightforward calculations could be performed to select a suitable capacity. With the obvious goals to reduce complexity, size, and cost, the primary battery became further attractive. Inductive couplings as used by Orthoload and D’Lima were completely infeasible for this usage case because they were only suitable for taking measurements while the patient was in the lab coupled to the master coil and this device must passively collect information for weeks at a time. Ultimately, the biggest motivation for the primary cell implementation was complete autonomy from patient adherence issues. As envisioned, the patient should not even have to think about their instrumented knee spacer for the 6–10 week duration of implantation.

2.4.1

Concept Generation, Selection & Implementation

This team was uninterested in creating a custom battery due to the regulatory concerns. Due to the already expansive scope of this project, it made logistical sense to outsource the battery development. Several companies were consulted to better understand available options for the optimal solution.

1) Integer/Electrochem

Electrochem is a battery manufacturer that sells specialized cells for a variety of applications. They offer several different battery chemistries, and one huge advantage of their product is that they can provide integrated undervoltage protection, saving PCB space. Unfortunately, their catalogue offerings for implants are only approved for usage up to 60°C. While this is acceptable in use, during the setting process of bone cement

internal temperatures are expected to reach approximately 80–86°C so implantation would be infeasible [79] [80].

2) Eagle Picher

This company is one of the better established in the industry. They were notable for a few reasons. Their customer service was quick and extremely knowledgeable. When contacted, they provided access to one of their engineers free of charge to discuss options and offer more information than was available on their data sheets. Notably they offer batteries in a variety of chemistries, with several options of regulatory rigour for various applications.

3) Tadiran Batteries

Tadiran is a prominent manufacturer of lithium thionyl chloride batteries, specifically designed for high temperature implantable use [81]. Their designs and testing procedures conform to regulatory requirements in many regions of the world for implant safety [82]. When contacted they were also quite responsive, knowledgeable, and eager to help.

Electrochem was eliminated at a preliminary stage as none of their offerings were suitable to withstand the temperatures required or offered appropriate capacity in an acceptable form factor for this application.

Quickly this team narrowed down the desired chemistry to lithium thionyl chloride (LTC). Of the battery types suitable for this environment and regulatory requirements, these were the highest power density offerings available [83].

These can be a volatile type of primary battery and are generally avoided for consumer electronics, but manufacturers like Tadiran and Eagle Picher have invested significant R&D to design casings suitable for regulatory approval [82].

Unfortunately, there are still drawbacks. Any device undergoing rigorous regulatory approval is quite expensive, the selected model for example was quoted at \$250 USD with a minimum \$5000 USD order. Also, as of yet, the smallest capacity offered by either manufacturer was 350mAh in this chemistry, roughly twice the capacity required for an

acceptable operational lifetime including a healthy factor of safety for this specific device. Higher capacity translates to a higher casing size and the overall implant package is heavily impacted by the battery geometry.

Ultimately an Eagle Picher 3PN-LTC-M1 implantable class battery was selected. Eagle Picher offers this battery with a preferable casing geometry over Tadiran for project needs and were excellent to work with throughout the development process. They offered a nearly identical battery, the 3PN-LTC-S2, which shares most specifications with the medical variant but lacks the rigorous regulatory approvals. This was instrumental for developing a minimum viable product as each battery cost only \$16 USD but are a plug and play substitute for the \$250 USD medically approved sibling. Eagle Picher is also a manufacturer of custom sized batteries. In the future if this sensing package requires a smaller custom battery or one of a different geometry for placement somewhere else in the body, Eagle Picher would be an excellent partner to collaborate with.

By selecting a battery that already satisfies the design, manufacturing, and quality assurance stipulations over something like a common coin cell, a great deal of engineering/testing responsibility was mitigated. The only component left to the design team was appropriate implementation.

The primary concern for battery safety in any device is rupture. Rupture is generally accompanied by explosion, venting or leakage, these are all generally undesirable. There are four main ways to cause these problems: a mechanical interference (crushing/piercing), over charging, over discharging, or overheating [84].

Mechanical interferences will be discussed in subsequent sections, while over charging is not a concern for non rechargeable batteries. Overheating and over discharge protection however, were both taken extremely seriously during implementation.

The selected batteries are suitable for temperatures up to 95°C so the casting procedure of the bone cement is of no concern with ~10°C of headroom [79] [80] [85]. The real concern comes from short circuiting. One common mechanism of protection from short circuits or other sources of rapid current discharge are polymeric positive temperature

coefficient (PPTC) devices. These are compact, self resetting fuses that operate as a tiny thermostat. If installed in series with the battery they reach a threshold temperature either by a high current throughput or environmental heating condition they will open the circuit [86]. A surface mount PPTC was selected for use in redundancy to existing overheating protection fail-safes offered by the CC2650 processor and battery management hardware commonly integrated into the casings of medical grade LTC batteries. Note that self resetting functionality was critical as the 80–86 °C setting temperature of antibiotic bone cement is likely to trip many current threshold thermal fuses that are otherwise suitable for this application [79] [80]. When temperatures return to normal levels the circuit will reactivate.

Over discharge protection is commonly designed with an all in one “low voltage cut-off” device coupled with a transistor to disconnect the battery when the voltage drops below the desired threshold and two resistors to tune the boundaries of cut-off hysteresis [87]. This strategy was suggested for the final design in redundancy with the existing undervoltage cut-off integrated into to the CC2650 programming. This redundancy was especially critical as the FDA critically evaluated a Medtronic implantable device’s ability to create an open its circuit during undervoltage conditions [88]. The final electrical schematic for the device is seen in Figure 2.4 below.

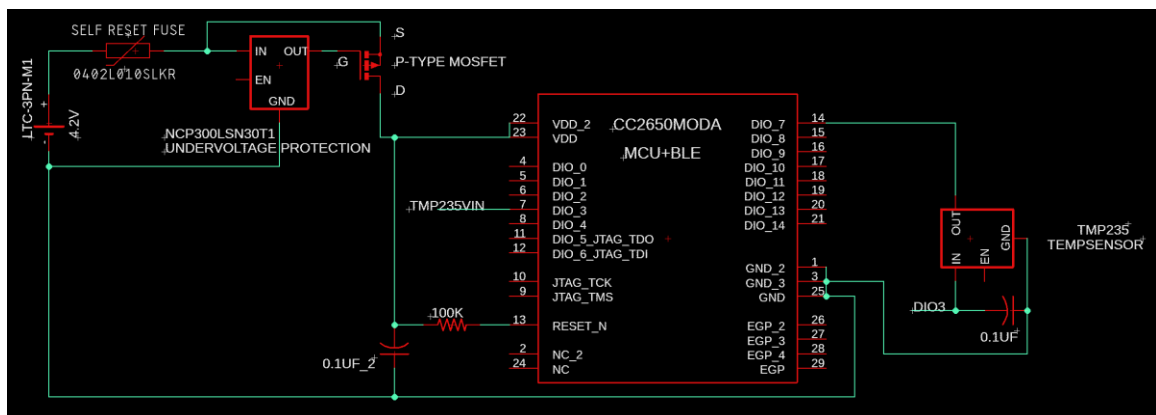


Figure 2.4—Schematic of the custom printed circuit board layout which depicts the battery, short circuit/undervoltage protection, sensor and microcontroller with integrated antenna.

Following the development of the circuit, shown finalized in Figure 2.4, custom boards were printed and assembly/testing could begin. Simultaneously a discussion of encapsulation was also underway as the final geometry of the electronics was at this stage better understood. Section 2.5 details how this process was conducted. A completed example of the electronics package can be seen below in 2.5.7 (Figure 2.6).

Encapsulation Strategy

2.5 Encapsulation of implantable electronics is a complex topic requiring consideration from several different perspectives. High level strategy is discussed in Section 2.5.1, while the nuances of functionality, safety and assembly technique are covered in the remainder of Chapter 2.

Hermetic, Near-Hermetic & Non-Hermetic Implant Packaging

2.5.1 When encapsulating medical devices there are three predominant strategies: hermetic, near-hermetic, and non-hermetic.

The classical definition of the term “hermetic” is thousands of years old, simply meaning “airtight” [89]. However, for a device to be considered “hermetic” by United States FDA standards, it must specifically satisfy MIL-STD-883 TM 1014 [90]. This evaluation involves extended exposure to high pressure helium followed by an observation period in a mass spectrometer under vacuum, which measures the leakage rate of helium previously forced into the package [91].

Usually, devices satisfying these requirements must be designed for simple parting lines with fused seams rather than a mechanical mate. Metallic casings are most common, while several strategies are applied for sealing. It has been preferred to avoid adhesives when sealing a device hermetically and rather fuse the casing together through a technique like electron beam, laser or friction welding. Although, interest in alternatives has been growing [92] [93]. Recently ceramics and polymers have also garnered interest as viable possibilities for hermetic casings. The Orthoload instrumented tibial component is a classical example of a hermetic casing. Their sealed housing is machined in three titanium components, the electronics are placed inside, the housing is electron beam and

laser welded together before being tested for hermeticity, calibrated, and sterilized using ethylene oxide (ETO) [94].

At the opposite end of the spectrum are completely non-hermetic encapsulants. These are epoxy resins or silicones designed to permit a degree of liquid ingress. They use an entirely different mechanism to protect the circuitry from the body and vice versa. Where the hermetic seal operates by completely isolating the inside of the casing from the outside, non-hermetic encapsulants simply conform very aggressively to the surface of the internals, allowing no air pockets to form between the surface of the electronics and the encapsulant. Although the encapsulant may be saturated with bodily fluids, short circuiting, corrosion or mixing with any contaminants cannot occur as there is no air volume for the fluids to condense within [95]. This strategy is advantageous in circumstances where the operation of the proposed device requires sampling of bodily fluids.

Considering most hermetic casings are made of titanium or 316 stainless steel, many of those devices require metal-on-glass feedthroughs and a secondary encapsulation mechanism for an antenna, which adds complexity and cost [96]. With most non-hermetic encapsulants, wireless transmission is unimpeded thus greatly simplifying design [97]. One drawback to consider is that any batteries would still need to be hermetically sealed before the overall device was encapsulated non-hermetically or an external excitation mechanism could be used.

A gastrointestinal stimulator designed by Laurent Lonys *et al.* in 2015 is a prime example of an implantable embedded system. It was designed to help manage obesity by leveraging non-hermetic encapsulant. They published an interesting article on the design challenges of encapsulation in a highly acidic environment and why their externally powered silicone encapsulated solution was well suited to the application [98].

Somewhere between the two other strategies falls near-hermetic encapsulation. Although just beginning to gain momentum, there is high potential in this space for innovative encapsulation strategies to emerge. A wide variety of materials can be considered for a near-hermetic package. These are generally categorized with the understanding that there

is some inherent material porosity. This disqualifies them for hermetic status as defined by MIL-STD-883. Many would still prevent meaningful amounts of water ingress for months or years when submerged [99]. Furthermore, some non-metallic materials that would make eligible capsule options such as reinforced polyether-ether ketone (PEEK) or ultra high molecular weight polyethylene (UHMW), have excellent mechanical properties for loadbearing orthopaedic applications *and* RF transmission [97] [100]. Unfortunately, at this time there is no evidence of FDA approval or *in vivo* studies of electronics packaged near-hermetically.

Additive & Subtractive Manufacturing of Case Materials

2.5.2 For reasons discussed in Section 2.5.7, ultimately a solid external casing, hermetic or otherwise, would be required. There are very few ISO 13485 approved manufacturing facilities available for contract prototyping in this space, which somewhat restricted materials, methods, and geometries to options they were able to provide.

Additive manufacturing methods (3D Printing) generally offer looser tolerances, reduced material selection, and increased surface roughness relative to a subtractive method like CNC machining or turning. However, they also have the advantage of generally lower cost for small scale production and complex geometries can be more easily created without the need for custom fixturing or 4–6 axis milling operations [101]. ADEISS, an ISO 13485 additive manufacturing facility is local to Western University so there was incentive to design a solution compatible with their manufacturing capabilities as this logistically simplified the potentially iterative design process.

ADEISS offers 3D printed Ti6Al4V ELI-0406. This is a titanium alloy specifically designed to produce excellent biocompatibility results for implantable applications and is highly thermally conductive (6–8 W/mK), which was preferred over some of the previously considered PEEK options for this temperature sensing application [102].

Using a 3D printing methodology also permitted straightforward texturing of the external faces to promote bone cement integration without intensive milling operations. The only serious concern was the challenge titanium alloy raised for RF penetration. With

relatively high confidence in the use of this casing strategy for structural protection, a compatible electrical encapsulation strategy was investigated next.

Conformal Encapsulant

As discussed previously, there are silicone options for encapsulation that conform aggressively to PCBs and prevent moisture from condensing on the internal components.

- 2.5.3 There are a number of these options manufactured by several mainstream companies suitable for implantation such as Elkem's Silbione line, Dow Corning's Silastic MDX4-4210, and NuSil's Avantor lineup [103] [104] [105]. These products are generally designed to be poured into a captive volume and cured under vacuum or injection molded although some sprayable options are also available.

One other notable technology is Parylene deposition. Parylene is a generic name for a series of polymers based on paraxylene. Parylene C coatings are prolific in the protection of circuit boards in high risk environments. There are several FDA approved implantable devices leveraging the protective properties of Parylene C coatings to derive their hermeticity [106]. It appears much like a thin acrylic coating on the PCB but the application process is drastically different (and its primary disadvantage). Parylene requires a vapour deposition process. The parylene dimer is heated to 100–150°C under vacuum. This extracts the vapour. This vapour is drawn through a furnace to split the molecules into monomers. In the coating chamber (at ambient temperature) the vaporous components rapidly seek a substrate to condense on the PCB, which causes aggressive conformity to the circuit board components. Finally, the coating chamber is rapidly cooled to remove any residual vaporous parylene and evacuated to a “cold trap” at -90–120°C [107]. There were two major issues with parylene coatings for this application. The first was cost and the second was the limitation it put on future sensing options. As parylene is a hermetic coating, it would not allow sampling of any fluidic properties. While this is acceptable for the current temperature sensing embodiment, it could limit future options.

Bone Cement & Potting Considerations

Other aspects of this solution to consider were three design elements that might be impacted by the cement potting process of this device:

2.5.4 1) Slip conditions and stresses at capsule/cement interface

Bone cement relies on a mechanical interlock at a micro scale rather than adhesive properties to anchor orthopaedic components [79]. There is extensive and conflicting literature examining various implant surface features and the relationship to PMMA bone cement adhesion. Some suggest that beginning with a smooth surface and subjecting it to an acidic passivation process provides superior locking to roughened surfaces as they found air pockets more likely to form between PMMA and rough features [108]. Another study showed that the preparation and contaminant removal on the implant surface is more critical than any surface features [109]. A more recent study shows that a laser peening process to produce roughened grooves significantly increased bone cement adhesion to titanium alloys [110]. Ultimately, it was likely that implant surface geometry would have an impact on the adhesion of the bone cement to the implant, although it was not obvious which surface characteristics would be optimal. It became a constraint to select a material/manufacturing process permitting flexibility in surface condition so this could be easily iterated upon if needed.

2) Elevated cure temperature

Depending on the source, bone cement is expected to heat to 80–86°C during the curing process that occurs during implantation [79] [80]. This constrains allowable materials to ones unlikely to deform at temperatures in this range.

3) Fluidic penetration

PMMA bone cement is intended to completely envelop this implanted sensing package. Over the length of this implant's lifespan, bone cement is suitably resistant to fluidic absorption, so no bodily fluids should ever reach the implant package [111]. Efforts invested in designing a package to be hermetic, near-hermetic or conformal non-hermetic

were likely to be redundant design choices. Regardless, the plausibility of error during installation or PMMA fracture *in vivo* and the objective to reduce any doubts of safety were strong motivations to constrain the material selection process to solutions offering one of these types of encapsulation.

Thermal Insulation of the Sensor

2.5.5 On a separate, but tangentially related thought, a common question received throughout the design process regarded the amount of thermal insulation the package is expected to impart. There was an objective to have the sensor operate with minimal thermal impedance and therefore react quickly to any changes of joint temperature. This was impacted by the geometry and materials selected. However, this objective took relatively low priority for three reasons. First, soft tissues and skin surrounding the joint offer insulation, thermally stabilizing the sensing region, although it is difficult to determine by how much. Second, this device does not require the acquisition time of a usual medical thermometer. This device is meant to log slow changes to mean temperature over weeks at a time. If this capsule were to filter out short fluctuations due to increased friction while the patient ascends stairs or walks in the cold air from their car to the entrance of a shopping mall, it was of little concern. Finally, any efforts taken to assemble a capsule with high thermal conductivity would be stifled by the poor thermal conductivity (0.19 – 0.24 W/mK) of the PMMA bone cement mantle. For reference, the titanium commonly used in implants is approximately 100 times more thermally conductive than bone cement 2.5.6 at 21.9W/mK [112].

Kinematic Loading Expectations

Another area that was originally a major design concern surrounded the effective elastic modulus of the overall package and how it would interact with the bone cement under loading.

A core more resistant to deformation than the surrounding bone cement could cause delamination of the bone cement from the surface of the package and accelerate fatigue failure of the PMMA.

On the other hand, a core much more deformable than the PMMA could result in overall loss of mechanical integrity of the keel component as thin walled features attempted to withstand loads formerly supported by a much larger cross section.

Another issue was providing the appropriate cross-sectional area on the implant casing to support the loading without piercing the PMMA. Initially, finite element analysis (FEA) was discussed to determine how sensitive the structural integrity of the overall keel components would be to changes in geometry and tensile moduli but finding appropriate boundary conditions proved difficult. It was not clear how much axial loading, initially the primary mode of concern, to expect on the bone cement spacer keel. There have been studies on TKA stress shielding and discussions on primary TKA keel/bone interaction but they indicate that keel length outweighs material considerations anyway [113]. There was also extensive information on how the tibial tray component and the femoral bearing surfaces interact as this research was the output of the D'Lima and Orthoload research [55] [114]. Little comprehensive evidence was found on force absorbed by the planed tibial/femoral surfaces vs. transferred loading to interfering surfaces in the intermedullary canal.

Ultimately, an orthopaedic surgeon was consulted. It was determined that the region of the spacer keels containing the sensing packages were unlikely to experience any significant axial loading. There are two reasons for this. The keel of a knee spacer is designed to prevent implant movement about the plane of the articular surface. They anchor the TKA components against sliding transversally rather than absorbing significant axial load, which is instead absorbed by the tibial tray/femoral condyle interface planed perpendicular to the loading. Also, when installing a spacer, the physician avoids packing the intermedullary canal as tightly as a TKA in anticipation of having to remove the spacer a few weeks later. This puts the spacer at greater risk of implant loosening, but this is preferable to difficult extraction procedure when revising to the second TKA and consequently removes most of the material needed to cause any keel loading. A suggestion from this discussion was to focus on avoiding features that might increase the likelihood of the keels separating from the pre-formed articulating components under (the more significant) torsional/transverse loading. A 2014 study by S.

Garcia David *et al.* supports this anecdote through FEA of a primary TKA with a winged keel [115]. With transverse loading of the keel identified as the more pressing concern than axial, the objective to select a material/geometry less likely to result in keel separation.

Another concern involved the spacer extraction procedure specifically. Extraction of a total knee spacer can appear much like carpentry. The consulting surgeon suggested selection of a casing likely to withstand a violent extraction, specifically to protect the battery from becoming ruptured.

Concept Selection & Implementation

2.5.7 As seen from the widely variable discussions featured in Sections 2.5.1–2.5.6, the selection of an encapsulation strategy is a complex decision. Accordingly, an engineering design process was required to select an optimal solution.

To begin, a list of objectives and constraints were generated to discern a preferred solution. Recall, constraints are stipulations that *must* be met for the project to be a success. Objectives are criteria differentiating an optimal solution from a selection of options that have already satisfied the constraints.

There are five constraints identified from the above investigation:

- 1) The encapsulation strategy must isolate the body from potential contaminants.
- 2) It must protect electrical components from bodily fluids.
- 3) The package materials must be compatible with a sterilization method adopted by other FDA approved implants like ethylene oxide, radiation or autoclaving.
- 4) All components of the package must be protected from physical or thermal damage. This is especially relevant to the installation and removal of the implant.
- 5) Although Bluetooth compatibility is not a requirement, the capsule must permit some form of wireless communication to be acceptable.

Additionally, nine objectives were selected to derive the best solution possible:

- 1) The design should permit straightforward iteration to allow an easy pivot if issues were observed with the first attempt. This was of extremely high importance as there were many questions that could only be answered experimentally.
- 2) It would ideally accept alternative sensing modalities besides temperature with ease. This was of medium importance as although future applications for this device were envisioned, it was not pivotal to the success of this thesis project.
- 3) The overall design and manufacturing strategy should aim to reduce project costs if possible. While important for a commercial product, at the prototype phase, low cost was more of an advantage than a necessity.
- 4) Ideally the selected design would permit Bluetooth communication as this is the preferred wireless communication strategy. The circuitry and programming had already been designed/manufactured by this stage, switching communication strategies would have been a major inconvenience so this was a high priority objective.
- 5) The materials, manufacturing, and sterilization method suggested should not be novel to the medical implant space to streamline the regulatory process. There was a goal to have the proposed design backed up by precedent. While not essential for a functioning solution as unconventional projects do sometimes succeed, it was extremely advantageous to avoid this.
- 6) The design chosen should offer a clear, streamlined, pathway to a functioning minimum viable product. This project had an 18 month design runway from ideation to validation, which did not permit extended lead time for specialized manufacturing. This was high priority for project success.
- 7) The materials selected and overall geometry should ideally provide relatively fast thermal response to changing conditions. Although certainly a positive quality, for the reasoning discussed previously, this was not a high priority objective.

- 8) The capsule design should avoid the possibility of keel separation from the tibial tray or femoral condylar geometry. While most envisioned solutions would not compromise this junction, it was still important to device success. Note that even passive spacers do fail at this junction without catastrophic consequence, but it is still to be avoided.
- 9) There was a goal to design this device to use readily available materials and processes to avoid a production bottleneck. Although, for testing purposes a similar material could be used without dire concern.

With these in mind, several potential solutions were generated:

- 1) Hermetic titanium unibody with pass through design

This design is most analogous to other commercial devices like pacemakers. It would consist of the electronics being secured inside a hermetic titanium enclosure made of two parts electron beam welded together. It would require a passthrough and external cap somehow adhered to route the antenna.

- 2) Non hermetic, windowed titanium superstructure with silicone encapsulant

Without dependence on a hermetic seal, this device would not be a conventional “capsule” and would not require helium leak testing. A titanium shroud could be locally 3D printed and used to a) protect the silicone encapsulated circuitry inside from installation/extraction procedures and b) to support the implant/PMMA interface. Windows in the superstructure would permit a variety of radiofrequency transmission modalities.

- 3) Near hermetic, carbon fiber reinforced PEEK capsule

This concept follows the work of Nathaniel Dahan *et al.* who showed the viability for a PEEK capsule for short term implantable devices [92]. This capsule would be a two-piece design that threads together before sealing by a thermal plastic weld. This material would provide easy RF transmission and has excellent mechanical properties for the reduction of stress shielding.

4) Near hermetic, titanium superstructure with polyethylene cap

The final generated concept involves a titanium superstructure similar to the second concept, but instead of relying on silicone for a non-hermetic conformal coating, it would incorporate a polyethylene (or similar material) cap. This would retain the compact titanium superstructure while avoiding the additional complication of a passthrough and an electron beam welding process. However, it does raise its own concerns in lacking precedent and a challenging sealing process.

First, the generated concepts were compared against the design constraints in a go/no-go screening seen in Table 2.2. Any solutions that did not pass all constraints would not be eligible for consideration as they would fail to solve the problem.

Table 2.2—Go/No-Go screening of encapsulation strategies. This is an engineering selection tool used to filter potential solutions.

	Hermetic Capsule	Non-Hermetic Superstructure w/ Silicone	Near Hermetic PEEK Capsule	Near Hermetic Ti/Polymer
Demonstrated ability to isolate the body from contaminants	Go	Go	Go	No Go
Protect electrical components from fluids	Go	Go	Go	Go
Compatible materials for an FDA approved sterilization method	Go	Go	Go	Go
Protect internals from physical/thermal damage	Go	Go	Go	Go
Permit some wireless communication	Go	Go	Go	Go
Result:	Pass	Pass	Pass	Fail

Seeing three viable options, the objectives were assigned a relative weight out of 1–3 with 1 being a “low priority” objective and 3 being a “top priority”. In an engineering decision matrix (Table 2.3) each solution’s ability to meet the objectives was also ranked from 1–3.

Table 2.3—Engineering decision matrix for optimal encapsulation strategy. This is a secondary design tool to select the optimal solution from a list of feasible ones.

	Objective Weight	Hermetic Capsule	Non-Hermetic Superstructure w/ Silicone	Near Hermetic PEEK Capsule	Near Hermetic Ti/Polymer
Permit straightforward design iteration	3	1	3	3	
Afford future flexibility to alternate sensing modalities	2	2	3	3	
Reduce costs	1	1	2	2	
Permit Bluetooth communication	3	3	3	3	
Supported by regulatory precedent	3	3	2	1	
Reduce time to minimum viable product	3	1	3	2	
Permit faster thermal sensing response	1	2	2	1	
Avoid features that increase the likelihood of keel separation	3	2	2	2	
Be manufacturable through readily available materials	2	2	3	1	
Score:		41	55	45	

Following this investigation, it was clear that the optimal solution was the non hermetic option utilizing a titanium superstructure and silicone conformal coating/suspension. One takeaway was that several other strategies could have also been feasible in other circumstances. Access to the materials/equipment locally with ADEISS and previous in-house medical silicone molding projects made the selected solution ideal for a rapid turnaround time.

In implementation, the design began by considering the geometry of the circuitry and battery. It was desirable to maintain at least 1 mm of silicone on all sides to account for any assembly misalignment as it would be unacceptable to have the circuit board short against the conductive casing. Then, after the internal geometry of the casing was determined, several variations were manufactured, and a wall thickness was chosen offering a good balance of deformation resistance, reduction in volume, and permitted experimentation with various textures to improve PMMA integration. Leveraging the capabilities of additive manufacturing, an initial surface geometry was chosen that offers many micro dimples for the PMMA to purchase with no sharp corners, which might prevent stress raisers and avoid premature fracture and a completely smooth alternative, seen below in Figure 2.5.



Figure 2.5—Two titanium superstructures, pictured with the intentionally textured pattern (left) and the smooth alternative (right).

While the regions surrounding the battery remain solid titanium, the area of the titanium superstructure surrounding the Bluetooth antenna was designed with windows to encourage unimpeded RF transmission.

Silastic MDX-4210 was the selected encapsulant for the minimum viable product. It is manufactured by Dow Corning and is advertised as a short term implantable electronics silicone encapsulant.

Assembly was an 8 step process:

- 1) The exterior of the titanium superstructure was masked off to prevent leakage through the RF windows and maintain exterior cleanliness.
- 2) The MDX-4210 was mixed according to manufacturer's instructions and degassed at 710 mmHg at ~22°C for 30 minutes.
- 3) Approx. 5 mL of MDX-4210 was deposited into the bottom of the superstructure.
- 4) Using a custom fixture, the battery and circuit board were suspended centrally within the superstructure (Figure 2.7) and the assembly was further degassed at 150 mmHg for 15 minutes to encourage silicone conformity to the lower half of the circuitry.
- 5) The first silicone stage was then permitted to cure.
- 6) Step 2 was repeated.
- 7) With the circuitry partially enveloped in/supported by silicone, the suspension fixture was removed (Figure 2.8) and a second stage of MDX-4210 was poured to fill.
- 8) The assembly received a final degassing procedure at 150 mmHg for 15 minutes before being allowed to cure thoroughly for 72 hours. Seen curing in Figure 2.9.

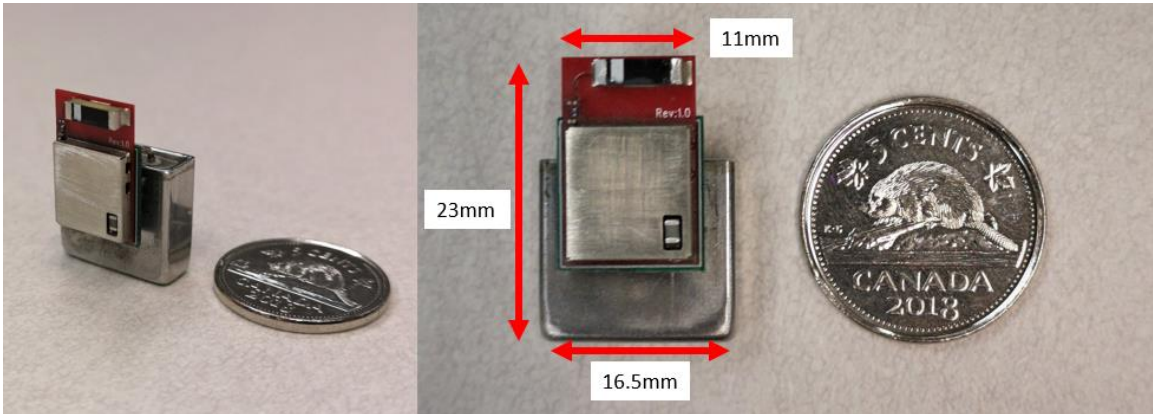


Figure 2.6—Completed instrumentation package including MCU, sensor and battery.

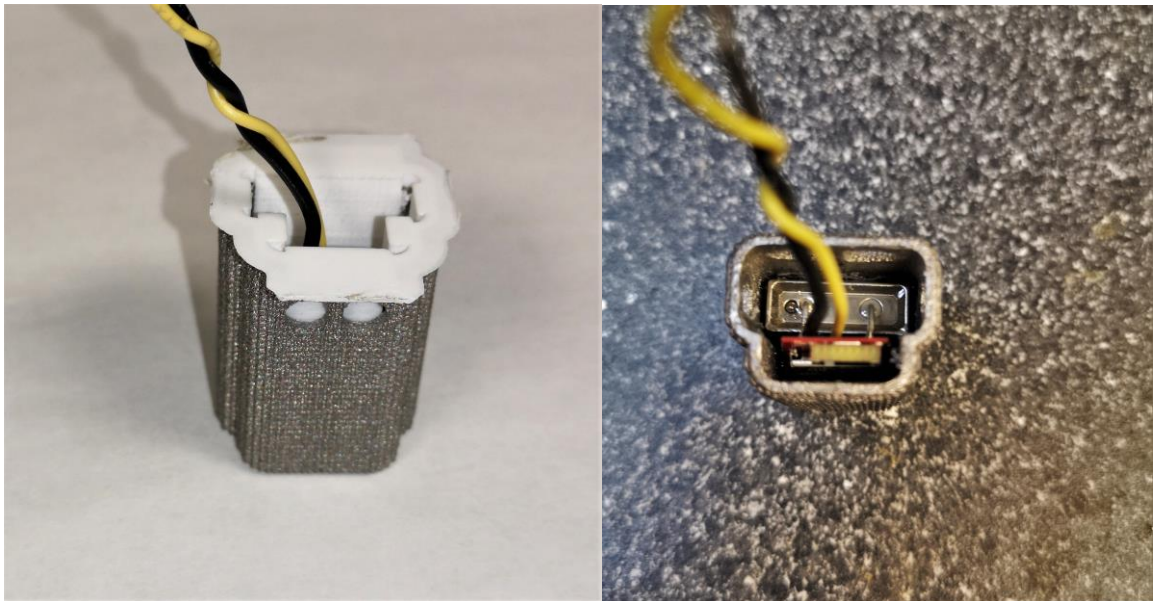


Figure 2.7—Custom fixture is installed, suspending instrumentation package for the first silicone stage.



Figure 2.8—The fixture is removed following Step 5 with the package suspended by cured first stage.

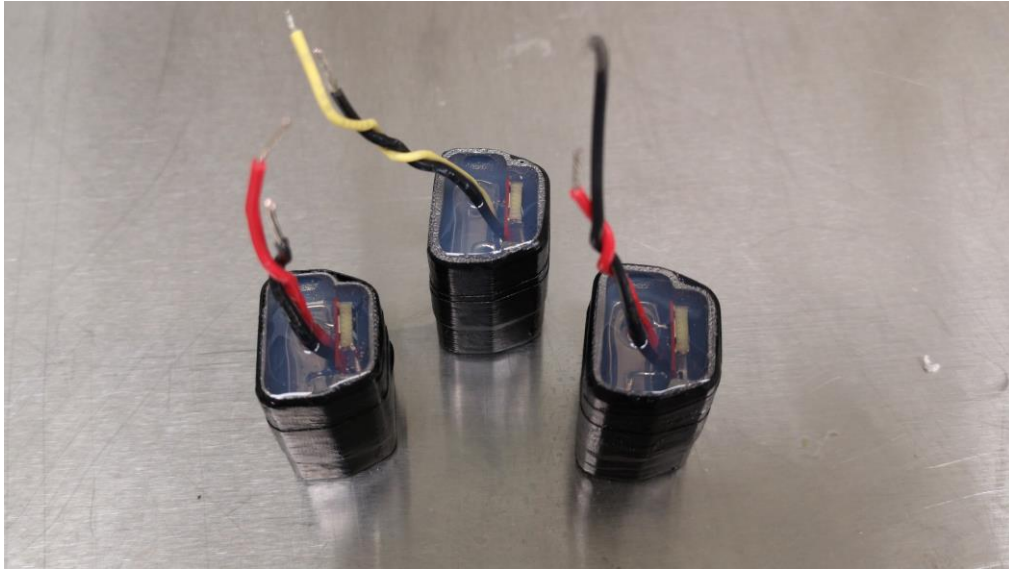


Figure 2.9—Sensing packages in Step 8 of assembly depicting the second silicone stage curing in vacuum chamber.

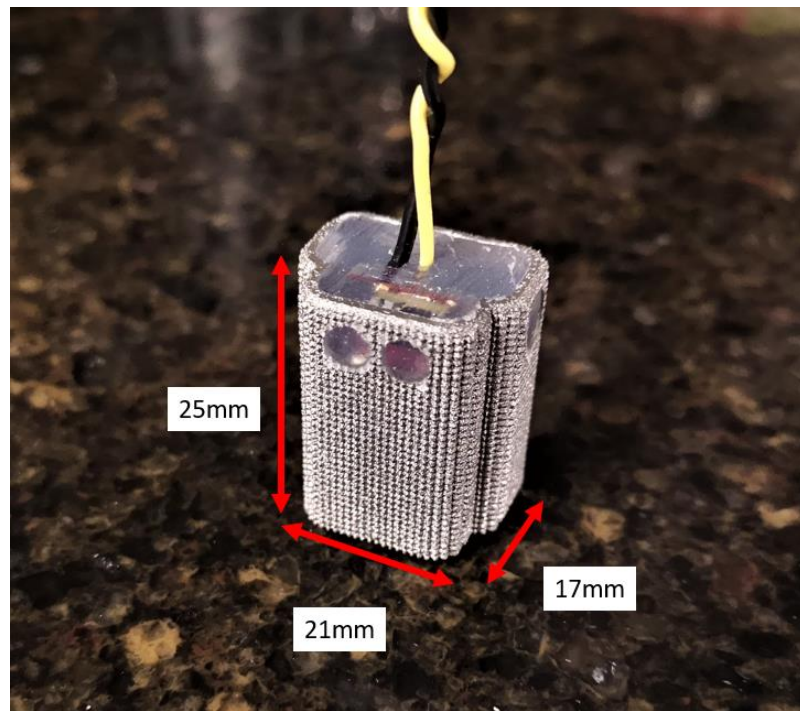


Figure 2.10— Depiction of the prototype encapsulated system. The protruding wires are only for prototype purposes and clipped before use.

In to conclude this chapter, several key technical elements of the proposed sensing package have been examined in the context of an engineering design process. One major learning from this process should be to design for failure. Redundancy where feasible, especially where safety is concerned and a clear “pivot” pathway if one component of the technology requires iteration to avoid overhaul of the entire project. Deliberate effort to design accordingly meant a functional prototype, closely resembling a final embodiment, was ready for cadaveric study within 18 months of idea inception despite some technical challenges.

3 Chapter 3—Experimental Evaluation of Prototype

Having completed the design process and assembly of a prototype, a series of evaluations were performed to inform the researchers of the device performance. This chapter describes the experimental evaluation of the instrumented knee spacer prototype, specific to temperature sensing for the application of infection monitoring in knee arthroplasty.

Introduction

3.1 Persistent infection of total knee arthroplasty is an issue resulting in serious long term mobility challenges, exorbitant healthcare expenses, and occasionally, morbidity for >20,000 North Americans annually [18] [24]. Primary infection management is handled relatively well, with only 1–3% of total knee arthroplasties (TKA) requiring revision due to infection [3] [4] [5] [21] [22] [23]. The gold standard treatment in these cases in North America is a two-stage revision. This involves the surgical removal of the infected implant and temporary installation of an antibiotic bone cement knee spacer for a period of 6–10 weeks while the infection is treated. When convinced the infection is cleared, the surgeon will perform a second procedure to remove the antibiotic spacer, remove any necrotic tissue, and install the permanent “revision” knee replacement. Unfortunately, this procedure has a much lower success rate with ~15% of revision patients maintaining infection after this extremely costly procedure [6]. A strong possibility is that many of these cases are persistent infection that were not completely cleared at the antibiotic spacer phase before final revision was completed. Further, when considering common evaluation methods, the most common tests for a primary infection plummet in reliability as soon as antibiotic treatment is started, or dynamic amounts of swelling are present [35] [36].

When a measured condition is relatively stable (pre-treatment), low frequency sampling is acceptable. However, the two-stage revision process is turbulent for the joint space, the trauma of surgery coupled with extensive local and systemic antibiotic or anti-inflammatory treatment results in dynamic fluctuation of common infection markers [35]. Taking temperatures, blood or serum samples only on occasion, when the patient visits the clinic, may be insufficient to form a comprehensive picture of the infection status, and

may contribute to the comparatively poor re-infection rate post revision. The same logic is applied to sampling rates in other biometric tracking. Lower frequency sampling is considered suitable to capture movement patterns of walking than a more dynamic activity state like running [116]. Therefore, diagnostic tools for infection status specifically designed for the dynamic nature of infection symptoms during treatment would provide physicians with more a representative dataset to improve treatment pathways.

Instrumented implants are devices surgically installed inside the body designed to collect some information regarding biological or kinematic status. Many of these implants combine instrumentation with other features such as an output transducer or wireless transmission interface. Some examples would include a pacemaker, a gastrointestinal stimulator, or a cardiac monitor. There has been some research performed regarding the use of instrumented implants in orthopaedics, especially for kinematic analysis, but so far there are no commercial products on the market [54] [55].

The proposed solution is intended to leverage low power embedded electronics to instrument the antibiotic spacer with temperature sensing and logging capability. This device would passively collect and store temperature readings directly from the implant site. When the patient visits the clinic, the physician will be able to wirelessly access logged information to observe trends in the joint space temperature over time.

Within this report, two hypotheses are tested. First, the sensing package developed will offer sufficient sensing, power management, and communication performance to be feasibly used for the application of infection diagnostics in a knee spacer. Second, the integration of the proposed instrumented package within a bone cement spacer is unlikely to cause mechanical or logistical issues during installation or use.

Methods

Study Design

In order to test these hypotheses, this study was divided into two stages. The first
3.2 rigorously evaluated the sensing performance of the developed instrumentation package
3.2.1 using a custom PID controlled temperature chamber while the second stage utilized a
cadaver knee and mechanical loading apparatus to demonstrate *in situ* device
performance within a simulated environment.

The first components of this research were benchtop evaluations specifically tailored to
examining three parameters determined critical for device success: precision and
accuracy of sensing in addition to the overall thermal time constant. Precision and
accuracy tests were performed using paired correlative sampling against a reference
temperature sensor while subjected to identical conditions. This maintains consistency
with prior art in the temperature sensing/characterization domain [117] [118]. The
thermal time constant was evaluated using an 8L stovetop water bath.

The second components were performed in an $n = 1$ cadaver trial. These were binary
evaluations of three parameters. First, could the device establish successful wireless
connection to a mobile device while impeded by the knee tissues? Second, could the
implant collect and store temperature readings while the knee is subjected to anatomical
loading? Third, would the introduction of the proposed instrumentation package cause
mechanical failure of the PMMA spacer under representative loading conditions?

Telemetric packages were molded into the keels of both a tibial and femoral knee spacer
and surgically implanted to a cadaveric specimen. A kinematic force loading apparatus
was used to apply loading representative of what a PMMA spacer might be subjected to
in vivo. Concurrently, Bluetooth communications were tested, collection of data was
observed. After loading cycles were performed, the specimen was debrided to inspect for
spacer fracture, and micro CT scanned to examine the possibility of internal fracture
propagation.

Specimen Design, Manufacture, and Inspection

3.2.2.1 Specimen A

This specimen was an unencapsulated version of the final device, electrically tethered to a CC2650 LaunchPad (Texas Instruments, TX, USA) for power and real time data transmission. It was capable of temperature sensing and serial transmission of environmental conditions. The custom circuit board was printed by PCBWay (Guadong, China), electrical components were purchased from Digikey (Digikey, MN, USA), hand soldered/assembled in house using a WS81 soldering station (Weller, Baden-Württemberg, Germany) and generic hotplate. Functionality was verified using a diagnostic program written in the Sensor Controller Studio (Texas Instruments, TX, USA).

3.2.2.2 Specimen B

This device is an encapsulated version of Specimen A. This device utilized a 3D printed Ti6Al4V ELI-0406 (Renishaw, Staffordshire, England) superstructure manufactured by ADEISS (ADEISS, ON, Canada). This casing was designed to protect the sensing equipment from loading or impact and to mechanically integrate with bone cement. The circuitry was suspended in a Silastic MDX-4210 (Dow Corning, MI, USA) implant grade silicone electrical encapsulant for contaminant separation according to manufacturer protocols. The entire package was coated in ~5 mm of Simplex antibiotic bone cement (Stryker, NY, USA). Assembly was performed in house. Following the assembly operations, sensing functionality was verified as for Specimen A and tested for waterproofing through overnight immersion. This device was designed to permit real-time temperature capture and transmission from within a package with similar thermal insulation to an in-vivo application for characterization of a thermal time constant. A visual representation of this variant is depicted below in Figure 3.1.



Figure 3.1—Specimen B, an encapsulated sensing package, which has been potted in bone cement to demonstrate similar thermal insulation characteristics to the implanted embodiment.

3.2.2.3 Specimens C1 & C2

The final specimens were duplicate, untethered versions of Specimen B, with the omission of bone cement. This version was fabricated for use in the cadaveric trials and closely represents the final embodiment of the proposed device. These specimens were programmed to take temperature measurements at 15 second intervals. Specimens C1 and C2 were powered by onboard 350 mAh lithium thionyl chloride batteries. The LTC-3PN-S2 (Eagle Picher, OH, USA) was used for testing purposes but could be replaced by the ISO 13485 certified variant (LTC-3PN-M1) for *in vivo* use. Note that due to (resolved) software issues, a physical reset mechanism was required that protruded from the silicone encapsulant and was clipped off prior to specimen use. At this stage, the entire device should be compatible with ethylene oxide sterilization although it was untested and unnecessary for this study [119]. Functionality was verified using a custom Bluetooth handshaking protocol initiated from a mobile phone.

CAD Workflow, Manufacture, and Programming

The circuitry for all specimens was laid out in EAGLE (v9.6.2, Autodesk, CA, USA).

3.2.3 The PCB parameters were intentionally selected for the application (dual layered, 0.4 mm thick, FR-4, immersion gold plated contacts) and manufactured by PCBWay (Guangdong, China).

Physical design work was performed in Solidworks (2018 & 2019, Dassault Systèmes, Versailles, France). Solidworks was also used to mesh the STL files of the casings provided to ADEISS (ON, Canada) for manufacturing.

Programming of the temperature controlled chamber was performed in Arduino Code Composer (v1.8.8, Arduino, Turin, Italy). Programming of the designed implant was performed in Code Composer Studio (v8.3.1, Texas Instruments, TX, USA) and Sensor Controller Studio (v2.4.0.793, TX, USA).

3.2.4 Testing

3.2.4.1 Thermal and Sensing Characterization

3.2.4.1.1 Sensor Precision Test

To facilitate characterization of temperature sensing performance, a custom apparatus was constructed so temperature conditions could be driven to a programmable curve over extended periods of time. This apparatus consisted of an insulated chamber with a resistive heating element and a sensing array of three MCP9808 automotive grade temperature sensors (Microchip Technologies, AZ, USA). Over the relevant 35–40°C sensing range the MCP9808 reports a typical accuracy of $\pm 0.25^\circ\text{C}$ and a maximum $\pm 0.5^\circ\text{C}$. Critically, the MCP9808 is precise to 0.0625°C [67]. The system was managed by a Feather M0 (Adafruit, NY, USA) using a custom program based on the proportional, integral, derivative control scheme.

The temperature controlled chamber was programmed to maintain 35°C for an indefinite period. Specimen A was suspended centrally within the chamber. After a 1 hour heat soak, the 10 minute test was started. Sampling was performed at 200 ms intervals and

divided into 5 sample non overlapping windows. The median of each window represented one “reading”. The 200 ms sampling rate was chosen because this is the intended “in use” frequency for this device. The number of samples per window is inversely correlated to the observed precision (approaching a lower asymptote), 5 sample windows were likely to yield acceptable ($< 0.2^{\circ}\text{C}$) sensor precision based on similar literature characterising temperature sensors and some preliminary evaluation [117] [118]. The length of the test was chosen to yield > 100 independent readings affording a 95% confidence interval on the standard deviation, where standard deviation is equivalent to sensing precision [120]. The ability to maintain a temperature inside the controlled chamber for an indefinite period easily permitted gathering $> 100,000$ readings. This allowed several repetitions of the test and experimentation with various window lengths.

3.2.4.1.2 Sensor Characterization and Accuracy Test

The second thermal test determined both the characteristic equation relating unitless analog sensor readings to tangible values in $^{\circ}\text{C}$ and to evaluate the sensing accuracy of Specimen A relative to a reference sensor. Specimen A was suspended centrally within the chamber. After a 1 hour, 35°C heat soak, the test began. The chamber was programmed to hold stable temperatures at 0.25°C increments for 10 minute periods stepping from $35.5\text{--}40^{\circ}\text{C}$. The readings were captured using the same 5 sample, non overlapping windows at 200 ms frequency. Values collected during the transient period between temperatures were discarded to remove potential error caused by different thermal time constants between the reference and experimental sensing boards. Thermal rise time was characterized separately. A paired correlative sampling technique was applied as depicted by other similar characterizations [117] [118]. The readings were regressed against the reference sensor readings integral to the PID controlled chamber to generate a characteristic equation. This procedure was repeated twice to provide a “calibration” dataset and a “validation” dataset. The characteristic equation generated from the calibration set was used to regress the validation numbers. Accordingly, the root-mean-squared error of the validation set relative to paired correlated samples across the entire sensing range represented the sensor accuracy. Further, hysteresis was considered by evaluating the mean difference between samples collected at each

temperature while the chamber was sequentially increasing in temperature versus while the chamber was sequentially decreasing in temperature.

3.2.4.1.3 Thermal Equilibrium Test

Using an identical sampling protocol to the previous analyses, Specimen B was permitted to thermally stabilize for a period of 5 hours at room temperature ($\sim 21^{\circ}$). For this test, a large volume water bath (8L) was utilized as is common to other experiments designed to ascertain a thermal time constant of an unknown device [121]. The water bath was heated to a randomized temperature between 35–55°C and permitted to reach thermal equilibrium over a 5 hour period. Data logging then began and 100 readings were taken at room/initial temperature before submersion in the water bath. Timestamped values were collected until readings suggested Specimen B had reached thermal equilibrium with the water bath at the “final” temperature. This process was repeated for a total of 15 trials. Following all trials, each dataset was normalized between 0 (initial temperature) and 1 (final temperature) before superimposition of all curves on a single plot. Finally, a thermal rise coefficient was measured along with 95% confidence bounds. Note the comparatively large volume water bath was assumed to be thermally unaffected by the submersion of the cooler specimen and the submersion process was assumed to be instantaneous as reflected in previous literature [117] [118].

3.2.4.2 Cadaveric Investigation

3.2.4.2.1 Cadaver Preparation

After a medial parapatellar arthrotomy was performed to expose the knee joint, Triathlon (Stryker, NY, USA) instruments were utilized to perform the bone cuts. The patella was everted, and the fat pad, ACL, PCL, and meniscus were resected. Using an intramedullary guide, the distal femoral cut was made at 10 mm depth and at 6 degrees to the anatomic axis. The anterior and posterior cuts based on measured resection principles resulted in appropriate bone resections. The proximal tibial cut was made using an extramedullary guide, at 9 mm of depth based on the lateral tibial plateau and 3 degrees of slope.

After checking the balance, the anterior and posterior chamfer cuts were performed. Trialing demonstrated a balanced knee after appropriate sizing. Simplex antibiotic bone cement (Stryker, NY, USA) was used to cement Specimens C1 and C2 into the femoral notch and tibial intermedullary canal respectively. Preformed InterSpace (Exactech, FL, USA) articulating spacer components were cemented in, with removal of excess cement. Figure 3.2 shows the general location of where both sensing packages would reside in the knee before bone cement application. Implementation seen in Figure 3.3 and Figure 3.4, which depict the knee with the installed spacer in flexion and extension respectively. Finally, the mid femur, mid tibia, and mid fibula were skeletonized and cemented into polyvinyl chloride pipe for mounting to the anatomic motion simulator.

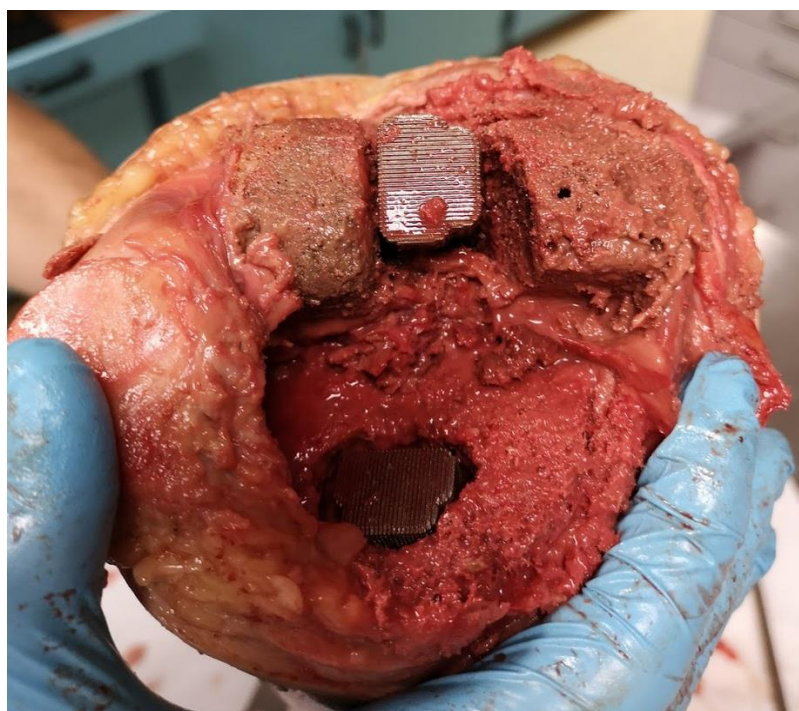


Figure 3.2—Approximate location of the Specimens C1 & C2 within the cadaveric specimen prior to bone cement application. The femur is above, while the tibia is below.

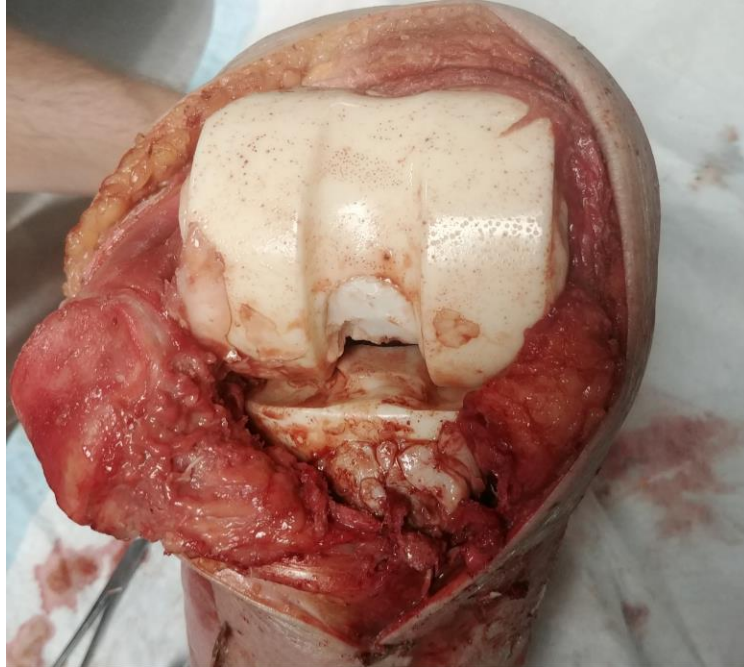


Figure 3.3—Cadaveric knee featuring InterSpace articulating components and novel instrumentation as seen in flexion

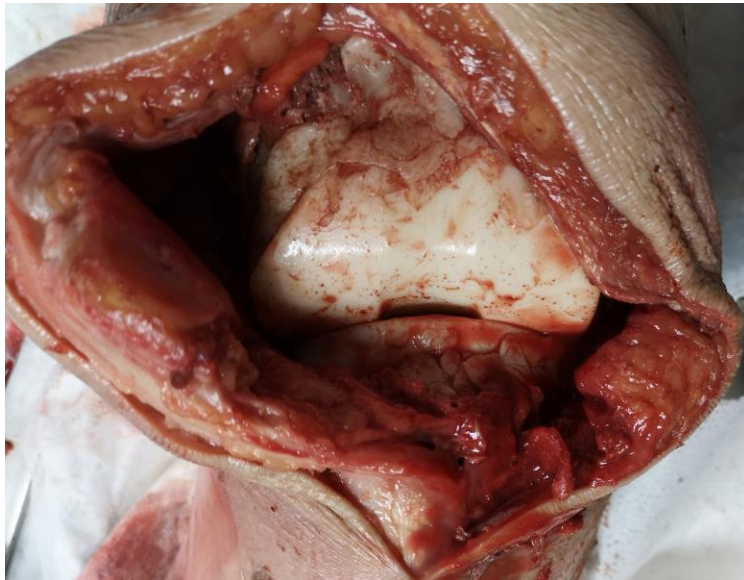


Figure 3.4—Cadaveric knee featuring InterSpace articulating components and novel instrumentation as seen in extension

3.2.4.2.2 Anatomic Loading Profile

The VIVO 6 Degree of Freedom (DoF) joint motion simulator (Advanced Medical Technologies Inc., MA, USA) was used to apply anatomically representative loading to the knee/spacer. The mounting and implementation can be seen below in Figure 3.5. This device was capable of loading both the femur and tibia independently. It permitted anatomically correct, axial tibial rotation throughout each “stride”. The system was closed loop with forces being measured by a 6 DoF load cells attached to the tibia. Setup of the system was performed in accordance with previous literature [122]. The selected loading profile included reduced magnitude (~500 N) loading for 30,000 cycles, cycled at 0.5 Hz, with a 60° flexion range about the joint axis and permission for 20° rotation about the tibia longitudinal axis.



Figure 3.5—Depiction of the cadaveric knee with the installed articulating spacer and sensors mounted to the VIVO apparatus for the purposes of anatomic loading.

3.2.4.2.3 Radio Frequency Penetration Check

This test was performed using both a Huawei P20 Pro (Huawei, Guangdong, China) running Android 9.1 and a 2019 Apple iPad (Apple, CA, USA) running iOS 12.1. Both devices were running LightBlue (Punch Through, CA, USA), a free software designed for low level Bluetooth communication. Immediately before and after the “Cadaver Preparation”, Bluetooth connection was established with both specimens (C1 and C2) from a distance of 30 cm. Signal strength was recorded as reported on both mobile devices, for both specimens, at both time points.

3.2.4.2.4 Data Collection During Anatomic Loading Check

This test was intended to demonstrate the ability of the implant to collect/transmit meaningful data while installed in an antibiotic knee spacer being subjected to anatomical loading. Testing was performed using a Huawei P20 Pro (Huawei, Guangdong, China) running Android 9.1 and the LightBlue (Punch Through, CA, USA) Bluetooth sniffer. Following the completion of the Anatomic Loading Profile, a Bluetooth connection was established with one of the implanted specimens and commands were issued to wirelessly offload the collected temperature readings from within the implant taken during the loading cycle. The same procedure was attempted for Specimen C2. The values were then exported and checked for coherency.

3.2.4.2.5 Mechanical Integrity Check

This test was intended to examine if the knee spacer demonstrated any modes of obvious mechanical failure due to instrumentation integration. Limited literature is available on the topic of anatomic spacer loading. Two examples used a 5000 cycle protocol with increasing force from 400–1200 N although this protocol was designed to identify modes of failure rather than replicate real usage to see if failure would occur [123] [124]. This team selected an approach that might replicate real world usage. The loading profile involved 30,000 cycles of net 500 N loading as a resultant component of force about the medial/lateral, anterior/posterior, and vertical axes. Two stage revision patients will likely only be walking with a walker or cane for the first 4–8 weeks following surgery, and with limited loading for the next several weeks, hence the reduced loading profile. Patient

activity information for the weeks immediately following knee replacement surgery is limited, but likely to be greatly reduced [125] [126] [127]. Primary (uninfected) TKA patients take an average of 5278 (SD 2999) steps/day preoperatively [128]. The testing cycle count was selected to reflect a generous 25% of preoperative step rate, every day for ~8 weeks, a reasonable amount of time to revision [129] [130].

Following the anatomical loading cycle, the cadaveric specimen was skeletonized and visually inspected for tibial tray separation or other obvious fracture. Then both the femoral and tibial knee regions were micro CT scanned at 154 μm resolution, 120kV tube voltage, and 20 mA tube current. The images captured were evaluated for any internal cracking or stress fractures around both specimens (C1 and C2). This radiographic analysis was valuable because it is non-destructive. Observations made essentially involve an inspection of the boundaries where the bone cement mated with the encapsulated electronics and the bone. Telling features include voids/cracking, which are indicated by darkened regions.

The last element of this investigation involved a manual debridement process to extract the implants. This was undertaken after imaging with the understanding that damaging the implanted spacer in ways additional to the intended testing was possible. It was still valuable for visually confirming the findings from the non-destructive imaging above.

3.2.5

Statistical Analysis

All datum handling throughout this investigation was performed in either Excel (365 Pro Plus, Microsoft, WA, USA) or MATLAB (v2018, MathWorks, MA, USA). The Curve Fitting App within MATLAB was used for datum regression and prediction boundary tabulation for all of three of the thermal and sensing characterization tests. Final plots for presentation were generated in Prism (v8.4.2, GraphPad, CA, USA).

Results

Specimen Manufacturing

Specimens A and B were manufactured as planned and performed as expected during 3.3 testing.

3.3.1

For Specimens C1 & C2, after external power wires were removed, the batteries were installed, and communication functionality was confirmed. An issue with the ability to wirelessly reset the device was observed. Hardware level reset was required to rectify the issue. This resulted in the need for two wires to protrude from the silicone so the device could be reset immediately prior to implantation during the cadaveric study.

Approximately three hours following implantation, communication was lost with C1, the tibial sensor. Post study dissection and analysis revealed a short circuit where the protruding hardware reset wires had permitted fluids to condense on the circuit board surface (Figure 3.6). C2, the femoral sensor performed properly for the duration of the test and continued to do so for several weeks following the test.

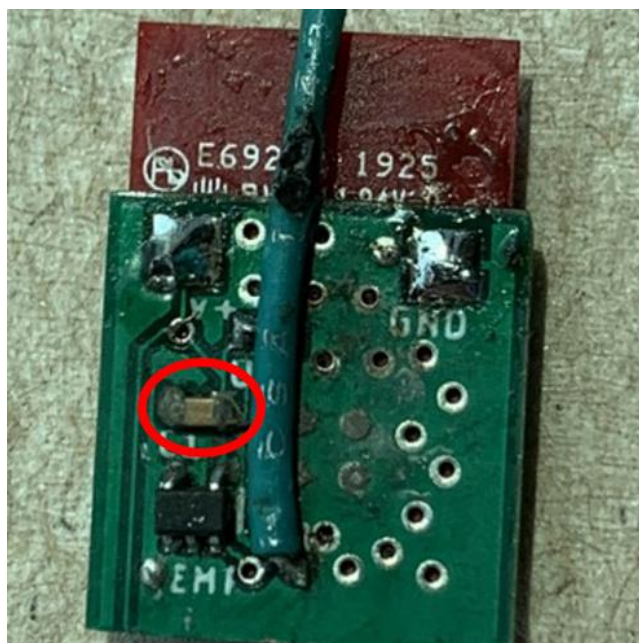


Figure 3.6—Retroactively identified oxidation on decoupling capacitor as a result of fluidic condensation during testing and delay before debridement.

Sensing Precision

3.3.2 The sensor precision was measured at a constant 35°C temperature using 100 consecutive 5 sample, averaged, non overlapping windows. Precision was recorded to be 0.0928°C, or 0.09°C when considering significant figures, with 95% confidence by calculating the standard deviation of the 100 measurements captured at steady state condition.

Sensor Characterization, Sensing Accuracy & Hysteresis

3.3.3 Sensor characterization was performed on the calibration dataset. This equation regresses the arbitrary units read from the experimental sensor analog output to a useful value in °C as determined from the reference sensor's paired correlative data points. This regression, performed on the calibration data set, can be observed in Figure 3.7. The characteristic equation was $T[°C] = 0.3411 \times \text{Measurement} - 54.55$ with 0.995 R-squared correlation. Sensor accuracy was tabulated by applying this characteristic equation to the validation dataset and measuring the root-mean-squared error, producing $\pm 0.24°C$ accuracy with 95% confidence throughout the sensing range.

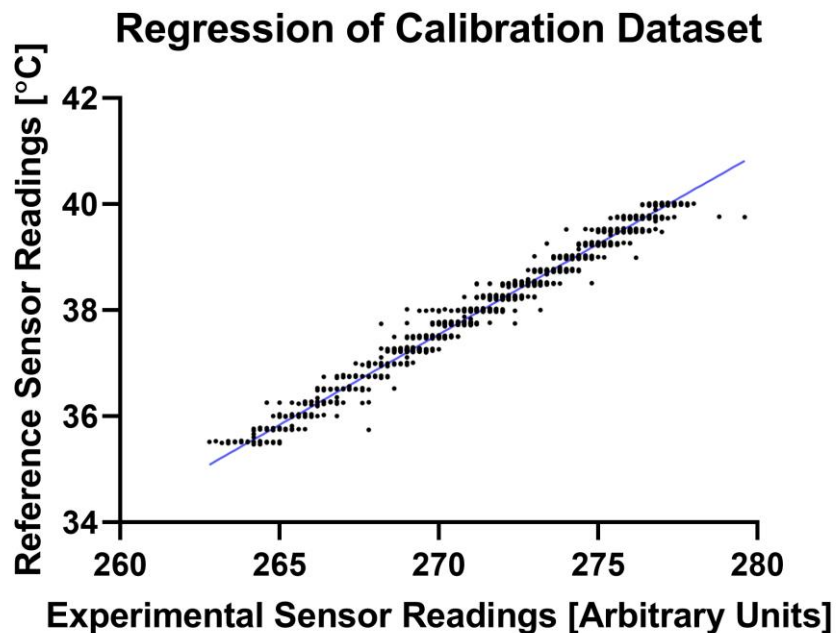


Figure 3.7—Graph depicting the comparison of the reference sensor readings vs. the experimental sensor readings and visualization of the characteristic equation of the calibration dataset.

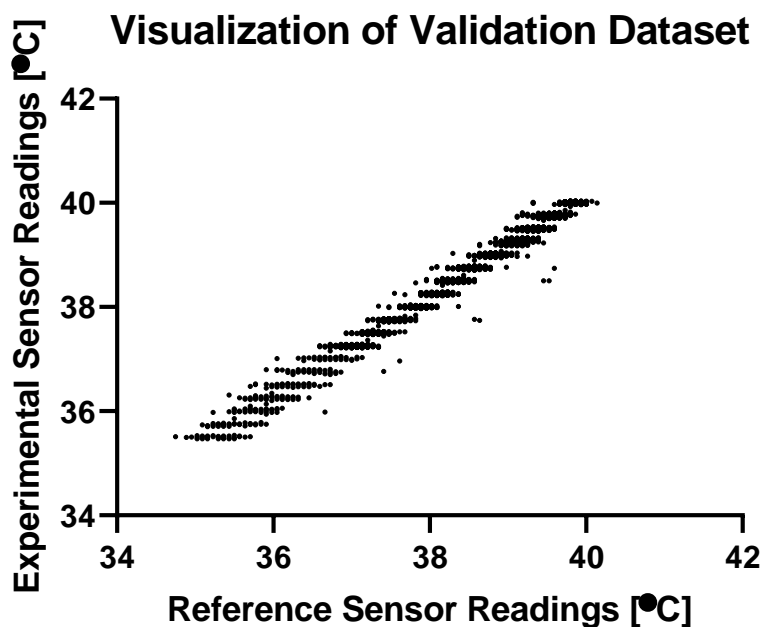


Figure 3.8—A visual representation of the validation dataset. This depicts the relationship between the experimentally captured values regressed to degrees Celsius and their paired samples from the reference sensor.

In Figure 3.8 the validation dataset is displayed. On the y axis are the experimental sensor readings (as in Figure 3.7) but on the x axis the reference sensor readings have already been converted to degrees by the characteristic equation found from the calibration.

Hysteresis was also observed in the validation data set to have a mean value of -0.001°C across the entire $35.5\text{--}40^{\circ}\text{C}$ sensing range with a SD of 0.007°C . Each bar on Figure 3.9 below represents the difference between the average recorded temperature while the chamber was maintained at a given condition as the temperatures were increased, minus the equivalent value during the descending phase of the test. Each “step” consisted of $N=350$ sequential measurements. It should be noted that the largest individual hysteresis values observed were still well within the magnitude of the previously measured precision, so it is difficult to interpret this result as anything more than noise.

Hysteresis Observed at Each Temperature Step

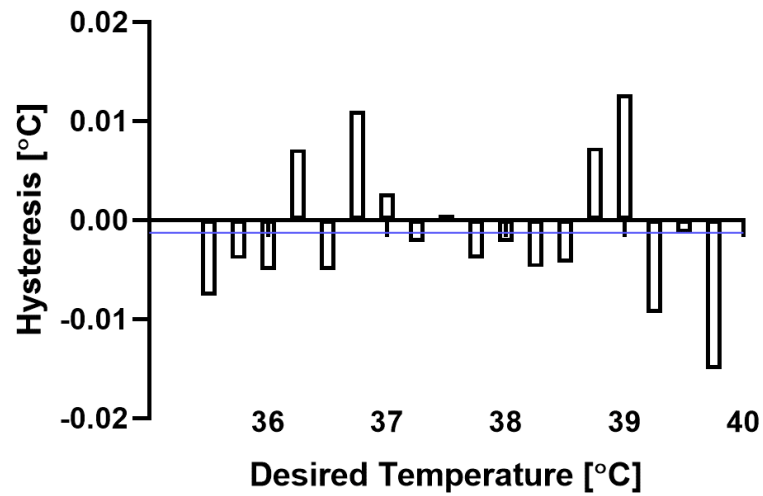


Figure 3.9—Graphical depiction of the hysteresis observed at each temperature step. The mean value (-0.001°C) is displayed in blue.

Thermal Equilibrium & Insulation

3.3.4 The thermal time constant of the cemented instrumentation package was measured. Note that the thermal time constant is a measurement of time between the moment of temperature “disturbance” (immersion in heated water bath) to when the system reaches 63.2% of the equilibrium temperature [131]. The result was $\tau = 262.67 \pm 4.56$ seconds was determined empirically and an associated settling time of $T_s = 1027.57 \pm 17.84$ seconds (~17 min) was tabulated assuming a lumped thermal capacitance model. Figure 3.10 below displays the repeated trials superimposed and the dotted lines highlight the point where the thermal time constant may be measured.

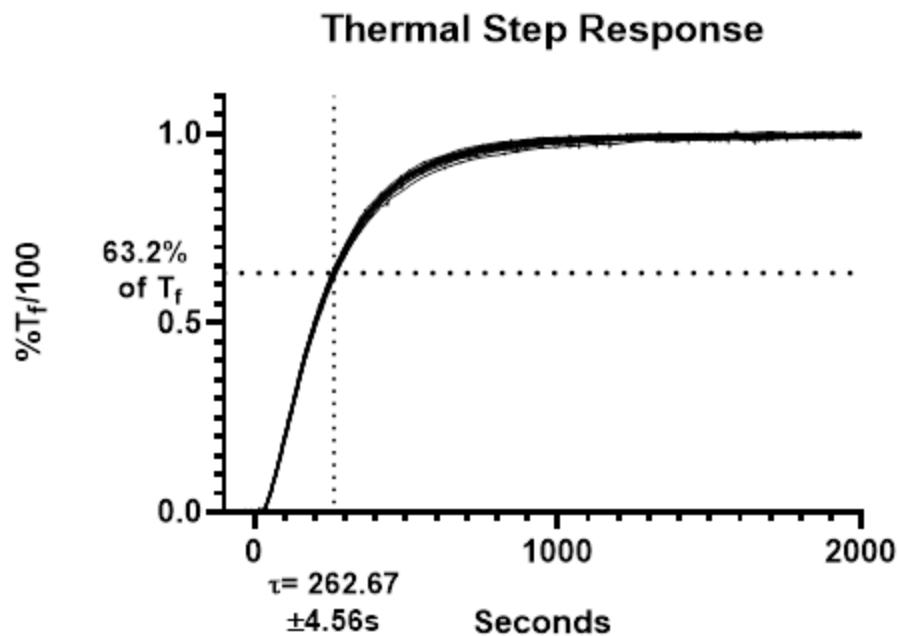


Figure 3.10—Graph of "Thermal Step Response" with 15 repeated trials of package temperature rise superimposed. Dotted lines highlight the average amount of time required for 63.2% of rise, also known as the thermal time constant.

Radio Frequency Penetration

Bluetooth connection strength was evaluated for Specimen C1 and C2, using both an iPad and Huawei P20 Pro, before and after surgical implantation. Table 3.1 displays the recorded signal strength, noting that closer to zero is a “stronger” signal. Superior performance was observed with the latter, but both devices were determined suitable.

Table 3.1—Bluetooth Signal Strength Before & After Implantation

	iPad		P20 Pro	
	C1 (Tibia)	C2 (Femur)	C1 (Tibia)	C2 (Femur)
External Signal Strength (dBm)	-65	-60	-53	-62
Implanted Signal Strength (dBm)	-97	-93	-78	-82

Data Collection During Anatomic Loading

Temperature readings captured at 15 second intervals during the anatomic loading test were retrieved from the femoral sensor without issue following the testing. These values can be seen depicted in Figure 3.11. As discussed in Section 3.3.3, the tibial mounted sensor failed before the anatomic loading test began and was not collecting data.

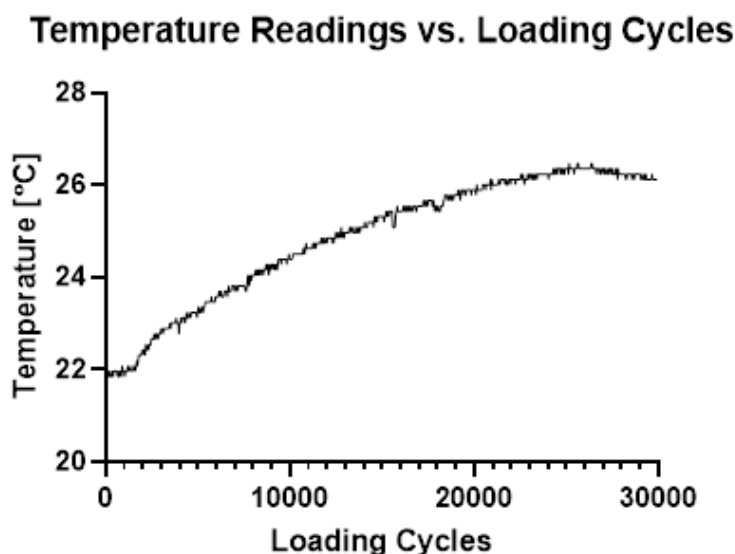


Figure 3.11— Graph of "Temperature Readings vs. Loading Cycles" depicting the temperature captured by the instrumented implant throughout cyclic loading.

Mechanical Integrity

3.3.7 The cadaveric knee was skeletonized following the anatomic loading profile. The specimen, with a clear view of the articulating surfaces, can be observed in Figures 3.12 and 3.13. No indication of tibial tray, femoral keel separation or other catastrophic failure was observed.



Figure 3.12—An axial view of the articulating surfaces following the loading cycle and debridement. Note excess bone cement on the tibial tray has been worn smooth.



Figure 3.13—An auxiliary view of the tibia and femur following the loading cycles and debridement. No spacer separation or major fracturing was observed.

Micro CT scans were examined for fine darkened lines propagating from the bone cement to titanium interface to indicate stress fracturing. Although no sign of stress fracture was found, some areas of poor bone cement integration with the textured surface sensing package were observed. This phenomenon can be seen highlighted by yellow circles in Figures 3.14 and 3.15.

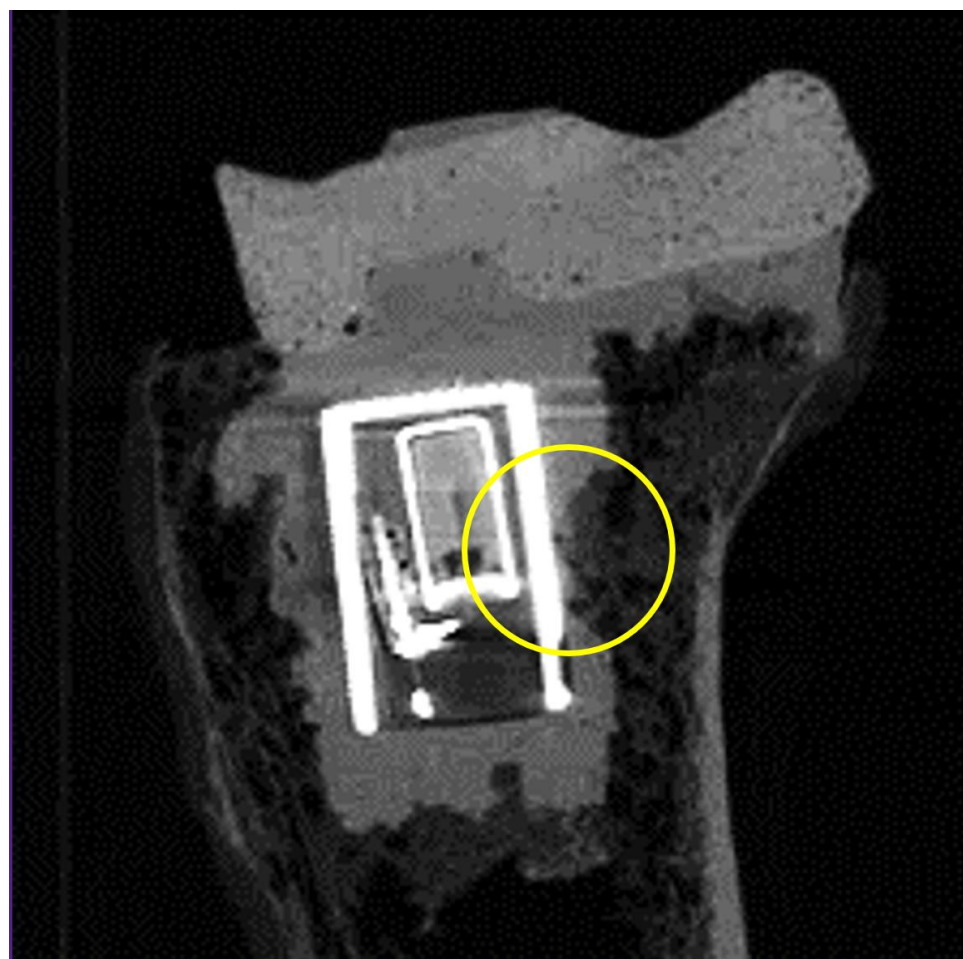


Figure 3.14—Micro CT image depicting a region on the posterior face of the potted sensing package in the tibia where poor bone cement coverage is observed.



Figure 3.15—Micro CT image depicting a sagittal view of the tibial implant where three regions of poor bone cement integration with the implanted instrumentation can be observed.

When examining the femoral component's imaging results, no similar voids were observed. These findings were corroborated by manual removal of the spacer from the bones and conducting a visual inspection. Shown in Figures 3.16 and 3.17, there are areas of the tibial spacer where the titanium casing can be clearly seen uncovered.



Figure 3.16—Two areas with insufficient bone cement can be observed on the tibial keel.



Figure 3.17—A third area with a void of bone cement coverage on the tibial keel.



Figure 3.18—Explanted femoral spacer component clamped in a bench vice displaying superior bone cement coverage of the sensing package.

Upon the completion of the extraction procedure, it was clear that the femoral component showed far superior coating of bone cement, evident in Figure 3.18. Although not directly visible in the above image, the PMMA mantle was approximately 5mm thick in most places.

Discussion

3.4 The performed testing implies an optimistic future for this novel sensing implant augment for orthopaedic infection diagnostics. Tight sensing precision coupled with reasonable relative accuracy and thermal capacitance revealed solid performance characteristics. The confirmation of Bluetooth penetration through knee tissues, logging capability *in situ* and the absence of any structural spacer issues under kinematic loading implies real world feasibility for this device to be of value beyond the benchtop.

Because there are no competitive devices or true precedent in this space, it is unfair to estimate this implant's performance at detecting a periprosthetic joint infection without a clinical trial. Beyond impressive sensing characteristics, there are two good indicators that this device will be successful. First, existing diagnostic protocols already perform well while recognizing infection at steady state, they only lose efficacy during the dynamic infection conditions caused by treatment [35] [36]. Basic control systems theory then indicates that existing measurement types *are* likely satisfactory, but lack the appropriate sampling rate (once per clinical visit) to properly represent the true dynamic infection status [132]. Second, even if early trials reveal that temperature sensing is not the ideal modality, this device has been designed to accept any analog or serial interface sensor that physically fits, so a rapid pivot would be trivial.

However, the testing was not a unilateral success. Premature failure of one sensing package was the result of a sequence of events caused by a software issue, which required some improvisation. Issues with wireless/software reset functionality meant a physical switch had to protrude from the sensing capsule and clipped off before implantation. This resulted in moisture condensation against a decoupling capacitor causing a short circuit. With soft reset functionality rectified, the protruding wires would not have been required and this short circuit would not have occurred. One interesting takeaway from this failure was that the femoral component is perhaps a preferred location to embed this sensor over the tibial spacer. The femoral notch offers space for increased cement volume relative to the intermedullary canal of the tibia and permits a more thorough coating of the sensor with bone cement. A likely reason the femoral sensor did not fail in the same way as the

tibial was the more generous application of bone cement permitted by the femoral spacer geometry, thus preventing moisture from ever reaching the sensor package.

From the testing performed, it was observed with 95% confidence that the temperature sensing hardware was accurate to $\pm 0.24^{\circ}\text{C}$ in the anticipated sensing range (relative to reference) and precise to 0.09°C with hysteresis found effectively negligible when compared to the precision. Accuracy is of lower priority in this context because nobody knows the temperature threshold for “infected” vs. “healthy”, as that value may vary from one patient to the next. Still, this accuracy is superior to some thermometers used for assessing elevated knee temperatures post surgery [65] [133]. The high precision sensing is the more meaningful result for this application. This indicates reliable, trended data will be collected meaning patterns can be observed with confidence. Two studies evaluating operative vs. non operative knee surface skin temperature found a temperature differential of healthy patients peaking 7 days post surgery at $+ 2.4^{\circ}\text{C}$ and $+ 2.9^{\circ}\text{C}$ respectively [65] [134]. Another study examined systemic effects of TKA infection and found core temperature might increase by 1.2°C from the fever response, although unclear what the localized response magnitude might be [135]. A fourth study investigates the temperature of an infected wound relative to skin surface temperature and found a gradient of $4\text{--}5^{\circ}\text{C}$ but more critically was able to observe infections at different stages showed that patients’ deep wound temperatures decrease by $0.8\text{--}1.1^{\circ}\text{C}$ mean temperature as their infections are cleared. This was measured with long wave IR thermography [66]. Considering the proposed device demonstrated sensing precision 1–2 orders of magnitude tighter than the anticipated fluctuations, this device is suitable for its application.

The sensing package has memory for 5500 individual temperature readings. With a goal of a 6 week logging period before requiring a clinical visit to offload the data, measurements can be taken at 20 minute intervals. The device’s battery life is well in excess of any period the patient might keep their antibiotic spacer before revision so absolutely no patient input is required for operation including charging. The thermal time constant analysis revealed $\tau = 262.67 \pm 4.56$ seconds and an associated settling time of $T_s = 1027.57 \pm 17.84$ seconds (~ 17 min). The settling time during dynamic conditions

being shorter than the programmed sampling rate implies that the thermal capacitance of the encapsulation materials and bone cement is unlikely to “filter out” meaningful patterns in temperature fluctuation.

Bluetooth penetration and signal drop when implanted was inline with literature estimations [58]. Especially while using more recent smartphone hardware, stability was excellent. This was ideal for commercial feasibility because Bluetooth connectivity is native to most smartphones and a dedicated transceiver can be replaced by a simple phone application downloaded by the physician.

The culmination of the results collected from these evaluations suggest a positive resolution to the first hypothesis. The electronics of this package (with rectification of the protruding wires) offer suitable characteristics for the intended usage of this device moving forward.

Mechanical results of the test were also promising with no indication of internal stresses or catastrophic spacer failure revealed by micro CT scans or manual debridement and inspection. Previous literature implies that this result would be common for a patient adhering to reduced loading guidelines. Mechanical failure of spacer components was only prevalent in patients that disregarded instructions to avoid full loadbearing. In patients receiving identical Exactech spacer components to ones used in this study, some reported modes of failure include fracture of the femoral component or subluxation of the tibial component [126]. Another study evaluated spacer performance using a very similar apparatus to this investigation observed failure in the form of aseptic loosening or femoral component fracture [124]. One study evaluating patients with PROSTELAC spacers and another study cementing in explanted and sterilized knee components observed fractures of the tibial component [136] [137]. No cases were found suggesting that fracture of the keel components is particularly likely and the observations made in this study do not suggest any new cause for concern caused by the inclusion of the instrumentation package. It is worthwhile considering the superior bone cement mantle consistency in the femoral component though. It was obvious that in the femoral embodiment, the notch geometry offers more room, and crucially better surgeon access

for bone cement application than the intermedullary canal of the tibial location. Based on the available information, especially in the femoral embodiment, the results depict an affirmative response to the second hypothesis. This evaluation has not uncovered any concerns of mechanical spacer failure as a result of introducing the proposed instrumentation package.

This study does have some limitations. First, because the reference sensor was externally validated and delivered with a calibration certification, the PID chamber was assumed to be satisfactory when driving conditions to within the least significant digit of desired temperature. That said, the overall apparatus was not validated externally and there is room for fair criticism. Precision could have been measured at several different temperatures but in this case was not. The study assumes precision to be constant throughout the relatively small 35–40°C sensing range. Also, battery capacity was more than satisfactory for the usage case and device lifetime is several times longer than the implantation period, so power consumption was not prioritized as an investigation objective, but as the device is redesigned with new (smaller) battery technology this question becomes more important. Perhaps the largest limitation lies in the cadaveric testing method. Due to COVID-19 challenges, the *in situ* tests only included one cadaveric specimen with a total of two sensing packages installed and anatomically loaded. While the findings were optimistic, this latter component of the study lacks the power to draw statistical confidence in the observations and would benefit from additional cadaveric specimens to improve this.

In conclusion, observed device performance was satisfactory relative to the application conditions. The sensing performance regarding precision, accuracy, and thermal insulation are suitable for the envisioned infection diagnostics application and the sensing package appears to be capable of seamless mechanical integration with the existing two stage total knee revision procedure. However, the inception of this device may be even greater than the performance information presented here. Data logging and measured decision making are already changing the cardiac field, there is hope that this device might begin a trend of similar technology trickling into the orthopaedic field, beginning with infection.

4 Chapter 4—Summary, Discussion, and Conclusion

The final chapter of this thesis reflects a summary of the findings throughout this project. Crucially, it covers some limitations observed with these evaluations and prototype. Further, it revisits the problem definition and research questions along with a discussion on next steps. This chapter begins with a retrospective glance at the prototype performance.

Summary of Device Performance

4.1 As discussed in Sections 3.3 and 3.4, overall device performance is encouraging despite the issues with prototype manufacturing. To clearly reiterate, the sensing device has demonstrated a precision of 0.09°C , $\pm 0.24^{\circ}\text{C}$ accuracy relative to reference with 95% confidence and a characteristic equation was generated for translation of analog readings to tangible temperatures. Note that precision is tabulated based on a 5 sample non overlapping window while accuracy is reported through paired correlative sampling and is therefore relative to the accuracy of the reference (MCP9808) sensor.

During the evaluation of thermal response time, a thermal time constant of $\tau = 262.67 \pm 4.56$ seconds was measured over 15 independent trials to various temperatures. This results in a settling time of 1027.57 ± 17.84 seconds assuming lumped thermal capacitance (discussed below in Section 4.2).

When surgically installed in a cadaveric knee, the Bluetooth signal strength was measured before and after the procedure using both an Apple iPad and a Huawei P20 Pro Android device. Overall, when implanted in the femoral component, an average transmission strength drop of 26.5 dBm was observed and 28.5 dBm in the tibial component.

Between the Bluetooth measurements and the beginning of the anatomic loading, connection was lost with the tibial sensing package. The femoral package performed as anticipated throughout the test and continued to operate post extraction.

During cyclic anatomic loading, the femoral sensing package demonstrated the ability to collect and store sensor readings at the programmed 15 second interval. Following the test, it was able to wirelessly export the values to either the iPad or P20 Pro when given the wireless command to do so.

Following anatomic loading, micro CT scans were taken to observe any evidence of internal spacer fracturing, which may have been caused by the integration of the proposed sensing package, but no damage was observed. There were some regions immediately adjacent to the sensing packages with air pockets present. Full manual debridement of the spacers from the knee joint following these scans revealed areas where the bone cement was not uniformly applied around the sensing packages, but no mechanical issues were observed as a result beyond increased fluidic exposure of the tibial sensing package.

During the manual debridement, the malfunctioning tibial sensing package was further analyzed. An issue with the software before the test resulted in the temporary need for a hardware level reset mechanism. As a result, two wires had to protrude from the silicone mantle. Silicone adhesion to the wire sheathing was insufficient for moisture sealing, coupled with inconsistent bone cement coverage of the tibial component, this permitted fluidic penetration, which ultimately caused a short circuit. This did not result in any battery leakage, swelling or other safety concern, only an inactive sensing board. In future iterations, the root cause of this issue was addressed with a software revision eliminating the need for protruding wires.

4.2 Section 4.2 is meant to contextualize some of these observations in a way that might reflect more meaningfully on the conclusions to be drawn and the impact on research questions.

Ramifications of Performance on Utility

Sensor accuracy was a lower priority for this application. As previously discussed in detail, it is far more likely that infection monitoring will involve mean temperature monitoring with no absolute thermal threshold pointing to a diagnosis. Still, it could be convenient for future sensing applications that have not yet been identified to offer

respectable sensing accuracy. As it stands, the accuracy measured is superior to medical grade radio frequency thermometers used in similar literature such as the MS LT series devices manufactured by Optris or the popular 0S530LE from OMEGA Engineering that report $\pm 0.4^{\circ}\text{C}$ and $\pm 0.37^{\circ}\text{C}$ accuracy respectively at 37.0°C [65] [133].

Sensor precision was more critical. Other studies imply that over a daily period, natural body temperature fluctuation may easily exceed 1°C [51] [64]. When examining operative knees in general temperature increases of $> 2^{\circ}\text{C}$ [65] [134]. Deep wounds temperatures have been correlated against infections and a thermal increase of $0.8\text{--}1.1^{\circ}\text{C}$ might be expected in infected patients [66]. Daily body temperature fluctuation is of no concern, as this is easily averaged out. There is some concern that in patients, future work might observe a mean temperature decrease and find it difficult to differentiate between infection subsidence and the surgical healing process slowing down. It is hypothesized that a key infection indicator separated from the natural healing process might be mean temperature *increase* following the end of an antibiotic bout, implying infection resurgence. Regardless, if there is a meaningful trend of temperature to correlate with infection, as suggested by Chanmugam *et al.*, the sensing precision of 0.09°C offers suitable performance for confident capture considering the anticipated fluctuation [66].

The thermal time constant was used to tabulate a settling time of roughly 17 minutes. Accordingly, in patient use, the sensing device will be programmed to collect a temperature reading once every 20 minutes. This calculation was done by modelling the system assuming lumped thermal capacitance. This methodology is common for small solids with relatively large conducting surface area when the exact thermal properties of the materials used are unknown. The operative feature for lumped thermal capacitance to be valid is a Biot number ≤ 0.1 . Practically speaking, thermal conduction at the surface of the object must be 10 times (or more) greater than the convection within the object [138] [139]. Solids, like the proposed sensing package, have effectively no internal convection as convection requires fluidic movement. As a result, any amount of thermal conduction at the surface of the spacer, with negligible convection, makes this device a candidate for this representation. A critical feature of this model is that the ΔT does not matter; the system will equilibrate in the same amount of time regardless of a 0.1°C or 10°C change.

Accordingly, the temperature of this device may be represented by the following equation [138].

$$\frac{(T(t) - T_f)}{(T_i - T_f)} = e^{(-\frac{t}{\tau})}$$

T(t) = Instrumented spacer temperature at time of interest

T_f = System final temperature

T_i = System initial temperature

t = Time elapsed since temperature change in seconds

τ = Measured thermal time constant in seconds

Note that settling time is commonly observed as the amount of time from disturbance (temperature change) to when the system reaches, and stays within, 2% of the final value [140].

Successful Bluetooth transmission through the knee tissues was encouraging. Although observed signal strength drops were substantial after implantation, they were manageable. Few, if any, mobile phones or tablets are natively equipped for low frequency transmission, while application development and support for independent development of Bluetooth devices is prolific. With the eligibility of Bluetooth connectivity confirmed for this application redesign of the circuitry will not be necessary and a dedicated transceiver device to collect information wirelessly is not required. This shortened the development timeline and may improve adoption by healthcare practitioners if additional hardware is unneeded.

The learnings from the cadaveric debridement and imaging process were just as valuable as the test itself. For example, it became clear that the titanium housing designed easily protects the circuitry within from the relatively violent extraction process. It was also clear, both during implantation and removal, that the femoral spacer represents a far more accessible location than the tibia for placement this sensing device for *in vivo* use.

Another question regarded the surface texture of the sensing package. During manufacturing, two surface finishes were made. One was intentionally textured to discourage slip conditions between the package and the bone cement while the other was relatively smooth. Recall that the previous literature comes to no clear consensus on the topic of which is better [108] [109] [110].

For the test performed, exclusively the textured titanium samples were used. In some cases the debridement procedure showed excellent integration. However, in other areas, clearly adhesion was not well maintained with the observation of voids. It was clear that the coverage of the femoral component was better than the tibial stem, the geometry of the cavity the femoral sensor resides within lends itself to more thorough PMMA packing. Given only a single cadaveric specimen was used, this study was unable to investigate the integration of various titanium surface textures. This is understood as a distinct limitation of this research but a truly rigorous evaluation on this topic could be an independent thesis project of its own.

One regret from the study was the lack of attention to preprocessing of components before assembly. Literature read afterwards discussed cleaning procedures with alcohols for circuit boards prior to encapsulation [141] [142]. Other literature discusses degreasing of metallic components prior to implantation in cemented applications [109]. It is plausible that the electrical failure of the tibial sensor may not have occurred with better conformal coating or more thorough PMMA encapsulation.

Another component of the manufacturing process not initially considered was the lack of vacuum rating for the selected battery. The silicone encapsulant manufacturer's instructions prescribe curing under vacuum to avoid air pockets (unacceptable in this application) [104]. The battery was not rated for vacuum. After contacting the battery manufacturer, clearance was given to place the battery under 10 mmHg of vacuum, but this was only a third of the recommended vacuum for the silicone. A change to the manufacturing process involving one more curing step may be in order to ensure the circuit board is conformally coated before battery installation.

Limitations, Recommendations & Future Work

4.3 As highlighted by section 4.2, this study admittedly, has several limitations at a higher level than the specific ones discussed in Section 3.4. A dedicated study to the integration of bone cement with the instrumented package may be required if future cadaveric specimens continue to show voiding issues. A direct limitation of the N=1 cadaveric study is the uncertainty of how consistent this issue is. Should future cadaveric testing reveal this problem is prolific, a dedicated examination of this phenomenon and the solutions (textures, geometry, prep etc.) would be worthwhile. Also, while any minor current leakage in the circuit is of no consequence in the existing application (with surplus power reserves and a lack of regulatory oversight) this will require measurement before human use. Along the same line of reasoning, ETO sterilization protocols would have to be performed on the assembled device to ensure sanitation and technical compatibility.

The insights found in Section 4.2 directly correlate to a range of discussion on which steps could be taken going forward to improve the evidence generated, iterate and ultimately demonstrate improvement on the suggested solution.

Work following the cadaveric study involved an immediate priority to remove the need for a hardware reset interface. Now, the software permits a wireless command to be sent to wipe the sensor's onboard memory, which permits new data to be collected after offloading the old stored data.

The circuitry was simplified for the purposes of the above studies, without the redundant circuitry present to protect against short circuits and undervoltage cases. As it has become clear this device has value for clinical study, the next batch of sensing packages manufactured will be equipped with the full compliment of previously specified electrical protection.

Although unlikely, if moisture condensation continues to be an issue after the protruding reset wires became obsolete, revisiting an alternate generated solution for encapsulation (Parylene C) may be considered despite the drawbacks. Contaminant isolation for the

patient and circuit board protection are both obviously higher priority than the flexibility to potentially add different/incompatible sensors in the future.

Ultimately the next steps for this project includes two things. First, additional cadaveric trials will be needed to build statistical confidence in device performance and spacer mechanical integrity once instrumented. After the findings within this thesis are confirmed with greater confidence, a human trial will be performed in an attempt to correlate infection status with mean internal joint temperature.

Should a temperature/infection correlation not exist, hopefully some cutting edge sensing options such as ESR and CRP lab-on-chip devices will have migrated from research labs into production/implementation [49] [50]. As soon as these devices are commercially available, implementation into the sensing infrastructure presented in this thesis should be trivial, although characterization, precision, accuracy etc. of these new sensors would need to be revisited.

4.4 Conclusion

In summary of this thesis, a device has been envisioned, developed, and evaluated to support physicians in the ongoing initiative to improve two stage revision outcomes.

Reflecting on the previously proposed problem definition, to “*Develop a diagnostic solution specifically suitable for use during treatment for total knee arthroplasty infection*” it is clear that a purpose built device was engineered to serve exactly such a purpose.

Reconsidering the initial study objectives proposed in Section 1.4, an objective look at the research contributions of this thesis may be conducted. First, there was an objective to characterize the proposed sensing device and determine suitability of the sensing, logging, and transmission performance in an infection telemetry application. Based on inferences of the stimuli/environment according to existing literature, and the observations made, the device performance is certainly adequate for the intended usage case. Second, an evaluation of the mechanical performance of the device showed promise for the current embodiment’s compatibility with bone cement spacer applications,

although this will require further study to claim with statistical confidence. Finally, while this study does have some limitations and some iteration is required, the observed results certainly indicate the feasibility of instrumenting the knee spacer to improve the revision process going forward.

More critically, a thorough engineering design process has laid the groundwork for intelligent, efficient iteration of the proposed platform technology to address logistical challenges and streamline future success of this project. The outcome of this research offers unique opportunity to the field of sensing in orthopaedics and infection management. It has displayed with great clarity that technology in computing, batteries, sensing, and wireless communications is approaching, or perhaps has already reached, the point of widespread feasibility for a plurality of biotelemetric solutions to medical problems. Other groups developing solutions to sensing various biometrics should view this contribution as a platform technology. With minor iteration the proposed device could provide feasible path to implantation of novel sensing technology. Ideally this technology will inspire collaboration and ultimately expedite the application of several other developing projects within the space of infection monitoring.

References

- [1] National Health Service UK, "Overview: Knee Replacement," 2019 August 2018. [Online]. Available: <https://www.nhs.uk/conditions/knee-replacement/>. [Accessed 22 March 2020].
- [2] S. Lohmander, "Knee replacement for osteoarthritis: facts, hopes, and fears," *Medicographia*, vol. 35, no. 114, pp. 181–188, 2013.
- [3] N. Kalore, T. Gioe and J. A. Singh, "Diagnosis and Management of Infected Total Knee Arthroplasty," *Open Orthopaedics Journal*, vol. 5, pp. 86–91, 2011.
- [4] J. C. Martinez-Pastor, F. Macule-Beneyto and S. Suso-Vergara, "Acute Infection in Total Knee Arthroplasty: Diagnosis and Treatment," *Open Orthopaedics Journal*, vol. 7, pp. 197–204, 2013.
- [5] R. d. P. Cury, E. T. Cinagawa, O. P. A. Camargo, E. H. Honda, G. B. Klautau and M. J. C. Salles, "TREATMENT OF INFECTION AFTER TOTAL KNEE ARTHROPLASTY," *Acta Ortopedica Brasileira*, vol. 23, no. 5, pp. 239–243, 2015.
- [6] C. Pangaud, M. Ollivier and J.-N. Argenson, "Outcome of single-stage versus two-stage exchange for revision knee arthroplasty for chronic periprosthetic infection," *EFORT Open Reviews*, vol. 4, no. 8, pp. 495–502, 2019.
- [7] Open Stax College Resources, "Anatomy of the Human Knee," 19 June 2013. [Online]. Available: https://commons.wikimedia.org/wiki/Category:Anatomy_of_the_human_knee#/media/File:917_Knee_Joint.jpg. [Accessed 2 August 2020].

- [8] J. F. Abhulhasan and M. J. Grey, "Anatomy and Physiology of Knee Stability," *Functional Morphology and Kinesiology*, vol. 2, no. 4, p. 34, 2017.
- [9] A. Cassidy, "The Patella," TeachMe Anatomy, 22 December 2017. [Online]. Available: <https://teachmeanatomy.info/lower-limb/bones/patella/>. [Accessed 28 March 2020].
- [10] A. S. Gersing, M. Solka, G. B. Joseph, B. J. Schwaiger, U. Heilmeyer, G. Feuerriegel, M. C. Nevitt, C. E. McCulloch and T. M. Link, "Progression of Cartilage Degeneration and Clinical Symptoms in Obese and Overweight Individuals is Dependent on the Amount of Weight Loss: 48-Month Data from the Osteoarthritis Initiative," *Osteoarthritis Cartilage*, vol. 24, no. 7, pp. 1126–1134, 2016.
- [11] A. J. S. Fox, A. Bedi and S. A. Rodeo, "The Basic Science of Human Knee Menisci," *Sports Health*, vol. 4, no. 4, pp. 340–351, 2012.
- [12] Arthritis Foundation, "Osteoarthritis," [Online]. Available: <https://www.arthritis.org/diseases/osteoarthritis>. [Accessed 24 March 2020].
- [13] C. B. Little, A. Barai, D. Burkhardt, S. M. Smith, A. J. Fosang, Z. Werb, M. Shah and E. W. Thompson, "Matrix Metalloproteinase 13-deficient Mice Are Resistant to Osteoarthritic Cartilage Erosion but Not Chondrocyte Hypertrophy or Osteophyte Development," *Arthritis and Rheumatology*, vol. 60, no. 12, pp. 3723–3733, 2009.
- [14] M. J. Lespasio, N. S. Piuze, M. E. Husni, G. F. Muschler and A. M. M. A. Guarino, "Knee Osteoarthritis: A Primer," *Permanente Journal*, vol. 21, pp. 16–183, 2017.

- [15] J. Sellam and B. F. "The role of synovitis in pathophysiology and clinical symptoms of osteoarthritis," *Nature Reviews Rheumatology*, vol. 6, no. 11, pp. 625–635, 2010.
- [16] Y. Zhang and J. M. Jordan, "Epidemiology of Osteoarthritis," *Clinical Geriatric Medicine*, vol. 3, pp. 355–369, 2010.
- [17] S. Zanasi, "Innovations in total knee replacement: new trends in operative treatment and changes in peri-operative management," *European Orthopaedics and Traumatology*, vol. 1, no. 2, pp. 21–31, 2011.
- [18] Canadian Institute for Health Information, "Hip and Knee Replacements in Canada, 2016–2017," 2018. [Online]. Available: https://secure.cihi.ca/free_products/cjrr-annual-report-2018-en.pdf. [Accessed 1 April 2020].
- [19] M. L. D. Varacallo and N. A. Johanson, "Total Knee Arthroplasty (TKA) Techniques," 15 March 2020. [Online]. Available: <https://www.ncbi.nlm.nih.gov/books/NBK499896/>. [Accessed 1 April 2020].
- [20] W. Cheadle, "Risk Factors for Surgical Site Infection," *Surgical Infections*, vol. 7, no. 1, pp. 7–11, 2006.
- [21] C. M. Mallon, R. Gooberman-Hill and A. J. Moore, "Infection after knee replacement: a qualitative study of impact of periprosthetic knee infection," *BMC Musculoskeletal Disorders*, vol. 19, no. 1, p. 352, 2018.
- [22] B. D. Springer, S. Cahue, C. D. Etkin, D. G. Lewallen and B. J. McGrory, "Infection burden in total hip and knee arthroplasties: an international registry-based perspective," *Arthroplasty Today*, vol. 3, no. 2, pp. 137–140, 2017.

- [23] J. Lu, J. Han, C. Zhang, Y. Yang and Z. Yao, "Infection after total knee arthroplasty and its gold standard surgical treatment: Spacers used in two-stage revision arthroplasty," *Intractable & Rare Disease Research*, vol. 6, no. 4, pp. 256–261, 2017.
- [24] J. R. H. Foran, "Total Knee Replacement," OrthoInfo, August 2015. [Online]. Available: <https://orthoinfo.aaos.org/en/treatment/total-knee-replacement/>. [Accessed 18 April 2020].
- [25] K. C. Chun, K. M. Kim and C. H. Chun, "Infection Following Total Knee Arthroplasty," *Knee Surgery & Related Research*, vol. 25, no. 3, pp. 93–99, 2013.
- [26] A. J. Moore, A. W. Blom, M. R. Whitehouse and R. Goberman-Hill, "Deep prosthetic joint infection: a qualitative study of the impact on patients and their experiences of revision surgery," *BMJ Open*, vol. 5, pp. 1–13, 2015.
- [27] T. Gehrke, P. Alijanipour and J. Parvizi, "The management of an infected total knee arthroplasty," *Bone & Joint Journal*, vol. 97, no. B, pp. 20–29, 2015.
- [28] B. Zmistowski, J. Karam, J. Durinka, D. Casper and J. Parvizi, "Periprosthetic Joint Infection Increases the Risk of One-Year Mortality," *Journal of Bone and Joint Surgery*, vol. 95, no. 24, pp. 2177–2184, 2013.
- [29] J. Cahill, B. Shadbolt, J. Scarvell and P. Smith, "Quality of Life after Infection in Total Joint Replacement," *Journal of Orthopaedic Surgery*, pp. 58–65, 2008.
- [30] C. Li, N. Renz and A. Trampuz, "Management of Periprosthetic Joint Infection," *Hip & Pelvis*, vol. 30, no. 3, pp. 138–146, 2018.

- [31] N. Greidanus, B. Masri, D. Garbuz, D. Wilson, G. McAlinden, M. Xu and C. Duncan, " Use of Erythrocyte Sedimentation Rate and C-reactive Protein Level to Diagnose Infection Before Revision Total Knee Arthroplasty. A Prospective Evaluation," *Bone and Joint Surgery*, vol. 89, no. 7, pp. 1409–1416, 2007.
- [32] P. Reinartz, "FDG-PET in patients with painful hip and knee arthroplasty: technical breakthrough or more of the same," *Journal of Nuclear Medicine and Molecular Imaging*, vol. 53, no. 1, pp. 41–50, 2009.
- [33] Johns Hopkins, "Joint Aspiration," [Online]. Available: <https://www.hopkinsmedicine.org/health/treatment-tests-and-therapies/joint-aspiration>. [Accessed 28 April 2020].
- [34] E. Ghanem, J. Parvizi, S. Burnett, P. Sharkey, N. Keshavarzi, A. Aggarwal and R. Barrack, "Cell Count and Differential of Aspirated Fluid in the Diagnosis of Infection at the Site of Total Knee Arthroplasty," *Journal of Bone and Joint Surgery (American Volume)*, vol. 90, no. 8, pp. 1637–1643, 2008.
- [35] M. Mont, B. Walman and D. Hungerford, "Evaluation of Preoperative Cultures Before Second-Stage Reimplantation of a Total Knee Prosthesis Complicated by Infection. A Comparison-Group Study," *Journal of Bone and Joint Surgery (American Volume)*, vol. 82, no. 11, pp. 1552–1557, 2000.
- [36] J. Lonner, J. Siliski, C. Della Valle and P. Lotke, "Role of Knee Aspiration After Resection of the Infected Total Knee Arthroplasty," *American Journal of Orthopedics*, vol. 30, no. 4, pp. 305–309, 2001.
- [37] K. Reddy, J. Shah, R. Kale and T. J. Reddy, "Fungal prosthetic joint infection after total knee arthroplasty," *Indian Journal of Orthopaedics*, vol. 47, no. 5, pp. 526–529, 2013.

- [38] B. J. Kildow, C. J. Della Valle and B. D. Springer, "Single vs 2-Stage Revision for the Treatment of Periprosthetic Joint Infection," *Journal of Arthroplasty*, vol. 35, no. 3, pp. S24-S30, 2020.
- [39] L. Mazzucchelli, F. Rosso, A. Marmotti, D. E. Bonasia, M. Bruzzone and R. Rossi, "The use of spacers (static and mobile) in infection knee arthroplasty," *Current Reviews in Musculoskeletal Medicine*, vol. 8, no. 4, pp. 373–382, 2015.
- [40] K. Merollini, R. Crawford and N. Graves, "Surgical treatment approaches and reimbursement costs of surgical site infections post hip arthroplasty in Australia: a retrospective analysis," *BMC Health Services Research*, vol. 13, no. 91, 2013.
- [41] R. Juul, J. Fabrin, K. Poulsen and H. M. Schroder, "Use of a New Knee Prosthesis as an Articulating Spacer in Two-Stage Revision of Infected Total Knee Arthroplasty," *Knee Surgery & Related Research*, vol. 28, no. 3, pp. 239–244, 2016.
- [42] T. A. G. van Vugt, J. J. Arts and J. A. P. Geurts, "Antibiotic-Loaded Polymethylmethacrylate Beads and Spacers in Treatment of Orthopedic Infections and the Role of Biofilm Formation," *Frontiers in Microbiology*, vol. 10, p. 1626, 2019.
- [43] L. Coelho, "C-reactive protein and procalcitonin in the assessment of infection response to antibiotic therapy," *Acute Care Testing*, January 2009. [Online]. Available: <https://acutecaretesting.org/en/articles/creactive-protein-and-procalcitonin-in-the-assessment-of-infection-response-to-antibiotic-therapy>. [Accessed 2 May 2020].
- [44] MathWorks, "System Identification Overview," 2020. [Online]. Available: <https://www.mathworks.com/help/ident/gs/about-system-identification.html>. [Accessed 21 April 2020].

- [45] A. Johnson, M. Zyweil, A. Stroh, D. Marker and M. Mont, "Serological markers can lead to false negative diagnoses of periprosthetic infections following total knee arthroplasty," *International Orthopaedics*, vol. 35, no. 11, pp. 1621–1626, 2011.
- [46] P. Bogarty, J. Brophy, L. Boyer, S. Simard, L. Joseph, F. Bertrand and G. Dagenais, "Fluctuating Inflammatory Markers in Patients With Stable Ischemic Heart Disease," *Archives of Internal Medicine*, vol. 165, no. 2, pp. 221–226, 2005.
- [47] F. Baker, J. Waner, E. Vieira, S. Taylor, H. Driver and D. Mitchell, "Sleep and 24 hour body temperatures: a comparison in young men, naturally cycling women and women taking hormonal contraceptives," *Journal of Physiology*, vol. 530, no. 3, pp. 565–574, 2001.
- [48] M. Maines, A. Zorzi, G. Tomasi, C. Angheben, D. Catanzariti and M. Del Greco, "Clinical impact, safety, and accuracy of the remotely monitored implantable loop recorder Medtronic Reveal LINQ," *EP Europace*, vol. 20, no. 6, pp. 1050–1057, 2018.
- [49] Y. J. Kang and B. J. Kim, "Multiple and Periodic Measurement of RBC Aggregation and ESR in Parallel Microfluidic Channels under On-Off Blood Flow Control," *Micromachines*, vol. 9, no. 7, p. 918, 2018.
- [50] C.-H. Chen, R.-Z. Hwang, L.-S. Huang, S.-M. Lin, H.-C. Chen, Y.-C. Yang, Y.-T. Lin, S.-A. Yu, Y.-S. Lin, Y.-H. C. N.-K. Wang and S.-S. Lu, "A Wireless Bio-MEMS Sensor for C-Reactive Protein Detection Based on Nanomechanics," *IEEE Transactions on Biomedical Engineering*, vol. 52, no. 2, pp. 462–470, 2009.

- [51] M. J. Buller, W. J. Tharion, R. W. Hoyt and O. C. Jenkins, "Estimation of Human Internal Temperature from Wearable Physiological Sensors," Brown Statistics, Providence, 2013.
- [52] T. A. English and M. Kilvington, " In Vivo Records of Hip Loads Using a Femoral Implant With Telemetric Output (A Preliminary Report)," *Journal of Biomedical Engineering*, vol. 1, no. 2, pp. 111–115, 1979.
- [53] R. H. Brown, A. H. Burstein and V. H. Frakel, " Telemetry in Vivo Loads From Nail Plate Implants," *Journal of Biomechanics*, vol. 15, no. 11, pp. 815–823, 1982.
- [54] D. D'Lima, C. Townshend, S. W. Arms, B. A. Morris and C. W. Colwell Jr., "An Implantable Telemetry Device to Measure Intra-Articular Tibial Forces," *Journal of Biomechanics*, vol. 38, no. 2, pp. 299–304, 2005.
- [55] Orthoload, "Loading of Orthopaedic Implants," 2020. [Online]. Available: <https://orthoload.com/>. [Accessed 8 April 2020].
- [56] T. Sanna, H.-C. Diener, R. S. Passman, V. D. Lazzaro, R. A. Bernstein, C. A. Morillo, M. M. Rymer, V. Thijs, T. B. F. Rogers, K. Lindborg and J. Brachmann, "Cryptogenic Stroke and Underlying Atrial Fibrillation," *New England Journal of Medicine*, vol. 370, pp. 2478–2476, 2014.
- [57] M. Khosrowpour, in *Information Technology & Organizations: Trends, Issues, Challenges & Solutions*, Philadelphia, Idea Group, 2003, p. 12.
- [58] A. Khaleghi and I. Balasingham, "On selecting the frequency for wireless implant communications," *Loughborough Antennas & Propagation Conference*, pp. 1–4, 2015.

- [59] mbientlab, "Metamotion C," [Online]. Available: <https://mbientlab.com/metamotionc/>. [Accessed 2 April 2020].
- [60] Texas Instruments, "CC2650MODA SimpleLink™ Bluetooth® low energy Wireless MCU Module," July 2019. [Online]. Available: <http://www.ti.com/lit/ds/symlink/cc2650moda.pdf>. [Accessed 3 May 2020].
- [61] ELSRA Smart, "Bluetooth & Biometrics," 2017. [Online]. Available: <https://www.elsra.com/BT03-1.html>. [Accessed 2 May 2020].
- [62] DF Robot, "Beetle BLE - The smallest Arduino bluetooth 4.0 (BLE)," [Online]. Available: <https://www.dfrobot.com/product-1259.html>. [Accessed 2 May 2020].
- [63] S. S. Evans, E. Repasky and D. T. Fisher, "Fever and the thermal regulation of immunity: the immune system feels the heat," *Nature Reviews Immunology*, vol. 15, no. 6, pp. 335–349, 2015.
- [64] R. Refinetti and M. Menaker, "The circadian rhythm of body temperature," *Physiology & Behavior*, vol. 51, no. 3, pp. 613–637, 1992.
- [65] Y. Zeng, W. Feng, X. Qi, J. Chen, L. Lu, P. Deng and J. F. L. Zeng, "Differential knee skin temperature following total knee arthroplasty and its relationship with serum indices and outcome: A prospective study," *Journal of International Medical Research*, vol. 44, no. 5, pp. 1023–1033, 2016.
- [66] A. Chanmugam, D. Langemo, K. Thomason, J. Haan, E. A. Altenburger, A. Tippett, L. Hernderson and T. A. Zortman, "Relative Temperature Maximum in Wound Infection and Inflammation as Compared With a Control Subject Using Long-Wave Infrared Thermography," *Advances in Skin and Wound Care*, vol. 30, no. 9, pp. 406–414, 2017.

- [67] Microchip, "MCP9808 Datasheet," May 2018. [Online]. Available: <http://ww1.microchip.com/downloads/en/DeviceDoc/MCP9808-0.5C-Maximum-Accuracy-Digital-Temperature-Sensor-Data-Sheet-DS20005095B.pdf>. [Accessed 2 May 2020].
- [68] Texas Instruments, "TMP23X Low-Power, High-Accuracy Analog Output Temperature Sensors," 2019 May. [Online]. Available: <https://www.ti.com/lit/ds/symlink/tmp235.pdf?ts=1587953510538>. [Accessed 2 May 2020].
- [69] Texas Instruments, "TMP117 high-accuracy, low-power, digital temperature sensor with SMBus™- and I2C-compatible interface," March 2019. [Online]. Available: <https://www.ti.com/lit/ds/symlink/tmp117.pdf?ts=1587953585232>. [Accessed 13 May 2020].
- [70] N. Soin, "Chapter 10 - Magnetic Nanoparticles—Piezoelectric Polymer Nanocomposites for Energy Harvesting," in *Magnetic Nanostructured Materials*, Amsterdam, Elsevier, 2018, pp. 295–322.
- [71] PowerWatch, "PowerWatch: Never Charge Again," [Online]. Available: <https://www.powerwatch.com/>. [Accessed 28 May 2020].
- [72] M. Hutin and M. LeBlanc, "TRANSFORMER SYSTEM FOR ELECTRIC RAILWAYS". France Patent 209,323, 5 November 1980.
- [73] Realinfo, "Oersted Law," Realinfo Encyclopedia of Electrical Engineering, [Online]. Available: https://www.realinfo.com/toc/Basic_Electrical_Engineering/Electricity_and_Magnetism/Magnetism/Oersted_law. [Accessed 12 May 2020].

- [74] Khan Academy, "What is Faraday's Law?," [Online]. Available: <https://www.khanacademy.org/science/physics/magnetic-forces-and-magnetic-fields/magnetic-flux-faradays-law/a/what-is-faradays-law>. [Accessed 11 May 2020].
- [75] X. Lu, P. Wang, D. Niyato, D. I. Kim and Z. Han, "Wireless Charging Technologies: Fundamentals, Standards, and Network Applications," *IEEE Communications Surveys & Tutorials*, vol. 18, no. 2, pp. 1413–1452, 2016.
- [76] V. Mallela, V. Ilankumaran and N. S. Rao, "Trends in Cardiac Pacemaker Batteries," *Indian Pacing and Electrophysiology*, vol. 4, no. 4, pp. 201–212, 2004.
- [77] CSA Group, "Making Sense of Regulations for Medical Device Batteries," 2020. [Online]. Available: <https://www.csagroup.org/article/making-sense-regulations-medical-device-batteries/>. [Accessed 5 May 2020].
- [78] L. Lao, Y. Su, Q. Zhang and S. Wu, "Thermal Runaway Induced Casing Rupture: Formation Mechanism and Effect on Propagation in Cylindrical Lithium Ion Battery Module," *Journal of The Electrochemical Society*, vol. 167, no. 9, 2020.
- [79] R. Vaishya, M. Chauhan and A. Vaish, "Bone cement," *Journal of Clinical Orthopaedics and Trauma*, vol. 4, no. 4, pp. 157–163, 2013.
- [80] G. Massazza, A. Bistofi, E. Verne, M. Miola, L. Ravera and F. Rosso, "9 - Antibiotics and cements for the prevention of biofilm-associated infections," in *Biomaterials and Medical Device - Associated Infections*, Woodhead Publishing, 2015, pp. 185–197.

- [81] Tadiran Batteries, "Lithium/Thionyl Chloride Batteries," 2020. [Online]. Available: <https://tadiranbatteries.de/eng/products/lithium-thionyl-chloride-batteries/overview.asp>. [Accessed 2 April 2020].
- [82] Tadiran Batteries, "Tadiran Batteries Technical Brochure," [Online]. Available: <https://tadiranbatteries.de/pdf/Technical-Brochure-LTC-Batteries.pdf>. [Accessed 2 May 2020].
- [83] Battery University, "BU-106a: Choices of Primary Batteries," 21 June 2019. [Online]. Available: https://batteryuniversity.com/learn/article/choices_of_primary_batteries. [Accessed 12 May 2020].
- [84] D. Knight, "Lithium Ion Cell Protection," DigiKey, 14 December 2015. [Online]. Available: <https://www.digikey.ca/en/maker/blogs/lithium-ion-cell-protection>. [Accessed 19 April 2020].
- [85] Eagle Picher, "LTC-3PM-M1 Datasheet," Eagle Picher Medical Power, [Online]. Available: <https://www.eaglepicher.com/sites/default/files/LTC-3PN-M1%200119.pdf>. [Accessed 4 April 2020].
- [86] Littell Fuse, "Portable Medical Devices Protection Quick Reference Guide," 2016. [Online]. Available: https://www.littelfuse.com/~media/electronics/application_guides/littelfuse_portable_medical_devices_protection_quick_reference_application_guide.pdf.pdf. [Accessed 29 January 2020].
- [87] ON Semiconductor, "NCP300, NCP301 Voltage Detector Series Datasheet," October 2017. [Online]. Available: <https://www.onsemi.com/pub/Collateral/NCP300-D.PDF>. [Accessed 28 January 2020].

- [88] US Food and Drug Administration, "Summary of Safety and Effectiveness Data: Micra Transcatheter Pacing System," 6 April 2016. [Online]. Available: https://www.accessdata.fda.gov/cdrh_docs/pdf15/P150033B.pdf. [Accessed 1 May 2020].
- [89] Merriam-Webster, "Hermetic," [Online]. Available: <https://www.merriam-webster.com/dictionary/hermetic>. [Accessed 2 June 2020].
- [90] TJ Green Associates, "Hermetic vs “Near Hermetic” Packaging A Technical Review," 2019. [Online]. Available: <https://www.tjgreenllc.com/2016/09/21/hermetic-vs-near-hermetic-packaging-a-technical-review/>. [Accessed 13 May 2020].
- [91] US Department of Defense, "Test Method Standard Microcircuits: MIL-STD-883E," 31 December 1996. [Online]. Available: <http://scipp.ucsc.edu/groups/fermi/electronics/mil-std-883.pdf>. [Accessed 19 January 2020].
- [92] N. Dahan, "The application of PEEK to the packaging of implantable electronic devices," Department of Medical Physics and Bioengineering - University College London, London, 2013.
- [93] S. M. Tavakoli, D. A. Pullen and S. B. Dunkerton, "A review of adhesive bonding techniques for joining medical materials," *Assembly Automation*, vol. 25, no. 2, pp. 100–105, 2005.
- [94] B. Heinlein, I. Kutzner, F. Graichen, A. Bender, A. Rohlmann, A. Halder, A. Beier and G. Bergmann, "ESB clinical biomechanics award 2008: Complete data of total knee replacement loading for level walking and stair climbing measured in vivo with a follow-up of 6–10 months," *Clinical Biomechanics*, vol. 24, no. 4, pp. 315–326, 2009.

- [95] A. Debelle, L. Hermans, M. Bosquet, S. Dehaeck, L. Lonys, B. Scheid, A. Nonclercq and A. Vanhoestenbergh, "Soft Encapsulation of Flexible Electrical Stimulation Implant: Challenges and Innovations," *European Journal of Translational Myology*, vol. 26, no. 4, pp. 292–296, 2016.
- [96] M. Birkholz, P. Glogener, F. Glos, T. Basmer and L. Theuer, "Continuously Operating Biosensor and Its Integration into a Hermetically Sealed Medical Implant," *Micromachines*, vol. 7, no. 10, p. 183, 2016.
- [97] B. Weishalla, "Smart Plastics for Bluetooth," RTP Co., Winona, 2001.
- [98] L. Lonys, A. Vanhoestenbergh, N. Julémont, S. Godet, M.-p. Delplancke, P. Mathys and A. Nonclercq, "Silicone rubber encapsulation for an endoscopically implantable gastrostimulator," *Medical and Biological Engineering and Computing*, vol. 53, no. 4, pp. 319–329, 2015.
- [99] N. Dahan, N. Donaldson, S. Taylor and N. Sereno, "Prolonging the Lifetime of PEEK Packages for Implantable Electronic Devices Using Commercially Available Vacuum Thin Film Coatings," *Journal of Microelectronics and Electronic Packaging*, vol. 11, no. 3, pp. 128–136, 2014.
- [100] R. M. Cowie, A. Briscoe, J. Fisher and L. M. Jennings, "Wear and Friction of UHMWPE-on-PEEK OPTIMA™," *Journal of the Mechanical Behavior of Biomedical Materials*, vol. 89, pp. 65–71, 2019.
- [101] H. Weiner, "Additive vs Subtractive Manufacturing – Simply Explained," All3DP, 2 January 2019. [Online]. Available: <https://all3dp.com/2/additive-vs-subtractive-manufacturing-simply-explained/>. [Accessed 25 May 2020].

- [102] Renishaw, "Data sheet: Ti6Al4V ELI-0406 powder for additive manufacturing," June 2017. [Online]. Available: <https://resources.renishaw.com/en/details/data-sheet-ti6al4v-eli-0406-powder-for-additive-manufacturing--94700>. [Accessed 15 January 2020].
- [103] Elkem, "Silicone keeping cardiac resynchronization devices safe from corrosive body fluids," 2018. [Online]. Available: https://silicones.elkem.com/EN/Our_offer/Market_And_Application/Pages/Cardiac-Resynchronization-Devices-.aspx. [Accessed 19 January 2020].
- [104] DuPont, "SILASTIC® MDX4-4210 BioMedical Grade Elastomer," 8 August 2005. [Online]. Available: <https://www.dupont.com/content/dam/Dupont2.0/Products/transportation/Literature/Downloaded-TDS/0901b803809b782d.pdf>. [Accessed 13 January 2020].
- [105] NuSil, "Biomaterials - Implant Line Product Guide," 2019. [Online]. Available: <http://nusil.cloudapp.net/~media/Files/Product%20Guides/Biomaterials/NuSil%20-%20Medical%20Implants%20Product%20Guide.pdf>. [Accessed 13 January 2020].
- [106] Simtal Coatings, "Applying Parylene for use in Medical and Bio-Medical Devices," [Online]. Available: <https://www.simtalltd.com/applications/medical/>. [Accessed 13 January 2020].
- [107] Diamond-MT, "Comparison of Parylene and Acrylic Coatings," 2020. [Online]. Available: <https://www.paryleneconformalcoating.com/parylene-vs-acrylic-conformal-coatings/#>. [Accessed 3 February 2020].
- [108] J. C. Keller, E. P. Lautenschlager, G. W. Marhall Jr. and P. R. Meyer Jr., "Factors affecting surgical alloy/bone cement interface adhesion," *Journal of Biomedical Materials Research*, vol. 14, no. 5, pp. 639–651, 1980.

- [109] T. Wang, M. H. Pelletier, N. Bertollo, A. Crosky and W. R. Walsh, "Cement-Implant Interface Contamination: Possible Reason of Inferior Clinical Outcomes for Rough Surface Cemented Stems," *Open Orthopaedics Journal*, vol. 7, pp. 250–257, 2013.
- [110] M. Khandaker, S. Riahinezhad, F. Sultana, M. B. Vaughan, J. Knight and T. Morris, "Peen treatment on a titanium implant: effect of roughness, osteoblast cell functions, and bonding with bone cement," *International Journal of Nanomedicine*, vol. 11, pp. 585–595, 2016.
- [111] W. N. Ayre, S. P. Denyer and S. L. Evans, "Ageing and moisture uptake in polymethyl methacrylate (PMMA) bone cements," *Journal of the Mechanical Behavior of Biomedical Materials*, vol. 32, no. 100, pp. 76–88, 2014.
- [112] J. Ikekwem, J. Chukwunke and S. Omenyi, "Thermal Behaviour of Bone Cement in Hip Replacement," *Physical Science International Journal*, vol. 17, no. 4, pp. 1–14, 2018.
- [113] B. Eidel, A. Gote, C. P. Fritzen, A. Ohrndorf and H. J. Christ, "Tibial Implant Fixation in TKA Worth A Revision?– How to Avoid Stress-Shielding Even for Stiff Metallic Implants," *arXiv: Medical Physics*, 2019.
- [114] D. D'Lima, S. Patil, N. Steklov, J. E. Slamin and C. W. Colwell Jr., "Tibial Forces Measured In Vivo After Total Knee Arthroplasty," *Journal of Arthroplasty*, vol. 21, no. 2, pp. 255–262, 2006.
- [115] S. García David, J. A. Cortijo Martínez, I. Navarro Bermúdez, F. Maculé, P. Hinarejos, L. Puig-Verdié, J. C. Monllau and J. A. Hernández Hermoso, "The geometry of the keel determines the behaviour of the tibial tray against torsional forces in total knee replacement," *Revista Española de Cirugía Ortopédica y Traumatología*, vol. 58, no. 6, pp. 329–335, 2014.

- [116] M. Reiman, in *Orthopedic Clinical Examination*, Human Kinetics, Inc., p. 209.
- [117] C. Goumopolus, "A High Precision, Wireless Temperature Measurement System for Pervasive Computing Applications," *Sensors*, vol. 18, no. 10, 2018.
- [118] C. A. Boano, M. Lasagni, K. U. Römer and T. Lange, "Accurate Temperature Measurements for Medical Research using Body Sensor Networks," *IEEE International Symposium on Object/Component/Service-Oriented Real-Time Distributed Computing Workshops*, pp. 189–198, 2011.
- [119] Medtronic, "Our Position on Ethylene Oxide (ETO) Sterilization," 2020. [Online]. Available: <https://www.medtronic.com/us-en/e/eto.html>. [Accessed 22 May 2020].
- [120] P. Anderson, "Accuracy and Precision," Sophia Learning, 2020. [Online]. Available: <https://www.sophia.org/tutorials/accuracy-and-precision--3>. [Accessed 17 January 2020].
- [121] V. Thomsen, "Response Time of a Thermometer," *The Physics Teacher*, Fitchburg, 1998.
- [122] R. Willing, A. Moslemian, G. Yamomo, T. Wood, J. Howard and B. Lanting, "Condylar-Stabilized TKR May Not Fully Compensate for PCL-Deficiency: An In Vitro Cadaver Study," *Journal of Orthopaedic Research*, vol. 37, no. 10, pp. 2172–2181, 2019.
- [123] A. Weimann, T. Heinkele, M. Herbort, B. Schliemann, W. Petersen and M. J. Raschke, "Minimally invasive reconstruction of lateral tibial plateau fractures using the jail technique: a biomechanical study," *BMC Musculoskeletal Disorders*, vol. 14, 2013.

- [124] S.-Y. Chong, L. Shen and S. Frantz, "Loading capacity of dynamic knee spacers: a comparison between hand-moulded and COPAL spacers," *BMC Musculoskeletal Disorders*, vol. 20, 2019.
- [125] J. R. H. Foran, "Total Knee Replacement Exercise Guide," OrthoInfo, February 2017. [Online]. Available: <https://orthoinfo.aaos.org/en/recovery/total-knee-replacement-exercise-guide/>. [Accessed 25 May 2020].
- [126] A. J. Johnson, S. A. Sayeed, Q. Naziri, H. S. Khanuja and M. A. Mont, "Minimizing Dynamic Knee Spacer Complications in Infected Revision Arthroplasty," *Clinical Orthopaedics and Related Research*, vol. 470, no. 1, pp. 220–227, 2012.
- [127] P. Garg, R. Ranjan, U. Bandyopadhyay, C. Shiv, S. Mitra and S. K. Gupta, "Antibiotic-impregnated articulating cement spacer for infected total knee arthroplasty," *Indian Journal of Orthopaedics*, vol. 45, no. 6, pp. 535–540, 2011.
- [128] C. Lutzner, S. Kirshner and J. Lutzner, "Patient Activity After TKA Depends on Patient-specific Parameters," *Clinical Orthopaedics and Related research*, vol. 472, no. 12, pp. 3933–3940, 2014.
- [129] Y.-T. Jia, Y. Zhang, C. Ding, N. Zhang, D.-L. Zhang, Z.-H. Sun, M.-Q. Tian and J. Liu, "Antibiotic-loaded Articulating Cement Spacers in Two-Stage Revision for Infected Total Knee Arthroplasty: Individual Antibiotic Treatment and Early Results of 21 Cases," *Chinese Journal of Traumatology*, vol. 15, no. 4, pp. 212–221, 2012.
- [130] C. R. Wheelless, "Staged Revision for Infected Total Knee Joint," *Duke Orthopaedics*, 10 June 2016. [Online]. Available: http://www.wheelsonline.com/ortho/staged_revision_for_infected_total_knee_joint. [Accessed 7 May 2020].

- [131] Littelfuse, "Thermal Time Constant," [Online]. Available: <https://www.littelfuse.com/technical-resources/technical-centers/temperature-sensors/thermistor-info/thermistor-terminology/thermal-time-constant.aspx>. [Accessed 28 January 2020].
- [132] H. Hirata and J. D. Powell, " Sample Rate Effects on Disturbance Rejection for Digital Control Systems," *1990 American Control Conference*, pp. 1137–1145, 1990.
- [133] OMEGA Engineering, "OMEGASCOPE™ Handheld Infrared Thermometer," 2019. [Online]. Available: <https://www.omega.ca/en/sensors-and-sensing-equipment/temperature/sensors/infrared-sensors/os532e-os533e-os534e/p/OS530LE>. [Accessed 25 May 2020].
- [134] S. G. Haidar, R. M. Charity, R. S. Bassi, P. Nicolai and B. K. Singh, "Knee skin temperature following uncomplicated total knee replacement," *The Knee*, vol. 13, no. 6, pp. 422–426, 2006.
- [135] T.-W. Tai, C.-W. Chang, C.-J. Lin, K.-A. Lai and C.-Y. Yang, "Elevated Temperature Trends After Total Knee Arthroplasty," *Orthopedics*, vol. 32, no. 12, p. 886, 2009.
- [136] R. M. D. Meek, D. Dunlop, D. S. Garbuz, R. McGraw, N. V. Greidanus and B. A. Masri, "Patient satisfaction and functional status after aseptic versus septic revision total knee arthroplasty using the PROSTALAC articulating spacer," *Journal of Arthroplasty*, vol. 19, no. 7, pp. 874–879, 2004.
- [137] M. Pietsch, S. Hofmann and C. Wenisch, "Treatment of Deep Infection of Total Knee Arthroplasty Using a Two-Stage Procedure," *Operative Orthopädie und Traumatologie*, vol. 18, pp. 66–87, 2006.

- [138] M. Bahrami, "Transient Heat Conduction," Simon Fraser University, [Online]. Available:
<https://www.sfu.ca/~mbahrami/ENSC%20388/Notes/Transient%20Heat%20Conduction.pdf>. [Accessed 22 February 2020].
- [139] J. Wotjtkowiak, "Lumped Thermal Capacity Model," Encyclopedia of Thermal Stresses, Springer, Dordrecht, 2014. [Online]. Available:
https://link.springer.com/referenceworkentry/10.1007%2F978-94-007-2739-7_393. [Accessed 28 May 2020].
- [140] MathWorks, "Stepinfo," 2020. [Online]. Available:
<https://www.mathworks.com/help/control/ref/stepinfo.html>. [Accessed 22 May 2020].
- [141] L. Hitchens, "Cleaning and conformal coating," Nexus, [Online]. Available:
<http://www.conformalcoatinghelp.com/index.php/ebook/production/cleaning/#3>. [Accessed 19 March 2020].
- [142] E. Peck, "Cleaning and Drying Before Conformal Coating: Why It's Important," MicroCare Electronics, [Online]. Available:
<https://electronics.microcare.com/resources/whitepapers/cleaning-and-drying-before-conformal-coating-why-its-important/>. [Accessed 19 March 2020].
- [143] C. Mallon, R. Goberman-Hill, M. Whitehouse and A. Moore, "Surgeons are deeply affected when patients are diagnosed with prosthetic joint infection," *PLOS ONE*, vol. 13, no. 11, 2018.
- [144] F. R. Kolisek, M. A. Mont, T. M. Syler, D. R. Marker, N. M. Jessup, J. A. Siddiqui, E. Monesmith and S. D. Ulrich, "Total knee arthroplasty using cementless keels and cemented tibial trays: 10-year results," *International Orthopaedics*, vol. 33, no. 1, pp. 117–121, 2009.

- [145] Q. Liu, L. Shao, H. Xiang, D. Zhen, N. Zhao, S. Yang and J. Xu, "Biomechanical characterization of a low density silicone elastomer filled with hollow microspheres for maxillofacial prostheses," *Journal of Biomaterials Science, Polymer Edition*, vol. 24, no. 11, pp. 1378–1390, 2013.

Curriculum Vitae

Name: Michael Konstantine Lavdas

Post-secondary Education and Degrees: University of Western Ontario
London, Ontario, Canada
2018-2020 MEng. – Biomedical Engineering

Ivey School of Business & WORLDiscoveries Patent Office
London, Ontario, Canada
2018-2019 Module – Graduate Student Innovation Scholar

The University of Western Ontario
London, Ontario, Canada
2013-2018 BEng. – Mechatronic Systems Engineering

Honours and Awards: Province of Ontario Graduate Scholarship (OGS)
Declined in lieu of NSERC CGSM
2019-2020

1st Place Poster Award – London Health and Research Day
Detection, Screening and Diagnosis of Health and Disease
2019

Canadian Graduate Scholarship (NSERC CGSM)
Natural Sciences and Engineering Research Council of Canada
2019-2020

1st Place Pitch – Graduate Student Innovation Scholars
Final Pitch Competition
2019

Transdisciplinary Training Award
Collaborative Program in Musculoskeletal Health Research
2018-2020

Scholarship of Professional Merit
Canadian Society of Manufacturers and Exporters
2017

Summa Cum Laude Abstract – Imaging Network Ontario
Presented by co-author Dr. Ali Tavallaei
National Symposium
2016

2nd Place Poster Award – Imaging Network Ontario
Presented by co-author Ali Tavallaei
National Symposium
2015

Publications:

M. Lavdas, B. Lanting, D. Holdsworth, M. Teeter. (2020). Characterization of an Embedded Temperature Sensor for Instrumenting Tibial Spacers Used in Two-Stage Revision Procedures for Infected Total Knee Arthroplasty. Abstract only. Orthopaedic Proceedings. 102-B(2)

M.A. Tavallaei, D. Gelman, **M.K. Lavdas**, A.C. Skanes, D.L. Jones, J.S. Bax, M. Drangova. (2016). Design, Development and Evaluation of a Compact Telerobotic Catheter Navigation System. International Journal of Medical Robotics and Computer Assisted Surgery (MRCAS). 12(2): 442-452

M.A. Tavallaei, **M.K. Lavdas**, M. Drangova. (2016). Magnetic Resonance Imaging Compatible Remote Catheter Navigation System With 3 Degrees of Freedom. International Journal of Computer Assisted Radiology and Surgery (IJCARS). 11(8): 1537-1545

Protected Intellectual Property & Applications:

Tongue Strengthening Device and Method For Use Thereof
Assigned to: Trudell Medical International
Application Serial No.: 62/743,156
Filed: 10/09/2019

Smart Valved Holding Chamber
Assigned to: Trudell Medical International
Application Publication No. US2019/0366019A1
Filed: 03/04/2019

System for Catheter Manipulation
Assigned to: Dr. Mohammad Ali Tavallaei and Dr. Maria Drangova
Pat No. US10,441,374 B2
Filed: 08/10/2015
Year Issued: 2019

Conference Presentations:

Alumni Pathways (Panellist)
Professional Development Conference
Western Undergraduate Engineering Society
2020

M. Lavdas, B. Lanting, D. Holdsworth, M. Teeter. Characterization of an Embedded Temperature Sensor for Instrumenting Tibial Spacers Used in Two-Stage Revision Procedures for Infected Total Knee Arthroplasty.
Young Investigator Podium Presentation
International Society for Technology in Arthroplasty
2019

M. Lavdas, B. Lanting, D. Holdsworth, M. Teeter. Validation of a Temperature Sensor for Implantable Infection Telemetry.
Podium Presentation
Canadian Society of Mechanical Engineering
2019

M. Lavdas, B. Lanting, D. Holdsworth, M. Teeter. Characterization of a Temperature Sensor for Implementation in Instrumented Orthopaedics.
Poster Presentation
Imaging Network Ontario
2019

Alumni Pathways (Panellist)
Professional Development Conference
Western Undergraduate Engineering Society
2018

Classroom to Career (Panellist)
Annual General Meeting
Ontario Society of Professional Engineers
2017

Intro to Personal Finances for Young Engineers
First Year (student) Integration Conference
Engineering Student Societies' Council of Ontario
2017

Crucial Conversations and Negotiation Tactics
Professional Engineers Ontario Student Conference
Engineering Student Societies' Council of Ontario
2016

M.A. Tavallaei, M.K. Lavdas, M. Drangova. Magnetic Resonance Imaging
Compatible Remote Catheter Navigation System With 3 Degrees of Freedom.
Poster Presentation (delivered by co-author)
Imaging Network Ontario
2016

M. Lavdas, J. Tse, M. Drangova. Development of an Electromechanical Micro CT
Scanning Peripheral to Allow Dual Energy Scanning
Podium Presentation
Bone & Joint Institute Trainee Symposium
2015

M.A. Tavallaei, D. Gelman, M.K. Lavdas, A.C. Skanes, D.L. Jones, J.S. Bax,
M. Drangova. Design, Development and Evaluation of a Compact Telerobotic Catheter
Navigation System.
Podium Presentation (delivered by co-author)
Imaging Network Ontario
2015